Politecnico di Milano

School of Industrial and Information Engineering

Thesis in Space Engineering

LUMIO orbit refinement in high fidelity model

Supervisor:
Prof. Francesco Topputo

Thesis of:
Samuele Sirani

Co-Supervisor:
Prof. Giordano Carmine

A.Y. 2021/2022

ACKNOWLEDGMENTS

Sono grato al prof. F. Topputo per la possibilità datami di approfondire questa bellissima materia che è la meccanica orbitale, in particolar modo, le moderne tecniche che vengono utilizzate per costruite traiettorie nella realtà.
Vorrei inoltre ringraziare il prof. G. Carmine per la sua continua disponibilità durante tutto il periodo di stesura di questa tesi.
Un ringraziamento particolare va anche ai miei genitori ed a mia sorella, per avermi supportato incondizionatamente anche nei momenti piu difficili.

ABSTRACT

Although the circular restricted three body problem gives accurate results of the dynamics of a satellite, in proximity of a binary system like the Earth and Moon, perturbations from other bodies can start to become important, especially in correspondence of unstable Lagrangian points, when integrating the trajectory for a long time. The aim of this thesis is to describe the tools available nowadays in order to construct closed orbits, using a more realistic model, around Lagrangian points and apply the results to LUMIO spacecraft, which is plan to orbit in proximity of one of these stationary points.
However, before learning to pedal, you need to know how to walk, therefore preliminary notion are necessary about easier dynamical models. Starting from the general N-body problem, the dynamics is simplified through some reasonable assumption, considering the circular restricted three body problem and the bicircular model, then, also a presentation about the low-energy transfer used by LUMIO is studied, in order to have an idea of how satellites can reach libration points, saving more propellant compared to traditional transfers. Successively the dynamic formulation of the rotopulsating N-body problem is presented and, combined with the multiple shooting technique, a non linear optimization is formulated, capable of generate orbits in a more realistic models. The results are then applied to the LUMIO satellite.

SOMMARIO

Sebbene il modello ristretto circolare dia risultati accurati della dinamica di un satellite, in prossimità di un sistema binari come la Terra e la Luna, perturbazioni di altri corpi possono iniziare a diventare importanti, specialmente in corrispondenza dei punti Lagrangiani instabili, quando la traiettoria è integrata per un lungo tempo. L'obbiettivo di questa tesi è descrivere gli strumenti disponibili oggigiorno in modo da costruire orbite chiuse, usando un modello più realistico, intorno ai punti Lagrangiani ed applicare i risultati al satellite LUMIO, il quale è pianificato che orbiti in prossimità di uno di questi punti stazionari.
Ad ogni modo, prima di iniziare a pedalare bisogna sapere camminare, perciò nozioni preliminari sono necessarie riguardo ai modelli dinamici più semplici. Iniziando da un problema generico a N corpi, la dinamica viene semplificata attraverso ragionevoli assunzioni, considerando il problema ristretto circolare e dal modello bicircolare, poi, anche una presentazione riguardante il trasferimento a bassa energia usato da LUMIO viene studiato, in modo da avere un idea di come i satelliti possono raggiungere i punti di librazione, salvando più propellente rispetto a un trasferimento tradizionale. Successivamente la formulazione dinamica del problema degli N corpi rotopulsante viene presentata e, combinata con una strategia di shooting multiplo, un ottimizzazione non lineare è formulata, in grado di generare orbite in un modello più realistico. I risultati sono poi applicati al satellite LUMIO.

Contents

List of Figures

1 Introduction

Since the beginning of space missions, the design of trajectories was dependent on the concept of solving, at each step, a two-body problem and then patch together the different branches using the patched conic approximation. However, with the increase of complexity of space mission's requirements and computing power, these classical methods are no more adequate and newer economic and feasible solutions are needed, exploiting more realistic dynamical models.

One of the new solutions was applied, for the first time, on the Japanese spacecraft Hiten that was launched in orbit in January 1990. During the mission, the Spacecraft fly-by with the Moon and the Hagoromo orbiter was released from Hiten and inserted into a lunar orbit. Unfortunately, Hagoromo failed during the insertion and was not able to perform its objective. At the end of the mission of Hiten, the satellite was in an Earth orbit and not capable to reach the Moon using a direct transfer.

In this situation E. Belbruno and J. Miller described a new design strategy ([1, 2]) to transfer the spacecraft into a lunar orbit, using a low-energy transfer based on the so-called weak stability boundaries, the trajectory was studied so that a spacecraft in an Earth orbit is temporarily and ballistically captured in a lunar orbit requiring a small fraction of fuel compared with the traditional transfers. This transfer was successful implemented and Hiten satellite was able to fly around the Moon until it was deliberately crashed on the lunar surface on April 1993.

Koon et al, explained the idea of low energy transfer using the patched circular restricted three-body problem approximation and manifold theory ([3]). Based on the work of Koon, Parker, was able to identify different families of low energy transfer, targeting Earth-Moon libration point or a lunar orbit, setting a certain time of flight and tuning opportunely some parameters of the trajectory ([4, 5, 6]), while a different partition in families is given in [7] where, low energy transfers with lunar fly-by are considered.

From the positive result of Hiten, low energy transfers became trajectories useful for transfer CubeSat in a lunar orbit, indeed, after Hiten, also other missions were designed to exploit low energy transfer, some examples are: GENESIS ([8]), used to obtain information on the origin of the solar system and then return safely to the Earth and GRAIL ([9]), which consisted on two satellite used to acquire data about the surface and internal structure of the Moon. Also, other missions are planned to use these trajectories in future like EQUULEUS ([10]), OMOTENASHI ([11]) and LUMIO.

LUMIO is a 12U CubeSat, winner of the ESA's competition "Lunar CubeSats for Exploration", used for the detection of flashes, on the dark side of the Moon, due to impact of asteroids on the lunar surface. Its design strategy ([12, 13]) is to transfer into a Halo orbit around L_2 point in the Earth-Moon system and observe the lunar surface for at least one year, giving important information's about the estimation flux of asteroids that

hit a spacecraft in orbit and can also give the possibility to understand the feasibility of a human colony on the Moon.
In this thesis, an analysis of LUMIO's orbit is studied in a high fidelity model, starting from a circular restricted three body problem, the orbit is then refined in a more realistic dynamics.

1.1 Summary

This thesis is organized as follows:

- In **Chapter** 2 we will discuss some different models that can be available in order to design low energy transfer.
  Initially the general n-body problem and its important features are presented, then the Circular restricted three body problem (CRTBP) model is derived, the main approximation and the equation of motion.
  Then a discussion of the existence of equilibrium solution and their stability analysis is carried out, studying the linear approximation of the perturbed trajectory.
  Successively an analysis related to the constant of motion on the CRTBP is presented, showing how influence the accessible regions where motion can happen.
  Finally a presentation of the four body problem is presented, in particular, the Bicircular model is investigated and the equation of motion are shown in the different reference frame.

- In **Chapter** 3 We will see how to design low-energy transfer targeting libration points, from how to construct periodic orbit around Lagrangian points in the CRTBP to the design of trajectories using Manifold theory and then a brief discussion of weak stability boundaries is also discussed.

- In **Chapter** 4 The RPRnBP model is presented and its equation of motion are derived. Then, an optimization analysis is carried out, different possible constraints, typical of space mission, are presented. Finally LUMIO orbit is optimize under the RPRnBP, exploiting the multiple shooting algorithm.

- In **Chapter** 5 we summarize the investigation did in chapter 4 and the final considerations.

2 Dynamical Models

The patched conic approximation is based on the definition of the sphere of influence, spherical region centred in an attracting body, where the trajectory of the spacecraft is subjected to the gravitational attraction of only that body, solving a two-body problem each time the satellite escape from a sphere of influence to another one and then patch together the different conics. The obtained trajectory is a good approximation near each body, becoming less accurate at the patch points.
More precise models are necessary to represent high-fidelity transfer during the entire mission of the satellite. However, the main disadvantage of considering more than two bodies is that no closed solution exists, and numerical solution are needed.
In this chapter an overview of only the most important dynamical models is presented, a more detailed classification is given in hierarchy order in [14].

2.1 n-body problem formulation

The most generic model is represented considering an arbitrary number n of bodies, in *Figure 1* is reported a schematic representation of the n-body problem. The axis $(O; X, Y, Z)$ denotes the inertial frame with the origin placed in O. The position of the q-*th* body, P_q respect to the origin and its mass are indicated as $\boldsymbol{r_q} = (r_q^x, r_q^y, r_q^z)$ and m_q respectively.

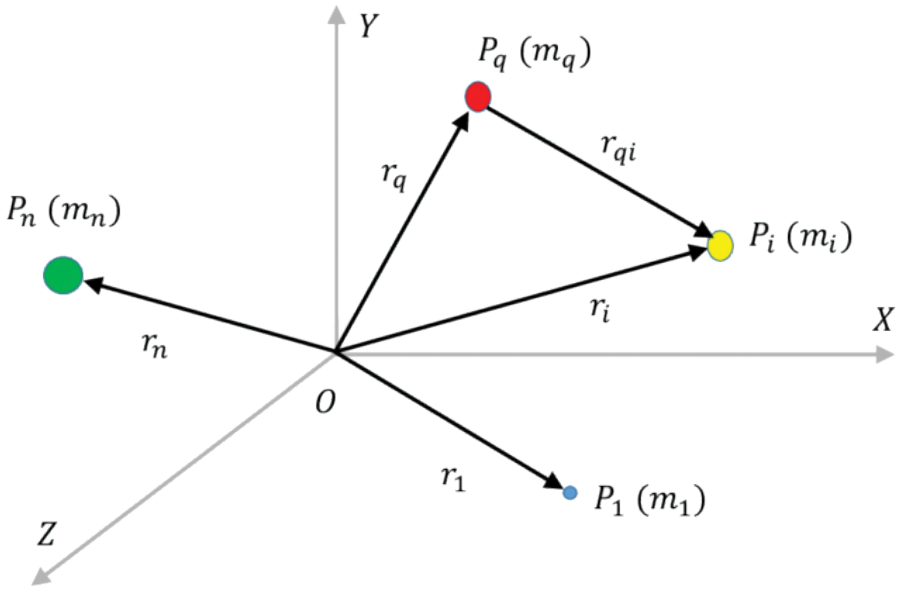

Figure 1: n-body problem

Each mass is subjected to the mutual attraction of the other bodies, the equations of motion in the inertial frame, are given from Newton's law:

$$m_i \ddot{\boldsymbol{r}}_{\boldsymbol{i}} = -G \sum_{\substack{j=1 \\ j \neq i}}^{n} \frac{m_i m_j}{r_{ji}^3} \bar{\boldsymbol{r}}_{\boldsymbol{ji}} = -G \sum_{\substack{j=1 \\ j \neq i}}^{n} \frac{m_i m_j}{r_{ji}^3} (\boldsymbol{r_i} - \boldsymbol{r_j}) \quad , \quad \forall i = 1, ..., n \tag{1}$$

Where $\boldsymbol{r_{ji}} = \boldsymbol{r_i} - \boldsymbol{r_j}$ is the vector distance from the j-th body to the i-th body, r_{ji} its norm and G the gravity constant ($G = 6.67 \times 10^{-11} \frac{Nm^2}{kg^2}$).
Each Eq. (1) can be rewritten using a system of six scalar, non-linear ordinary differential equations of the first order, a total of $6n$ coupled, scalar equations that represents the state/degree of freedom of each body (position and velocity in our case) that must be solved once an initial state is set. Another possible approach is to find $6n$ constant of motion since in that case it would be possible obtain the solution of the problem in closed form without integrated it numerically.
We remark that the constant of motion of a generic n-body problem are the following:

- Since gravitational forces are internal forces and no external forces $\boldsymbol{R}^{(ext)}$ act on the system, from the first cardinal equation we get:

$$\dot{\boldsymbol{Q}} = \sum_{i=1}^{n} m_i \boldsymbol{a}_{cm} = \boldsymbol{R}^{(ext)} = 0 \tag{2}$$

  This means that either the center of mass $\boldsymbol{r}_{cm}$ is at rest or it is moving with a constant velocity in a straight line with respect to the origin O.
  Eq. (2) introduce six constant of motion about the position and velocity of the center of mass.

- Since there are not external torque, the second cardinal equation written respect to the origin O becomes:

$$\dot{\boldsymbol{\Gamma}}_O = \frac{d}{dt} (\sum_{i=1}^{n} \boldsymbol{r_i} \times m_i \boldsymbol{v_i}) = \boldsymbol{M}_O^{(ext)} = 0 \tag{3}$$

  This means that the angular momentum $\boldsymbol{\Gamma}_O$ is constant and this introduce three integral of motion.

- We note that the gravitational force can be written as a gradient of a potential function U:

$$U = \sum_{1 \leq i < j \leq n} G \frac{m_i m_j}{r_{ji}} \tag{4}$$

Since:

$$\frac{\partial U}{\partial \boldsymbol{r_i}} = \sum_{j=1, j\neq i}^{n} -G\frac{m_i m_j}{r_{ji}^3}\boldsymbol{r_{ji}} \tag{5}$$

This means that, in a system of only conservative forces, the total mechanical energy E must be conserved:

$$E = E_k + U = const \tag{6}$$

with

$$E_k = \frac{1}{2}\sum_{i=1}^{n} m_i(\boldsymbol{v_i} \cdot \boldsymbol{v_i}) \tag{7}$$

The kinetic energy of the entire system.
This add another constant of motion of the n-body problem.

At the end of the analysis we have only 10 constant that are not sufficient, this means that unluckily we cannot obtain a closed form solution and numerical integration is the only way. A note must be done for the two body problem since we have 12 degree of freedom we should not obtain a closed solution, however, it is possible to define a relative motion subtracting the two Eq.(1) obtaining an ODE which is decoupled with the relative position as the only variable, which is easier to solve.

2.2 Circular restricted three body problem (CRTBP)

Even if the n-body problem is very accurate, in most cases, it is possible to obtain a good approximation of the satellite dynamic just considering a limited number of bodies that mainly affect the motion of the satellite.
One of the most important model is the circular restricted three body problem.
The circular restricted three body problem is an approximation of the three body problem when dealing with space mission involving the mutual interaction of just three bodies, the main approximations are the following:

- Since we are focus on space mission one of the bodies must be the satellite therefore, its mass m is negligible compared with the other two massive bodies, called primaries, M_1 and M_2, that can be planets, comets or satellites planet.
- M_1 and M_2 with $M_1 > M_2$, are not affecting by the presence of the satellite and their motion can be assumed as a solution of a two body problem, obtaining a

conic section whose solution is known. This seems to be a very strong assumption since we are actually reduce the degree of freedom of the dynamical system from 18 to only 6 related to the satellite, however this assumption is very accurate when the first hypothesis is verified.

- The two bodies are assumed to revolve on circular orbits around their center of mass, this is because in our solar system most of the orbits involving massive object are quasi circular orbit, a good example to take in mind is the Sun-Earth or Earth-Moon system.

Note that no restriction of the motion on the spacecraft is imposed, it is free to move in space.

2.2.1 Problem definition and Normalize coordinates

In this section we derive the equation of motion of the third body in the restricted three body problem.
We start to solve the problem as in [15], first of all we need to introduce some notation. Consider the set $(O;\xi,\eta,\zeta)$ of axis in the inertial frame, centered on the fixed origin O, the ξ-axis lies along the line joining the primaries at time $t=0$, which during the motion remain confined in the $\xi-\eta$ plane and let ζ the axis perpendicular to this plane.
The position of the primaries and the particle P, are denoted as $\boldsymbol{R}_1$, $\boldsymbol{R}_2$ and $\boldsymbol{r}$ respectively while the distances from M_1 and M_2 to P are $\boldsymbol{r}_1$ and $\boldsymbol{r}_2$ as shown in *Figure 2*, where the mass of the particle is denoted as m.
From the two-body problem, if the two masses, M_1 and M_2, move on circular orbits, the distance between them is constant and rotate around their center of mass with the same angular velocity ω. It is possible to introduce another reference frame $(O^{'};x,y,z)$ with the origin placed in $O^{'}$, coincident with the barycenter of the primaries, that we suppose at rest, rotating rigidly with M_1 and M_2, having the x-axis directed toward the smaller primary and the z-axis coincident with the ζ-axis of the inertial frame, the reason behind this choice of this frame will be clearer later.
Without loss of generality, we take, for simplicity, the two origin coincident and therefore, since the barycenter is fixed, they will be both fixed during the motion of the system.

In order to simplify further the equations, we consider new units of measurement, indicated as $\#^*$ and its associated quantity as $\hat{\#}$ defined as follows:

- The unit of mass m^*, is taken such that, in the new units, the sum of the masses

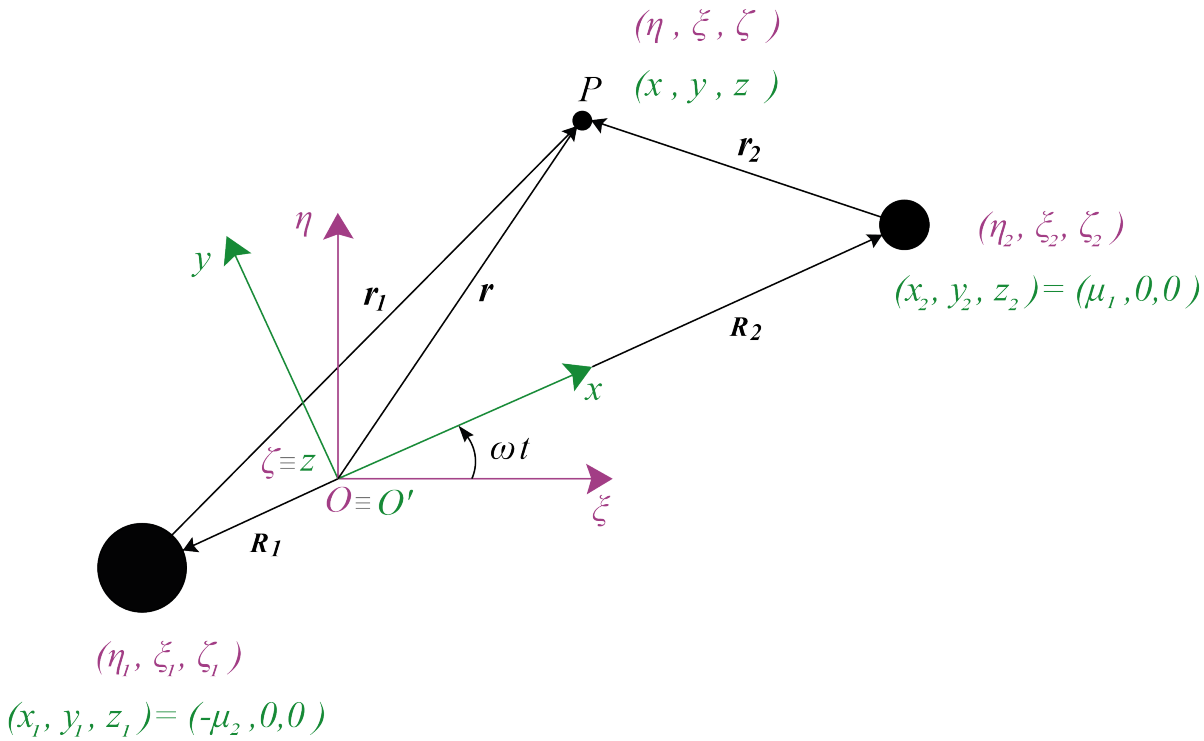

Figure 2: Restricted three body problem

of the primaries $\hat{M}_1$ and $\hat{M}_2$ is unitary:

$$\hat{M}_1 + \hat{M}_2 = 1m^* \tag{8}$$

Therefore the primaries, in this reference, have a mass given by:

$$\begin{aligned} \hat{M}_1 = \mu_1 &= \frac{M_1}{M_1 + M_2} \\ \hat{M}_2 = \mu_2 &= \frac{M_2}{M_1 + M_2} \end{aligned} \tag{9}$$

With $\mu_1 = 1 - \mu_2$.

- The unit of length d^*, is chosen such that, the distance between the primaries is unitary:

$$\|\hat{\boldsymbol{R}}_{\mathbf{2}} - \hat{\boldsymbol{R}}_{\mathbf{1}}\| = \hat{R}_{12} = 1d^* \tag{10}$$

Knowing that in the synodic frame $\hat{\boldsymbol{R}}_{\mathbf{1}}$ and $\hat{\boldsymbol{R}}_{\mathbf{2}}$ have only the x component different from zero and that the position of the barycenter of the system coincide with the origin:

$$\boldsymbol{r}_{\boldsymbol{cm}} = \frac{\hat{M}1\hat{\boldsymbol{R}}_{\mathbf{1}} + \hat{M}2\hat{\boldsymbol{R}}_{\mathbf{2}}}{\hat{M}1 + \hat{M}1} = \mathbf{0} \tag{11}$$

We can compute the position of the primaries in the synodic frame, obtaining:

$$\begin{aligned}\hat{\boldsymbol{R}}_{\mathbf{1}} &= (x_1, y_1, z_1) = (-\mu_2, 0, 0)\\ \hat{\boldsymbol{R}}_{\mathbf{2}} &= (x_2, y_2, z_2) = (\mu_1, 0, 0)\end{aligned} \tag{12}$$

- The unit of time s^* is selected in order that the angular rate ω is unitary:

$$\hat{\omega} = 1\frac{rad}{s^*} \tag{13}$$

With this choice we can also relate the time in the two different units, since the *rad* unit doesn't change, the angle spanned must be the same, therefore:

$$\theta = \omega t = \hat{t} = \hat{\theta} \tag{14}$$

With these new units we can also see that, from Kepler third law:

$$\hat{G} = \frac{\hat{\omega}^2 \hat{R}_{12}^3}{\hat{M}1 + \hat{M}2} = \frac{(1\frac{rad}{s^*})^2 (1d^*)^3}{1m^*} = 1\frac{N^* d^{*2}}{m^{*2}} \tag{15}$$

Therefore, also the gravity constant is unitary.

2.2.2 Equation of motion

Applying Eq.(1) with three body and to the motion of the third particle we obtain:

$$m\ddot{\hat{\boldsymbol{r}}} = -G\frac{mM_1}{r_1^3}\hat{\boldsymbol{r}}_{\mathbf{1}} - G\frac{mM_2}{r_2^3}\hat{\boldsymbol{r}}_{\mathbf{2}} \tag{16}$$

Making simplifications and introducing the new units discussed before we get:

$$\ddot{\hat{\boldsymbol{r}}} = -\frac{\mu_1}{\hat{r}_1^3}\hat{\boldsymbol{r}}_{\mathbf{1}} - \frac{\mu_2}{\hat{r}_2^3}\hat{\boldsymbol{r}}_{\mathbf{2}} \tag{17}$$

Where the derivatives are now in the normalized time and:

$$\hat{\boldsymbol{r}}_1 = \hat{\boldsymbol{r}} - \hat{\boldsymbol{R}}_{\mathbf{1}} = (\hat{\xi}, \hat{\eta}, \hat{\zeta}) - (\hat{\xi}_1, \hat{\eta}_1, \hat{\zeta}_1) = (\hat{\xi}, \hat{\eta}, \hat{\zeta}) - (-\mu_2 \cos\hat{t}, -\mu_2 \sin\hat{t}, 0) \tag{18a}$$

$$\hat{\boldsymbol{r}}_2 = \hat{\boldsymbol{r}} - \hat{\boldsymbol{R}}_{\mathbf{2}} = (\hat{\xi}, \hat{\eta}, \hat{\zeta}) - (\xi_2, \eta_2, \zeta_2) = (\hat{\xi}, \hat{\eta}, \hat{\zeta}) - (\mu_1 \cos\hat{t}, \mu_1 \sin\hat{t}, 0) \tag{18b}$$

are the positions of P respect to the primaries in these new units. From now on, we drop, for simplicity, the notation with $\hat{}$, remembering that we are in normalized coordinates, Eq.(17) can be written in scalar form:

$$\ddot{\xi} = -\frac{\mu_1}{r_1^3}(\xi + \mu_2 \cos\hat{t}) - \frac{\mu_2}{r_2^3}(\xi - \mu_1 \cos\hat{t}) \tag{19a}$$

$$\ddot{\eta} = -\frac{\mu_1}{r_1^3}(\eta + \mu_2 \sin\hat{t}) - \frac{\mu_2}{r_2^3}(\eta - \mu_1 \sin\hat{t}) \tag{19b}$$

$$\ddot{\zeta} = -\frac{\mu_1}{r_1^3}\zeta - \frac{\mu_2}{r_2^3}\zeta \tag{19c}$$

Eq.(19) are the equations of motion written in inertial and in normalized coordinate, a system like this is called $non - autonomous$ since the motion depend explicitly on the independent variable, the time.

At this point, it is natural to ask if there exist a particular reference such that the equations of motion are autonomous. Intuitively, the synodic frame is the frame that we are looking for, infect, as already discuss, in this frame the motion of the primaries is at rest and independent on time.

In order to write the Eq.(19) in the synodic frame, we apply a counterclockwise rotation around the out of plane axis, with $\omega = 1$. In this case the two generic positions can be related in the following form:

$$\begin{pmatrix} \xi \\ \eta \\ \zeta \end{pmatrix} = \begin{bmatrix} \cos t & -\sin t & 0 \\ \sin t & \cos t & 0 \\ 0 & 0 & 1 \end{bmatrix} \begin{pmatrix} x \\ y \\ z \end{pmatrix} = \boldsymbol{R} \begin{pmatrix} x \\ y \\ z \end{pmatrix} \tag{20}$$

Taking the derivative, we get the relations in the velocities:

$$\begin{pmatrix} \dot{\xi} \\ \dot{\eta} \\ \dot{\zeta} \end{pmatrix} = \frac{d\boldsymbol{R}}{dt} \begin{pmatrix} x \\ y \\ z \end{pmatrix} + \boldsymbol{R}\frac{d}{dt} \begin{pmatrix} x \\ y \\ z \end{pmatrix} = \begin{bmatrix} \cos t & -\sin t & 0 \\ \sin t & \cos t & 0 \\ 0 & 0 & 1 \end{bmatrix} \begin{pmatrix} \dot{x} - y \\ \dot{y} + x \\ \dot{z} \end{pmatrix} = \boldsymbol{R} \begin{pmatrix} \dot{x} - y \\ \dot{y} + x \\ \dot{z} \end{pmatrix} \tag{21}$$

Finally, the accelerations will be:

$$\begin{pmatrix} \ddot{\xi} \\ \ddot{\eta} \\ \ddot{\zeta} \end{pmatrix} = \begin{bmatrix} \cos t & -\sin t & 0 \\ \sin t & \cos t & 0 \\ 0 & 0 & 1 \end{bmatrix} \begin{pmatrix} \ddot{x} - 2\dot{y} - x \\ \ddot{y} + 2\dot{x} - y \\ \ddot{z} \end{pmatrix} = \boldsymbol{R}(\boldsymbol{a_{rel}} + \boldsymbol{a_{Coriolis}} + \boldsymbol{a_{Centr.}}) \tag{22}$$

We note that actually Eq. (22) is the representation of the relative kinematics using the apparent accelerations when $\omega = const = 1$ and when the origin of the rotating frame is fixed:

$$
\begin{aligned}
\boldsymbol{a_{inertial}} &= \boldsymbol{a_{O'}} + \boldsymbol{a_{rel}} + 2\boldsymbol{\omega} \times \boldsymbol{v} + \boldsymbol{\omega} \times (\boldsymbol{\omega} \times \boldsymbol{r}) + \frac{d\boldsymbol{\omega}}{dt} \times \boldsymbol{r} = \\
&= \boldsymbol{a_{rel}} + 2\boldsymbol{\omega} \times \boldsymbol{v} + \boldsymbol{\omega} \times (\boldsymbol{\omega} \times \boldsymbol{r}) = \\
&= \boldsymbol{a_{rel}} + \boldsymbol{a_{Coriolis}} + \boldsymbol{a_{Centr.}} = \boldsymbol{R} \begin{pmatrix} \ddot{x} - 2\dot{y} - x \\ \ddot{y} + 2\dot{x} - y \\ \ddot{z} \end{pmatrix}
\end{aligned}
\tag{23}
$$

Where $\boldsymbol{r}$, $\boldsymbol{v}$ and $\boldsymbol{a}$ are the position, velocity and acceleration of the third particle P respect to the synodic frame, a transformation through $\boldsymbol{R}$ is needed to obtain the corresponding inertial representation .
Substituting Eq. (20) and Eq. (21) into Eq. (19), we obtain:

$$
\begin{aligned}
&(\ddot{x} - 2\dot{y} - x)\cos t - (\ddot{y} + 2\dot{x} - y)\sin t = \\
&= \left(\mu_1 \frac{x_1 - x}{r_1^3} + \mu_2 \frac{x_2 - x}{r_2^3}\right)\cos t + \left(\frac{\mu_1}{r_1^3} + \frac{\mu_2}{r_2^3}\right) y \sin t
\end{aligned}
\tag{24a}
$$

$$
\begin{aligned}
&(\ddot{x} - 2\dot{y} - x)\sin t + (\ddot{y} + 2\dot{x} - y)\cos t = \\
&= \left(\mu_1 \frac{x_1 - x}{r_1^3} + \mu_2 \frac{x_2 - x}{r_2^3}\right)\sin t - \left(\frac{\mu_1}{r_1^3} + \frac{\mu_2}{r_2^3}\right) y \cos t
\end{aligned}
\tag{24b}
$$

$$
\ddot{z} = -\left(\frac{\mu_1}{r_1^3} + \frac{\mu_2}{r_2^3}\right) z \tag{24c}
$$

With:

$$
r_1 = \sqrt{(x + \mu_2)^2 + y^2 + z^2} \tag{25a}
$$

$$
r_2 = \sqrt{(x - \mu_1)^2 + y^2 + z^2} \tag{25b}
$$

The distances between the primaries and the particle P in the synodic frame.
It seems that Eq. (24) is much more complicated respect to what obtained in the inertial frame, however, multiplying Eq.(24a) by $\cos t$ and Eq.(24b) by $\sin t$, and add the results, and then multiply Eq.(24a) by $-\sin t$ and Eq.(24b) by $\cos t$ and add these together, the equation of motion in the rotating system become:

$$\ddot{x} - 2\dot{y} - x = -\left(\mu_1 \frac{x+\mu_2}{r_1^3} + \mu_2 \frac{x-\mu_1}{r_2^3}\right) \tag{26a}$$

$$\ddot{y} + 2\dot{x} - y = -\left(\frac{\mu_1}{r_1^3} + \frac{\mu_2}{r_2^3}\right) y \tag{26b}$$

$$\ddot{z} = -\left(\frac{\mu_1}{r_1^3} + \frac{\mu_2}{r_2^3}\right) z \tag{26c}$$

These accelerations can be written as the gradient of a scalar potential U so that:

$$\ddot{x} - 2\dot{y} = \frac{\partial U}{\partial x} \tag{27a}$$

$$\ddot{y} + 2\dot{x} = \frac{\partial U}{\partial y} \tag{27b}$$

$$\ddot{z} = \frac{\partial U}{\partial z} \tag{27c}$$

With:

$$U(x, y, z) = \frac{x^2 + y^2}{2} + \frac{\mu_1}{r_1} + \frac{\mu_2}{r_2} \tag{28}$$

Where U denotes the specific potential in this case.
First of all we note that Eq.(26) constitutes an *autonomous* system since are no more dependent on time.
Then, another consideration of its different term is done, if we multiply Eq.(23) by the mass m of the particle P and using Newton's law, we get:

$$\boldsymbol{F}_{grav.} = m\boldsymbol{a}_{rel} + \boldsymbol{F}_{Coriolis} + \boldsymbol{F}_{centr.} \tag{29}$$

From mechanics is known that a conservative force can be written as a gradient of a specific potential energy U (per unit of mass) defined in Eq.(28).
Manipulating Eq.(29):

$$\begin{aligned} \boldsymbol{a}_{rel} + \boldsymbol{a}_{Coriolis} &= \frac{\boldsymbol{F}_{grav.}}{m} - \frac{\boldsymbol{F}_{centr.}}{m} \\ \boldsymbol{a}_{rel} + \boldsymbol{a}_{Coriolis} &= \boldsymbol{\nabla}(U_{grav.} + U_{centr.}) = \boldsymbol{\nabla} U(x, y, z) \end{aligned} \tag{30}$$

Actually Eq.(26) and Eq.(30) are the same, this means that the term $\frac{x^2+y^2}{2}$ is the potential term associated to the centrifugal acceleration while the terms $\frac{\mu_1}{r_1}$ and $\frac{\mu_2}{r_2}$ are associated to the gravity acceleration due to the presence of the primaries.

We note that the Coriolis force is not inside the gradient, this because the Coriolis force is not capable of doing work since it is always perpendicular to the velocity in the synodic frame (its potential would be constant).
Equation of motion can also be written as a system of first order ordinary differential equation in order to represent explicitly the state of P.
Let $\boldsymbol{x} = (x_1, x_2, x_3, x_4, x_5, x_6)^T = (x, y, z, \dot{x}, \dot{y}, \dot{z})^T$ be the state of the satellite, we can write:

$$\dot{\boldsymbol{x}} = \boldsymbol{F}(\boldsymbol{x}) \tag{31}$$

Or equivalently:

$$\begin{pmatrix} \dot{x}_1 \\ \dot{x}_2 \\ \dot{x}_3 \\ \dot{x}_4 \\ \dot{x}_5 \\ \dot{x}_6 \end{pmatrix} = \begin{bmatrix} x_4 \\ x_5 \\ x_6 \\ 2x_5 + x_1 - (\mu_1 \frac{x_1+\mu_2}{r_1^3} + \mu_2 \frac{x_1-\mu_1}{r_2^3}) \\ -2x_4 + x_2 - (\frac{\mu_1}{r_1^3} + \frac{\mu_2}{r_2^3}) x_2 \\ -(\frac{\mu_1}{r_1^3} + \frac{\mu_2}{r_2^3}) x_3 \end{bmatrix} \tag{32}$$

With:

$$r_1 = \sqrt{(x_1 + \mu_2)^2 + x_2^2 + x_3^2} \tag{33a}$$

$$r_2 = \sqrt{(x_1 - \mu_1)^2 + x_2^2 + x_3^2} \tag{33b}$$

2.2.3 Jacobi Constant

Multiplying Eq.(27a) by $\dot{x}$, Eq.(27b) by $\dot{y}$ and Eq.(27c) by $\dot{z}$ and add all together we have:

$$\dot{x}\ddot{x} + \dot{x}\ddot{x} + \dot{x}\ddot{x} = \frac{\partial U}{\partial x}\dot{x} + \frac{\partial U}{\partial y}\dot{y} + \frac{\partial U}{\partial z}\dot{z} \tag{34}$$

And integrating gives:

$$\dot{x}^2 + \dot{y}^2 + \dot{z}^2 = 2U - C_J \tag{35}$$

Where C_J is a constant of integration.
Since $\dot{x}^2 + \dot{y}^2 + \dot{z}^2 = v^2$ is the velocity in the synodic frame, using eq.(28) we can write:

$$C_J = (x^2 + y^2) + 2\left(\frac{\mu_1}{r_1} + \frac{\mu_2}{r_2}\right) - \dot{x}^2 - \dot{y}^2 - \dot{z}^2 = 2U - v^2 \tag{36}$$

The constant C_J is called Jacobi constant and represent an integral of motion of the restricted three body problem.
We notice that C_J express the conservation of the energy in the synodic frame since:

$$-\frac{C_J}{2} = \frac{\dot{x}^2 + \dot{y}^2 + \dot{z}^2}{2} - U = e_k - U = e \tag{37}$$

With e_k the specific kinetic energy and e the specific mechanical energy.
Since we have added different approximation and decreased the degree of freedom of the system, we are tempted to say that we have enough integral of motions to solve Eq.(26) in closed form, however, this is not true, **the only constant of motion is the Jacobi constant in the restricted three body problem**. This because the approximation of considering circular orbits leads Eq.(1) to a two body formulation for the primaries while a classic three-body formulation for P, thus the considerations about the different integral of motion cannot be applied in this case.
Even if we write Eq.(11), the conservation of the position of the center of mass and its velocity, the motion associated to P doesn't appear and therefore can't be used as a constant of motion.
Analogous consideration can be done for the angular momentum that is constant for M_1 and M_2 but changes for P since exchange with the primaries is not taken into account while the energy in the inertial frame can be express as (see.[15] for more detail):

$$\frac{1}{2}(\dot{\xi}^2 + \dot{\eta}^2 + \dot{\zeta}^2) - \left(\frac{\mu_1}{r_1} + \frac{\mu_1}{r_1}\right) = \boldsymbol{h} \cdot \boldsymbol{\omega} - \frac{1}{2}C_J \tag{38}$$

which is not constant because the angular momentum of the spacecraft $\boldsymbol{h}$ is not constant. Therefore the circular restricted three body problem has 6 degree of freedom and only 1 constant of motion so, also here, no closed solution of Eq.(26) exist.

2.2.4 State Transition Matrix

It is possible to linearize the system in Eq.(32) in order to develop a method of computing an approximation of the possible trajectories that are near to a reference one.
Let $\bar{\boldsymbol{x}}(t) = (\bar{x}(t), \bar{y}(t), \bar{z}(t), \dot{\bar{x}}(t), \dot{\bar{y}}(t), \dot{\bar{x}}(t))^T$ be a reference trajectory, a close trajectory $\boldsymbol{x}(t)$ can be expressed as a perturbation of $\bar{\boldsymbol{x}}(t)$ in the following way:

$$\boldsymbol{x}(t) = \bar{\boldsymbol{x}}(t) + \delta\boldsymbol{x}(t) \tag{39}$$

Where $\delta\boldsymbol{x}(t)$ indicate the difference, in the state space, between the two trajectories.
Linearizing Eq.(31) along the reference trajectory, for small values of $\delta\boldsymbol{x}(t)$, we obtain:

$$\dot{\boldsymbol{x}} - \dot{\bar{\boldsymbol{x}}} = \delta\dot{\boldsymbol{x}}(t) = \boldsymbol{F}(\boldsymbol{x}) - \boldsymbol{F}(\bar{\boldsymbol{x}}) \approx \frac{\partial \boldsymbol{F}}{\partial \boldsymbol{x}}(\bar{\boldsymbol{x}})\delta\boldsymbol{x}(t) = \boldsymbol{A}(t)\delta\boldsymbol{x}(t) \tag{40}$$

Where $\frac{\partial \boldsymbol{F}}{\partial \boldsymbol{x}}$ is the Jacobian matrix evaluated at the reference trajectory $\bar{\boldsymbol{x}}(t)$.
Computing all the derivatives, the Jacobian becomes:

$$\boldsymbol{A}(t) = \begin{bmatrix} 0 & 0 & 0 & 1 & 0 & 0 \\ 0 & 0 & 0 & 0 & 1 & 0 \\ 0 & 0 & 0 & 0 & 0 & 1 \\ U_{xx} & U_{xy} & U_{xz} & 0 & 2 & 0 \\ U_{yx} & U_{yy} & U_{yz} & -2 & 0 & 0 \\ U_{zx} & U_{zy} & U_{zz} & 0 & 0 & 0 \end{bmatrix} |_{\bar{\boldsymbol{x}}(t)} \tag{41}$$

With:

$$U_{xx} = \frac{\partial^2 U}{\partial x^2} = 1 - \frac{\mu_1}{r_1^3} - \frac{\mu_2}{r_2^3} + 3[\mu_1 \frac{(x+\mu_2)^2}{r_1^5} + \mu_2 \frac{(x-\mu_1)^2}{r_2^5}] \tag{42a}$$

$$U_{yy} = \frac{\partial^2 U}{\partial y^2} = 1 - \frac{\mu_1}{r_1^3} - \frac{\mu_2}{r_2^3} + 3[\frac{\mu_1}{r_1^5} + \frac{\mu_2}{r_2^5}]y^2 \tag{42b}$$

$$U_{zz} = \frac{\partial^2 U}{\partial z^2} = -\frac{\mu_1}{r_1^3} - \frac{\mu_2}{r_2^3} + 3[\frac{\mu_1}{r_1^5} + \frac{\mu_2}{r_2^5}]z^2 \tag{42c}$$

$$U_{xy} = U_{yx} = \frac{\partial^2 U}{\partial x \partial y} = 3[\mu_1 \frac{(x+\mu_2)}{r_1^5} + \mu_2 \frac{(x-\mu_1)}{r_2^5}]y \tag{42d}$$

$$U_{xz} = U_{zx} = \frac{\partial^2 U}{\partial x \partial z} = 3[\mu_1 \frac{(x+\mu_2)}{r_1^5} + \mu_2 \frac{(x-\mu_1)}{r_2^5}]z \tag{42e}$$

$$U_{yz} = U_{zy} = \frac{\partial^2 U}{\partial y \partial z} = 3[\frac{\mu_1}{r_1^5} + \frac{\mu_2}{r_2^5}]yz \tag{42f}$$

Eq.(40) describe the evolution of the displacement between the nominal and another trajectory in the neighborhood, once initial displacement $\delta\hat{\boldsymbol{x}}_0 = \delta\hat{\boldsymbol{x}}(t=0)$ is set. Note also that in this case the Jacobian depends on time, this means that while the trajectory evolves the different weights of each state coordinate x_i, change in time so that their contribution have a different influence on the velocity of the deviation $\delta\dot{\boldsymbol{x}}(t)$ between the two trajectories, depending on the evolution of the satellite's state.
The solution of Eq.(40) will depend on the actual trajectory $\bar{\boldsymbol{x}}(t)$, to write it explicitly, let $\phi(t;\boldsymbol{x}_0)$ the generic trajectory that starts at $\boldsymbol{x}_0 = \boldsymbol{x}(t_0)$ and describing the trajectory at the generic time $t > t_0$ that is, $\phi(t^*;\boldsymbol{x}_0)$ is the state of the spacecraft obtained starting in $\boldsymbol{x}_0$ and propagating the trajectory until $t = t^*$. First of all we note that with this definition:

$$\frac{d}{dt}\phi(t;\boldsymbol{x}_0) = \boldsymbol{F}(\phi(t;\boldsymbol{x}_0)) \quad , \quad \phi(t_0;\boldsymbol{x}_0) = \boldsymbol{x}_0 \tag{43}$$

Meaning that the solution of the satellite dynamics is a curve $\phi(t;\boldsymbol{x}_0)$ in $\mathbb{R}^6$, such that its velocity is tangent to the vector $\boldsymbol{F}$ when moving along that curve.
Since $\phi(t;\boldsymbol{x}_0)$ can describe the motion of a fluid particle, it is also referred as "flow map". A generic trajectory that depart near the reference trajectory will evolve with a displacement given by:

$$\delta\boldsymbol{x}(t) = \phi(t, \boldsymbol{x}_0 + \delta\boldsymbol{x}_0) - \phi(t, \boldsymbol{x}_0) \quad , \quad \delta\boldsymbol{x}_0 = \delta\boldsymbol{x}(t_0) \tag{44}$$

If we linearized the first term we get:

$$\delta\boldsymbol{x}(t) = \frac{\partial\phi}{\partial\boldsymbol{x_0}}(t, \boldsymbol{x_0})\delta\boldsymbol{x}_0 = \boldsymbol{\Phi}(t, t_0)\delta\boldsymbol{x}_0 \tag{45}$$

Eq.(45) is the solution of Eq.(40), $\boldsymbol{\Phi}(t, t_0)$ is a 6×6 matrix called state transition matrix and relates the small displacement at $t = t_0$ with a generic one at $t > t_0$ with the following elements:

$$\boldsymbol{\Phi}(t, t_0) = \begin{bmatrix} \frac{\partial x}{\partial x_0} & \frac{\partial x}{\partial y_0} & \frac{\partial x}{\partial z_0} & \frac{\partial x}{\partial \dot{x}_0} & \frac{\partial x}{\partial \dot{y}_0} & \frac{\partial x}{\partial \dot{z}_0} \\ \frac{\partial y}{\partial x_0} & \frac{\partial y}{\partial y_0} & \frac{\partial y}{\partial z_0} & \frac{\partial y}{\partial \dot{x}_0} & \frac{\partial y}{\partial \dot{y}_0} & \frac{\partial y}{\partial \dot{z}_0} \\ \frac{\partial z}{\partial x_0} & \frac{\partial z}{\partial y_0} & \frac{\partial z}{\partial z_0} & \frac{\partial z}{\partial \dot{x}_0} & \frac{\partial z}{\partial \dot{y}_0} & \frac{\partial z}{\partial \dot{z}_0} \\ \frac{\partial \dot{x}}{\partial x_0} & \frac{\partial \dot{x}}{\partial y_0} & \frac{\partial \dot{x}}{\partial z_0} & \frac{\partial \dot{x}}{\partial \dot{x}_0} & \frac{\partial \dot{x}}{\partial \dot{y}_0} & \frac{\partial \dot{x}}{\partial \dot{z}_0} \\ \frac{\partial \dot{y}}{\partial x_0} & \frac{\partial \dot{y}}{\partial y_0} & \frac{\partial \dot{y}}{\partial z_0} & \frac{\partial \dot{y}}{\partial \dot{x}_0} & \frac{\partial \dot{y}}{\partial \dot{y}_0} & \frac{\partial \dot{y}}{\partial \dot{z}_0} \\ \frac{\partial \dot{z}}{\partial x_0} & \frac{\partial \dot{z}}{\partial y_0} & \frac{\partial \dot{z}}{\partial z_0} & \frac{\partial \dot{z}}{\partial \dot{x}_0} & \frac{\partial \dot{z}}{\partial \dot{y}_0} & \frac{\partial \dot{z}}{\partial \dot{z}_0} \end{bmatrix} \tag{46}$$

Taking the derivative of Eq.(45) and using Eq.(40) we can obtain the time evolution of the state transition matrix:

$$\frac{d}{dt}\boldsymbol{\Phi}(t, t_0) = \boldsymbol{A}(t)\boldsymbol{\Phi}(t, t_0) \quad \text{with} \quad \boldsymbol{\Phi}(t_0, t_0) = \boldsymbol{I} \tag{47}$$

Note that, deviation from the nominal trajectory can be obtained considering also small time variations δt at t so that:

$$\delta\boldsymbol{x}(t) = \phi(t + \delta t, \boldsymbol{x}_0 + \delta\boldsymbol{x}_0) - \phi(t, \boldsymbol{x}_0) \tag{48}$$

And the resulting linearized equation will be:

$$\delta\boldsymbol{x}(t) = \frac{\partial\phi}{\partial\boldsymbol{x_0}}(t, \boldsymbol{x_0})\delta\boldsymbol{x}_0 + \frac{\partial\phi}{\partial t}(t, \boldsymbol{x_0})\delta t = \boldsymbol{\Phi}(t, t_0)\delta\boldsymbol{x}_0 + \boldsymbol{F}(\boldsymbol{x}_0)\delta t \tag{49}$$

2.2.5 Equilibrium points and stability analysis

It is interesting to understand if there exist equilibrium points of the restricted three body problem, where a particle is at rest in the synodic frame, to do so, setting null velocity and acceleration in Eq.(27) we get the usual condition:

$$\frac{\partial U}{\partial x}(x,y,z) = x - \left(\mu_1 \frac{x+\mu_2}{r_1^3} + \mu_2 \frac{x-\mu_1}{r_2^3}\right) = 0 \tag{50a}$$

$$\frac{\partial U}{\partial y}(x,y,z) = y - \left(\frac{\mu_1}{r_1^3} + \frac{\mu_2}{r_2^3}\right) y = 0 \tag{50b}$$

$$\frac{\partial U}{\partial z}(x,y,z) = -\left(\frac{\mu_1}{r_1^3} + \frac{\mu_2}{r_2^3}\right) z = 0 \tag{50c}$$

That states the equilibrium about the apparent centrifugal force and the gravitational forces, without considering Coriolis force because the particle is stationary in the rotating frame.
From Eq.(50c) we note that this is satisfy only if $z = 0$ and this means that the set of all equilibrium points must lie in the plane of the primaries, this is not surprising since the centrifugal force acts only in this plane and the gravitational forces cannot be balanced in this direction.
A quick analysis of Eq.(50a) and Eq.(50b) shown that a possible solution is given imposing $r_1 = r_2 = 1$, in this case we have 2 equilibrium points where both forms an equilateral triangle with the primaries, their position, in normalized coordinates, is given by:

$$x = \frac{1}{2} - \mu_2 \quad \text{and} \quad y = \pm\frac{\sqrt{3}}{2} \tag{51}$$

These are called triangular equilibrium points and are indicated as L_4 and L_5, a satellite placed in one of this point at rest would be subjected to a centrifugal force, direct toward the center of mass, which is balanced by the gravitational forces of μ_1 and μ_2.
Other possible equilibrium points must be in the x-axis where all the forces are aligned, setting $y = 0$, Eq.(50b) is automatically satisfied, while Eq.(50a) becomes:

$$\frac{\partial U}{\partial x}(x,0,0) = x - \left(\mu_1 \frac{x+\mu_2}{|x+\mu_2|^3} + \mu_2 \frac{x-\mu_1}{|x-\mu_1|^3}\right) = 0 \tag{52}$$

Solution of Eq.(52) can't be written exactly since is quite complicated, anyway we can study it and it is possible to shown that there are other three equilibrium points indicated as L_1, L_2 and L_3 called collinear points, obtained depending on the different sign chosen, their approximated position can be found in the appendix.

- The point L_1 is placed between the primaries, in this case we have $(x+\mu_2) > 0$ and $(x-\mu_1) < 0$, a spacecraft put in this point can be used for a continuous monitor

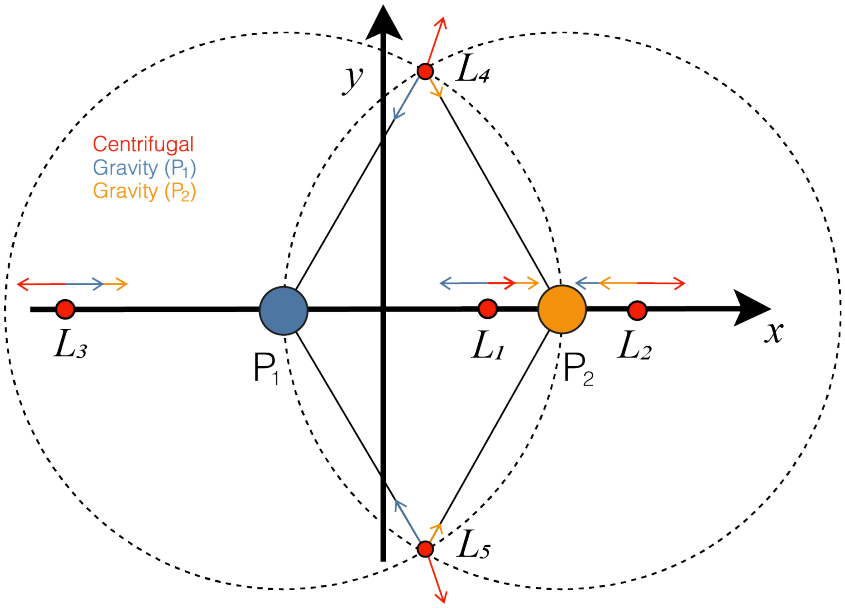

Figure 3: Lagrangian points position, adapted from [16]

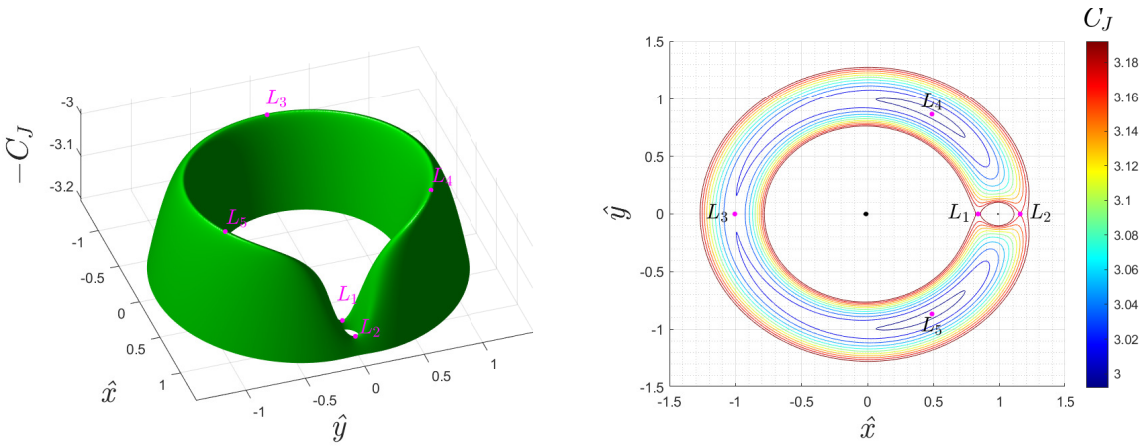

Figure 4: Plot of the Jacobi constant surface on the plane (left) and its associated contour levels (right)

of M_1 or M_2, considering the Sun-Earth system, L_1 it is useful for a continuous monitor of the Sun like the SOHO mission (see [17]).

- The point L_2 lies behind the smaller primary, μ_2 with $x + \mu_2 > 0$ and $x - \mu_1 > 0$ and in general can be used as a deep space observation mission like the James Webb Space Telescope (see [18]).

- The point L_3 lies behind the bigger primary, μ_1 with $x + \mu_2 < 0$ and $x - \mu_1 < 0$ and can be used for deep space observation or for monitoring the Sun, anyway this is not an interesting point since it is situated far away from the Earth and has an energy higher with respect to the other two collinear point meaning that more fuel consumption is needed to reach it.

In total we have five equilibrium points, as we can see in *Figure 3* and *Figure 4*, where forces are balanced.
If we rearrange Eq.(52) we obtain a quintic, a polynomial of 5-th degree of the form:

$$ax^5 + bx^4 + cx^3 + dx^2 + ex + f = 0 \tag{53}$$

Where the coefficients a, b, c, d, e, f depend on the collinear point considered.
Even if a spacecraft is placed in a equilibrium point, perturbations due to an-modeled dynamic are present so a stability analysis must be carried out.
To do so we apply a small disturb of the equilibrium state in order to study the deviation $\delta\boldsymbol{x}(t) = (X, Y, Z, \dot{X}, \dot{Y}, \dot{Z})$ of the resulting dynamics respect to the steady solution trajectory.
We note that the study of a neighborhood trajectory respect to a nominal one is already study in Section 2.2.4, where we have obtained the variational equation describing the time evolution of the displacement between the two close generic trajectories.
If we apply Eq.(40) in our case with $\bar{\boldsymbol{x}}(t) = (x_0, y_0, 0, 0, 0, 0)^T$ and setting $\delta\boldsymbol{x}(t) = (X, Y, Z, \dot{X}, \dot{Y}, \dot{Z}) = \boldsymbol{X}(t)$ the displacement of the satellite with respect to an equilibrium point, we get:

$$\dot{\boldsymbol{X}}(t) \approx \begin{bmatrix} 0 & 0 & 0 & 1 & 0 & 0 \\ 0 & 0 & 0 & 0 & 1 & 0 \\ 0 & 0 & 0 & 0 & 0 & 1 \\ U^0_{xx} & U^0_{xy} & U^0_{xz} & 0 & 2 & 0 \\ U^0_{yx} & U^0_{yy} & U^0_{yz} & -2 & 0 & 0 \\ U^0_{zx} & U^0_{zy} & U^0_{zz} & 0 & 0 & 0 \end{bmatrix} \boldsymbol{X}(t) = \boldsymbol{A}\boldsymbol{X}(t) \tag{54}$$

Where **A** is obtained evaluating the jacobian at the stationary equilibrium point and thus is independent on time.
We note that from Eq.(42e) and Eq.(42f), $U^0_{zx} = U^0_{zy} = 0$ for all equilibrium points, mining that the motion along the z direction is decoupled from the motion on the plane.
The general solution of Eq.(54) is well know and can be written in the form:

$$\boldsymbol{x} = \boldsymbol{v}e^{\lambda t} \tag{55}$$

where λ is called eigenvalue while $\boldsymbol{v}$ is a six dimensional vector, in our case, which is the associated eigenvector.
If we look to Eq.(55) we note that in order to have stability the only condition is that the real part of the eigenvalue is non-positive since in that situation the amplitude $\boldsymbol{v}$ will decrease exponentially if $Re(\lambda) < 0$ while it will be bounded if λ is pure imaginary.
Returning to our problem, restricting our analysis on the state Z we get:

$$\begin{pmatrix} \dot{Z} \\ \ddot{Z} \end{pmatrix} = \begin{bmatrix} 0 & 1 \\ U_{zz}^0 & 0 \end{bmatrix} \begin{pmatrix} Z \\ \dot{Z} \end{pmatrix} \tag{56}$$

The first equation is trivially satisfied while the second equation becomes:

$$\ddot{Z} - U_{zz}^0 Z = 0 \tag{57}$$

Substituting the general solution of Eq.(55), where $\boldsymbol{v} = \gamma_0$ is a scalar since we are looking only to the position state, we obtain:

$$(-\lambda^2 - U_{zz})\gamma_0 e^{\lambda t} = 0 \tag{58}$$

With $U_{zz}^0 = -(\frac{\mu_1}{(r_1)_0^3} + \frac{\mu_2}{(r_2)_0^3}) < 0$.
That is, in the z direction, the system has two pure imaginary eigenvalues $\lambda = \pm i\sqrt{|U_{zz}|}$ and therefore two distinct eigenvectors, the general solution is an harmonic oscillation with frequency given by $\omega_z = \sqrt{|U_{zz}|}$, also called natural frequency:

$$z(t) = \gamma_1 \cos(\omega_z t) + \gamma_2 \sin(\omega_z t) = \gamma \cos(\omega_z t + \phi_0) \tag{59a}$$

$$\text{with:} \quad z(0) = z_0 \quad , \quad \dot{z}(0) = \dot{z}_0 \tag{59b}$$

Where γ_1 and γ_2 or, equivalently, γ and ϕ_0 are constant determined from the initial conditions. For now on, since we have proved the stability in the out of plane motion, we focus in the stability motion on the plane.
In order to study the stability on the $x - y$ plane we start to eliminate the dependency of Z and $\dot{Z}$ in the linearized motion:

$$\frac{d\boldsymbol{X}}{dt} = \begin{pmatrix} \dot{X} \\ \dot{Y} \\ \ddot{X} \\ \ddot{Y} \end{pmatrix} = \begin{bmatrix} 0 & 0 & 1 & 0 \\ 0 & 0 & 0 & 1 \\ U_{xx}^0 & U_{xy}^0 & 0 & 2 \\ U_{xy}^0 & U_{yy}^0 & -2 & 0 \end{bmatrix} \begin{pmatrix} X \\ Y \\ \dot{X} \\ \dot{Y} \end{pmatrix} = \hat{\boldsymbol{A}}\boldsymbol{X} \tag{60}$$

Substituting the generic solution in Eq.(55) we obtain:

$$\hat{\boldsymbol{A}}\boldsymbol{v} = \lambda \boldsymbol{v} \tag{61}$$

Eq.(61) is how eigenvalue and eigenvector are defined from linear algebra.
If $\hat{\boldsymbol{A}}$ is thought of as a transformation matrix, the result of applying $\hat{\boldsymbol{A}}$ to the eigenvector $\boldsymbol{v}$ that satisfy Eq.(61) is to produce a vector in the same direction of $\boldsymbol{v}$ but with a different magnitude.

Even if we have obtained already the solution in the z-motion, in order to study the stability of the system an analysis of only the eigenvalues λ must be considered, a full derivation of the solution will be discussed in Section 2.2.7.
Eq.(61) can be written as an homogeneous system in the form:

$$(\hat{\boldsymbol{A}} - \lambda \boldsymbol{I})\boldsymbol{v} = 0 \tag{62}$$

Where $\boldsymbol{I}$ is the identity matrix.
Forcing the system to have non-trivial solution, $\boldsymbol{v} \neq \boldsymbol{0}$, we have:

$$det(\hat{\boldsymbol{A}} - \lambda \boldsymbol{I}) = 0 \tag{63}$$

Computing the determinant we obtain the following polynomial:

$$\lambda^4 + (4 - U^0_{xx} - U^0_{yy})\lambda^2 + U^0_{xx}U^0_{yy} - {U^0_{xy}}^2 = 0 \tag{64}$$

This is a quartic in the variable λ but also biquadratic in λ^2 with roots:

$$\lambda_{1,2} = \pm \left[\frac{1}{2}(U^0_{xx} + U^0_{yy} - 4) - \frac{1}{2}[(4 - U^0_{xx} - U^0_{yy})^2 - 4({U^0_{xx}U^0_{yy} - {U^0_{xy}}^2})^{\frac{1}{2}}]^{\frac{1}{2}} \right] \tag{65a}$$

$$\lambda_{3,4} = \pm \left[\frac{1}{2}(U^0_{xx} + U^0_{yy} - 4) + \frac{1}{2}[(4 - U^0_{xx} - U^0_{yy})^2 - 4({U^0_{xx}U^0_{yy} - {U^0_{xy}}^2})^{\frac{1}{2}}]^{\frac{1}{2}} \right] \tag{65b}$$

Note that in this case we have four different eigenvalues-eigenvectors pair, the analysis of stability doesn't change, in order to have stability all the eigenvalues must be with negative real part or pure imaginary, otherwise, if this is not verified, the system is unstable.
Now we can analyze the stability of each equilibrium point.

Collinear points In this case we have $y_0 = 0$, $(r_1^2)^0 = (x_0 + \mu_2)^2$, $(r_2^2)^0 = (x_0 - \mu_1)^2$ and hence:

$$U^0_{xx} = 1 + 2\bar{A} \quad , \quad U^0_{xx} = 1 - \bar{A} \quad , \quad U^0_{xy} = 0 \tag{66}$$

Where:

$$\bar{A} = \frac{\mu_1}{(r_1^3)^0} + \frac{\mu_2}{(r_2^3)^0} \tag{67}$$

Making the substitution $\beta = \lambda^2$ Eq.(64) becomes:

$$\beta^2 + (2 - \bar{A})\beta + (1 + \bar{A} - 2\bar{A}^2) = 0 \tag{68}$$

Eq.(68) is a quadratic function, in order to investigate its roots we use the Cartan rule. The equation has real solution since the discriminant $\Delta = 9\bar{A}^2 \geq 0$ moreover since we want negative solutions, that would generate imaginary stable eigenvalues, we require the coefficients to be positive:

$$\begin{cases} (2 - \bar{A}) > 0 \\ (1 + \bar{A} - 2\bar{A}^2) > 0 \end{cases} \tag{69}$$

This means that in order to be stable we need to have $-\frac{1}{2} < \bar{A} < 1$.
However if we compute $\bar{A}$ substituting the corresponding values of r_1^0 and r_2^0 for each collinear point we obtain that $\bar{A} > 1$ (given that $\mu_2 < \frac{1}{2}$), this indicate that the system has a positive eigenvalues so that small displacement around L_1, L_2 and L_3 will growth. Therefore we conclude that the collinear points are always unstable.

Triangular points In this case we have $r_1 = r_2 = 1$, $x = \frac{1}{2} - \mu_2$ and $y = \pm\frac{\sqrt{3}}{2}$ and so:

$$U_{xx}^0 = \frac{3}{4} \quad , \quad U_{xx}^0 = \frac{9}{4} \quad , \quad U_{xy}^0 = \pm 3\sqrt{3}\frac{(1 - 2\mu_2)}{4} \tag{70}$$

The characteristic equation becomes:

$$\lambda^4 + \lambda^2 + \frac{27}{4}\mu_2(1 - \mu_2) = 0 \tag{71}$$

And Eq.(65) reduce to:

$$\lambda_{1,2} = \pm\frac{\sqrt{-1 - \sqrt{1 - 27(1 - \mu_2)\mu_2}}}{\sqrt{2}} \tag{72a}$$

$$\lambda_{3,4} = \pm\frac{\sqrt{-1 + \sqrt{1 - 27(1 - \mu_2)\mu_2}}}{\sqrt{2}} \tag{72b}$$

Since $1-27(1-\mu_2)\mu_2 < 1$, $\lambda_{3,4}$ is always complex while in order to obtain pure imaginary solution also for $\lambda_{1,2}$, we need to have:

$$1 - 27(1 - \mu_2)\mu_2 \geq 0 \tag{73}$$

This implies that condition for stability reduces to:

$$\mu_2 \leq \frac{27 - \sqrt{621}}{54} \approx 0.0385 = \bar{\mu} \tag{74}$$

At the end we have that the collinear points are always unstable, this feature seams a disadvantage but in reality is a very useful property in order to construct low energy transfer since with a small maneuver the satellite can escape easily from these points while triangular points can have stable behaviour. Putting some numbers we see that within our system, each planet with the Sun have $\mu_2 < \bar{\mu}$ and therefore have the triangular points stable, this means that in such points asteroids belts can be found.

2.2.6 Zero velocity surfaces

If we look at Eq.(37) we see that as the spacecraft move far away from the center of mass of the primaries, its potential energy U increases and, accordingly, the kinetic energy decrease in order to maintain C_J constant. However, at a certain point where the spacecraft reach a condition where its kinetic energy is zero and the potential energy reach its maximum, if the spacecraft would move away after this point it would have a negative kinetic energy which is unfeasible, if we set $T = 0$ we get:

$$C_J = 2U \tag{75}$$

This equation defines different surfaces in space, according to the value of C_J, called zero-velocity surfaces that define regions where the motion can happen due to only energy considerations, the feasible regions are the accessible regions where the kinetic energy is positive:

$$C_J \geq 2U \tag{76}$$

It is possible to show how those surfaces evolve changing the values of C_J, in order to do that we compute the Jacobi constant at each equilibrium point, since they define limiting cases of accessible/forbidden regions. Substituting the position of L_1, L_2, L_3, L_4 and L_5 in Eq.(75) we get the zero surface associated to each equilibrium point, *Table 1* summarize the value of C_J of such a points in the Earth-Moon system.

Table 1: Values of C_j for each Lagrangian points in the Earth-Moon system

	L_1	L_2	L_3	L_4	L_5
C_J	3.188373	3.172188	3.012151	2.987994	2.987994

In *Figure 5* are analyzed the accessible and forbidden regions varying the Jacobi constant obtaining the following possible cases:

- For Values of $C_J \geq C_J^{L_1}$, the system is divided in 3 different accessible realm: the realm in proximity of each primaries and a region outside the system. In this case the regions can't communicate since the energy level is too small, a spacecraft put in each one of this zones remain there without moving to other possible realm since it would cross the forbidden regions.

- For values of $C_J^{L_2} \leq C_J \leq C_J^{L_1}$ the two realms around the primaries opens and a spacecraft can move from one body to another, this energy range is suitable for mission toward the Moon like the Apollo mission.

- If $C_J^{L_3} \leq C_J \leq C_J^{L_2}$ we are in a condition where the satellite has enough energy to move also outside the system of primaries.

- when $C_J^{L_4} \leq C_J \leq C_J^{L_3}$ the accessible region growth, the zero velocity surfaces moves away from the $x - y$ plane so that when $C_J = C_J^{L_4} = C_J^{L_5}$ the satellite is free to move in this plane even if there are still regions in the space where motion is not allowed.

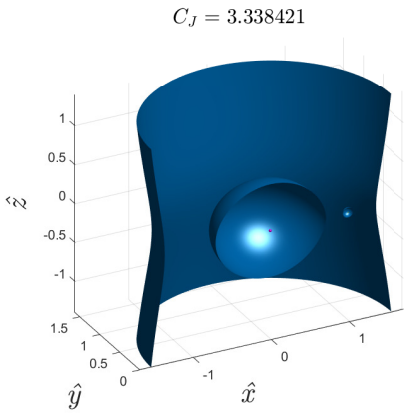

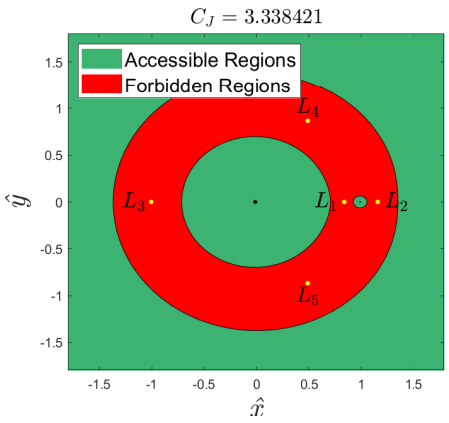

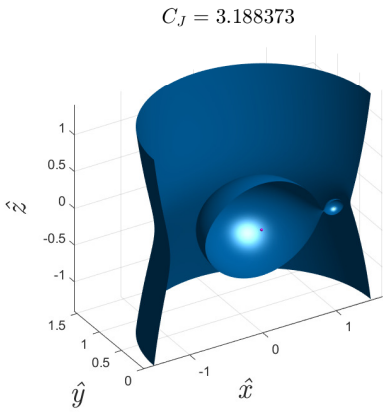

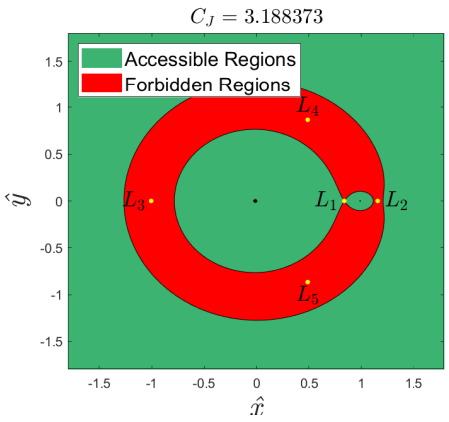

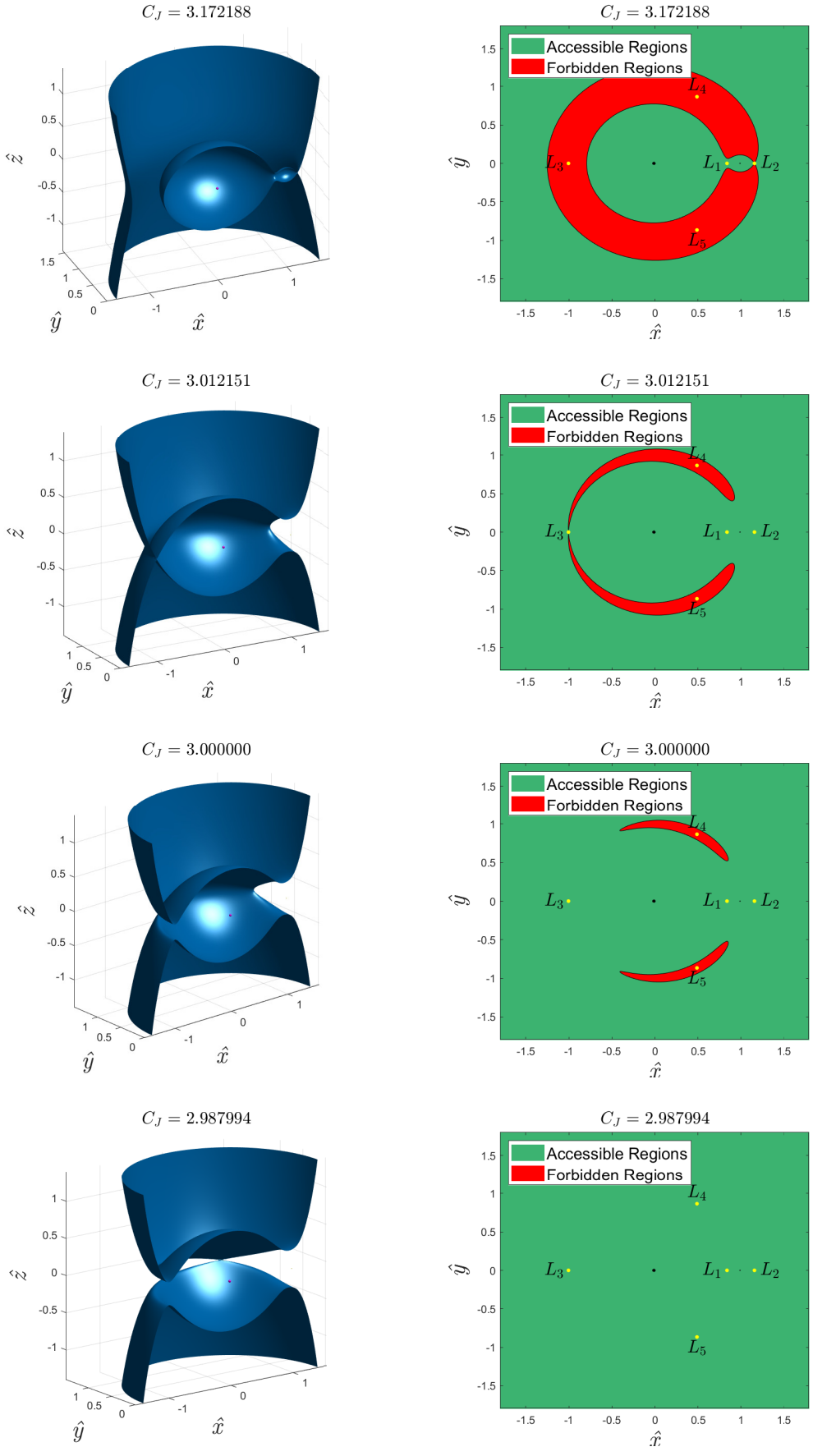

Figure 5: Zero velocity surfaces (left) and zero velocity curves in the plane (right) that highlight accessible and forbidden regions for different values of C_J

2.2.7 Linear solutions around Lagrange points

Since we have four different eigenvectors, the general linear solution is written, by superposition, as a linear combination of such a solutions:

$$X = \sum_{j=1}^{4} \alpha_j e^{\lambda_j t} \tag{77a}$$

$$Y = \sum_{j=1}^{4} \beta_j e^{\lambda_j t} \tag{77b}$$

$$\dot{X} = \sum_{j=1}^{4} \alpha_j \lambda_j e^{\lambda_j t} \tag{77c}$$

$$\dot{Y} = \sum_{j=1}^{4} \beta_j \lambda_j e^{\lambda_j t} \tag{77d}$$

$$Z = \gamma e^{\omega t} \tag{77e}$$

$$\dot{Z} = \gamma \omega e^{\omega t} \tag{77f}$$

Where α_j and β_j are, in general, complex.
We have already seen the solution in the Z-direction which is an harmonic undamped oscillation with solution given by:

$$z(t) = \gamma \cos(\omega t + \phi_0) \tag{78a}$$

$$\dot{z}(t) = -\omega\gamma \sin(\omega t + \phi_0) \tag{78b}$$

$$z(0) = z_0 \quad , \quad \dot{z}(0) = \dot{z}_0 \tag{78c}$$

In order to find also the solution in the $x - y$ plane, we compute the eigenvectors, substituting the expression of X, Y, $\dot{X}$ and $\dot{Y}$ in one of the last two equations of Eq.(60) (since they are linear dependent they express the same thing), we obtain the following relationship between α_j and β_j:

$$(\alpha_j \lambda_j^2 - 2\beta_j \lambda_j - U_{xx}\alpha_j - U_{xy}\beta_j)e^{\lambda_j t} = 0 \quad , \quad \forall j = 1, ..., 4 \tag{79}$$

Therefore:

$$\beta_j(\alpha_j) = \frac{\lambda_j^2 - U_{xx}}{2\lambda_j + U_{xy}}\alpha_j \tag{80}$$

So that the generic eigenvector $\boldsymbol{v}$ can be expressed in the form $\boldsymbol{v}_j = (\alpha_j, \beta_j(\alpha_j), \lambda_j\alpha_j, \lambda_j\beta_j(\alpha_j))^T$
Where α's can be computed from the initial condition at $t = t_0 = 0$:

$$\sum_{j=1}^{4} \alpha_j = X_0 \quad , \quad \sum_{j=1}^{4} \alpha_j \lambda_j = \dot{X}_0 \quad , \quad \sum_{j=1}^{4} \beta_j(\alpha_j) = Y_0 \quad , \quad \sum_{j=1}^{4} \beta_j(\alpha_j)\lambda_j = \dot{Y}_0 \tag{81}$$

Note that α_j is real if and only if λ_j is real.
The Eq.(77) represent the generic motion of a satellite around an equilibrium point. Althrougth the generic solution can contain unstable behaviour, it is possible to set initial conditions such that, the only eigenvalues excited by the system are only those related with pure imaginary eigenvalues related to oscillatory behaviour. In this particular condition periodic orbits around equilibrium points exist, note that the main difference with respect to the generic case is that we are removing part of the dynamics and therefore, given a certain position of the satellite along the orbit $\boldsymbol{X}(t)$, there is only one velocity vector $\boldsymbol{V}(t)$ that satisfy the motion, this means that the initial conditions are only defined in terms of position.
Here we can summarize the different possibilities of the motion of a satellite where we supposed $\mu_2 \leq \bar{\mu}$.

- **Saddle motion:** Is the solution that contains the unstable and asymptotic stable behaviour, it can be obtained for L_1, L_2 and L_3, having $Z(t) = 0$.
  The solution is written in the form:

$$\begin{pmatrix} X(t) \\ Y(t) \end{pmatrix} = \begin{bmatrix} \alpha_1 \\ \beta_1(\alpha_1) \end{bmatrix} e^{\lambda_1 t} + \begin{bmatrix} \alpha_2 \\ \beta_2(\alpha_2) \end{bmatrix} e^{\lambda_2 t} = \boldsymbol{a} e^{\lambda_1 t} + \boldsymbol{b} e^{\lambda_2 t} \tag{82}$$

  Where λ_1 and λ_2 are real and with different sign.
  In this case the motion is an hyperbolic motion in which the direction of the two asymptote are given by $\boldsymbol{a}$ and $\boldsymbol{b}$ that are the direction where the satellite leaves the point faster (unstable direction) or the direction where the satellite approach the equilibrium point asymptotically (stable direction).

- **Lissajous orbits:** Are quasi period orbits obtained eliminating the saddle motion from the general solution, in this case only two pure imaginary eigenvalues $\lambda_{1,2} = \pm i\omega_p$ in the plane are present:

$$\begin{pmatrix} X(t) \\ Y(t) \end{pmatrix} = \begin{bmatrix} \alpha_1 \\ \beta_1(\alpha_1) \end{bmatrix} e^{\lambda_1 t} + \begin{bmatrix} \alpha_2 \\ \beta_2(\alpha_2) \end{bmatrix} e^{\lambda_2 t} = \boldsymbol{a} e^{\lambda_1 t} + \boldsymbol{b} e^{\lambda_2 t} \quad , \quad Z(t) = \gamma_1 e^{i\omega_z t} + \gamma_2 e^{-i\omega_z t} \tag{83}$$

  Since we have $\omega_p \neq \omega_z$ the orbit is called quasi periodic since it is not closed oscillating in the z-direction with a frequency different from that of the plane as

we can seen in *Figure 6*.

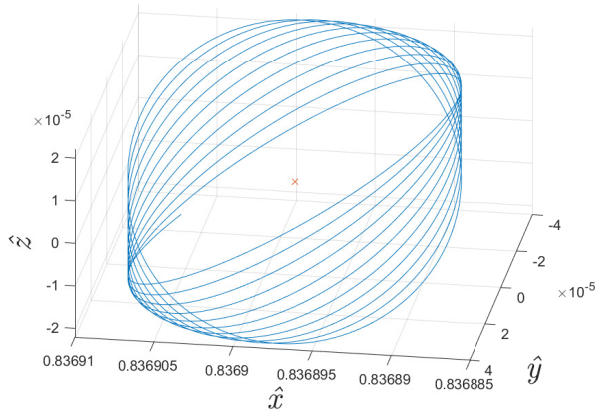

Figure 6: Lissajous orbit

- **Lyapunov orbits:** Are 2-D orbits obtained from Lissajous orbits setting $Z(t) = 0$, Eq.(83) becomes:

$$\begin{pmatrix} X(t) \\ Y(t) \end{pmatrix} = \begin{bmatrix} \alpha_1 \\ \beta_1(\alpha_1) \end{bmatrix} e^{\lambda_1 t} + \begin{bmatrix} \alpha_2 \\ \beta_2(\alpha_2) \end{bmatrix} e^{\lambda_2 t} = \boldsymbol{a} e^{\lambda_1 t} + \boldsymbol{b} e^{\lambda_2 t} \tag{84}$$

Those are periodic orbits that can be obtained around each Lagrangian point, they are ellipses, as can be seen in *Figure 7*, and can be found in all Lagrangian points, the size of this ellipse is related to $\boldsymbol{a}$ and $\boldsymbol{b}$.

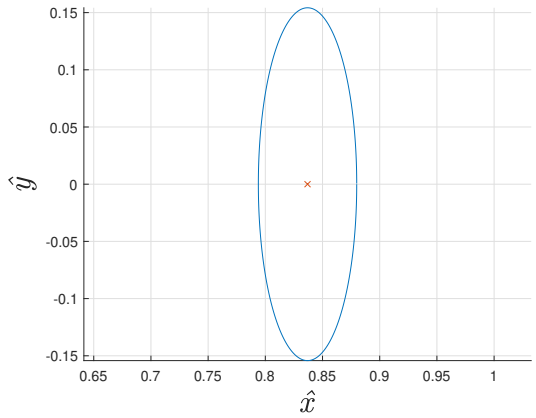

Figure 7: Lyapunov orbit

- **Trojan orbits:** Are particular orbits that exist only in L_4 and L_5 since they have 4 imaginary eigenvalues where are associated to two different frequencies ω_1 and

ω_2 such that $\lambda_{1,2} = \pm i\omega_1$ and $\lambda_{3,4} = \pm i\omega_2$, therefore the general solution in this case becomes:

$$\begin{pmatrix} X(t) \\ Y(t) \end{pmatrix} = \begin{bmatrix} \alpha_1 \\ \beta_1(\alpha_1) \end{bmatrix} e^{\lambda_1 t} + \begin{bmatrix} \alpha_2 \\ \beta_2(\alpha_2) \end{bmatrix} e^{\lambda_2 t} + \begin{bmatrix} \alpha_3 \\ \beta_3(\alpha_3) \end{bmatrix} e^{\lambda_3 t} + \begin{bmatrix} \alpha_4 \\ \beta_4(\alpha_4) \end{bmatrix} e^{\lambda_4 t} \tag{85}$$
$$= \boldsymbol{a} e^{\lambda_1 t} + \boldsymbol{b} e^{\lambda_2 t} + \boldsymbol{c} e^{\lambda_3 t} + \boldsymbol{d} e^{\lambda_4 t}$$

Figure 8 shown an example of those orbits note that the solution can be thought as a combination of two periodic motion.
Those orbits are common when dealing with asteroids belts inside our system, this because, as already mention, belts of asteroids orbiting in proximity of L_4 and L_5 can be found, those belts are also known as Trojan asteroids.

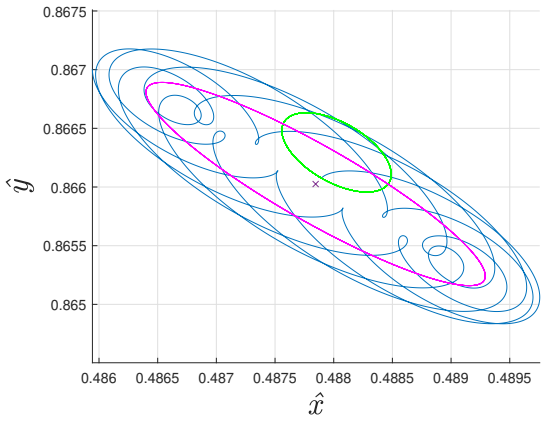

Figure 8: Trojan orbit

2.2.8 High order term orbits around Lagrangian points

In the previous section we have discussed the possible types of orbit around each equilibrium point, however those solutions are valid for small displacement respect to the stationary solution, in order to be able to search other possible orbits or the evolution of the previous orbits discussed, higher order terms must be considered.
First of all we note that no closed orbits in space exist in linear approximation since in general, $\omega_z \neq \omega_p$. However the in plane and out of plane frequencies are closed to each other in correspondence of the collinear points, therefore, if we consider higher order terms, the non-linearities alters the frequency of the linearized orbits so that, under particular constraints, $\omega_z = \omega_p$ and 3-D closed orbits, called Halo orbits, may exist (for more detail see the appendix).

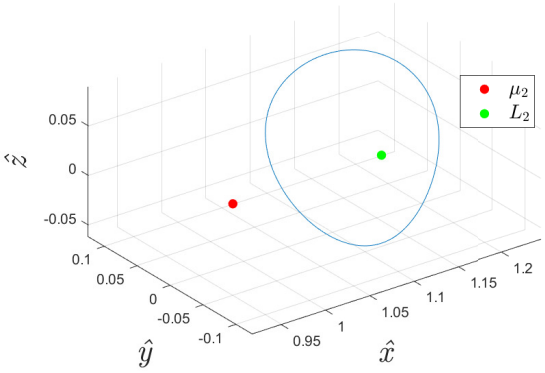

Figure 9: Halo orbit around L_2 in the Earth-Moon system

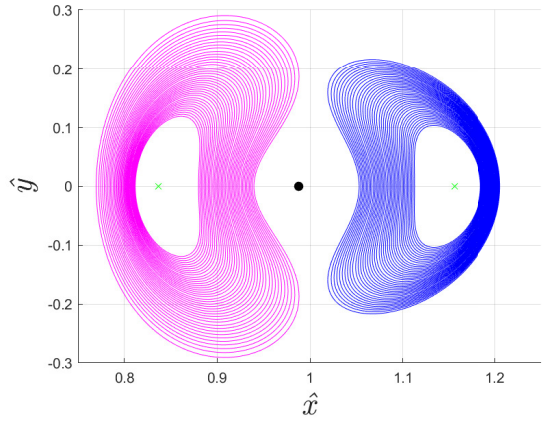

Figure 10: Lyapunov orbits around L_1 and L_2 in the Earth-Moon system

Note also that non linear term can also alters the preexisting orbits or introduce new kind of orbits, in *Figure 10* is reported the evolution of Lyapunov orbits increasing the distance from the equilibrium point, note how these orbits starts to deviate from the elliptical shape while in *Figure 11* is reported a tadpole and horseshoe orbits, special orbits obtained around triangular points, integrating the CRTBP for specific initial conditions.

2.3 Four body problem

Until now we have discussed the the motion under the three body problem approximation, that actually describe quite well the dynamics of the satellite in proximity of the primaries attraction.
However, it is possible that, during the flight, the spacecraft starts to go far away from the primaries or it remains around an equilibrium point for a long time so that perturbations due to other bodies start to become important, in those cases, a new dynamical model is needed, taking into account another body.

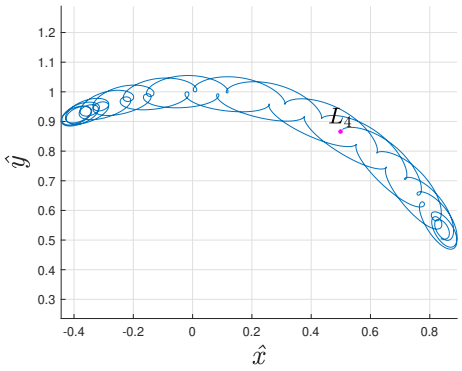

(a) Tadpole Orbit $\mu_2 = 0.001$, $X_0 = (x_0^{L_4} + 0.0065, y_0^{L_4} + 0.0065, 0, 0, 0, 0)$

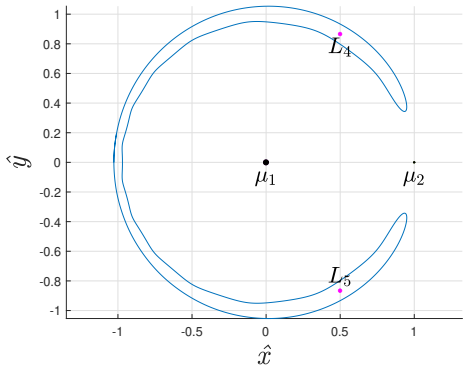

(b) Horseshoe Orbit $\mu_2 = 0.000953875$, $X_0 = (-1.02745, 0, 0, 0, 0.04032, 0)$

Figure 11: Example of Tadpole and Horseshoe orbits, from [15]

In our case, since we focus on the Earth-Moon system, the third primary that affect mainly the dynamics is the Sun, that dominate the motion of the spacecraft respect to the other planets due to its huge mass when moving toward the deep space.
As we have done with the three body problem we do some approximation regarding on the motion of the primaries so that, also in this case, the degree of freedom of the system are only six, related to the spacecraft.
The difference is that in the four body problem since the primaries are more than two, we can have two possible approximation about the motion of the primaries, indicating their masses as M_0, M_1 and M_2:

- **Concentric circular model**: In this case M_0 is the central body while M_1 and M_2 move on circular orbit around M_0, moreover the motion is assumed co-planar. This model is used for describing the dynamics of the Moons of a planet M_0 like Jupiter's moon and so on.

- **Bicircular model**: M_1 and M_2 are moving on circular orbits around their center of mass which is rotating in a circular orbit about the central body M_0. This model is also co-planar and is suitable, for example, in order to study the the motion of the Sun-Earth-Moon system.

In this thesis, we consider motion in the Earth-Moon system, where we neglect the inclination of the Moon with respect to the Sun-Earth system, therefore, the Bicircular model is adopted indicating the mass of the Sun, Earth and Moon as M_0, M_1 and M_2 respectively.

2.3.1 Equations of motion Bicircular model

Similarly with the circular restricted three body problem we can represent the problem in normalized coordinates in a rotating frame. However now we can have different possibilities to define those units since we can definite different rotating frame while the inertial frame $(O;\xi,\eta,\zeta)$ is considered centered in the fixed center of mass O of M_0 and M_1-M_2 barycenter.

Earth-Moon rotating frame The Earth-Moon rotating frame $(O';x,y,z)$ has the origin O' centered in the center of mass of the Earth-Moon system, the x-axis is taken aligned with M_1-M_2 and directed toward M_2, rotating rigidly with them. The z-axis is perpendicular to the plane coincident with the ζ-axis while the y-axis completes the frame, this choice is the same that we have seen in the restricted three body problem, note that in this case, the angular velocity of the rotating frame is $\boldsymbol{\omega} = (0,0,2.6644\times10^{-6})^T$ in the Earth-Moon system, obtained using Kepler's third law, which is unitary in normalized coordinate.
In order to write the equation of motion, first of all we consider again the general Eq.(23), the only difference is now that the center of mass of the Earth and Moon is moving, therefore:

$$\begin{aligned}\boldsymbol{a_{inertial}} &= \boldsymbol{a_{O'}} + \boldsymbol{a_{rel}} + 2\boldsymbol{\omega}\times\boldsymbol{v} + \boldsymbol{\omega}\times(\boldsymbol{\omega}\times\boldsymbol{r}) + \frac{d\boldsymbol{\omega}}{dt}\times\boldsymbol{r} = \\ &= \boldsymbol{a_{O'}} + \boldsymbol{a_{rel}} + 2\boldsymbol{\omega}\times\boldsymbol{v} + \boldsymbol{\omega}\times(\boldsymbol{\omega}\times\boldsymbol{r}) = \\ &= \boldsymbol{a_{O'}} + \boldsymbol{a_{rel}} + \boldsymbol{a_{Coriolis}} + \boldsymbol{a_{Centr.}}\end{aligned} \tag{86}$$

Multiplying by the mass m of the satellite and using again Newton's law, the dynamic of the particle becomes:

$$\boldsymbol{F}_{grav.} = m\boldsymbol{a_{O'}} + m\boldsymbol{a}_{rel} + \boldsymbol{F}_{Coriolis} + \boldsymbol{F}_{centr.} \tag{87}$$

Where here $\boldsymbol{F}_{grav.}$ takes into account also the gravitational interaction of the Sun.
If we now substitute each term and rearranging, we get:

$$\ddot{\hat{\boldsymbol{r}}} = -\frac{\mu_1}{\hat{r}_1^3}\hat{\boldsymbol{r}}_{\boldsymbol{1}} - \frac{\mu_2}{\hat{r}_2^3}\hat{\boldsymbol{r}}_{\boldsymbol{2}} - \frac{m_s}{\hat{r}_3^3}\hat{\boldsymbol{r}}_{\boldsymbol{3}} - 2\boldsymbol{\omega}\times\boldsymbol{v} - \boldsymbol{\omega}\times(\boldsymbol{\omega}\times\boldsymbol{r}) - \boldsymbol{a_{O'}} \tag{88}$$

The term $\boldsymbol{a_{O'}}$ is related to the acceleration of the Earth and Moon barycenter, since we supposed that O' moves on a circular orbit, in the barycenter O' should be applied a gravitational force that grants the centripetal acceleration needed in order to have a curved trajectory.
However this force is not present since O' is not a point mass in reality, what we can

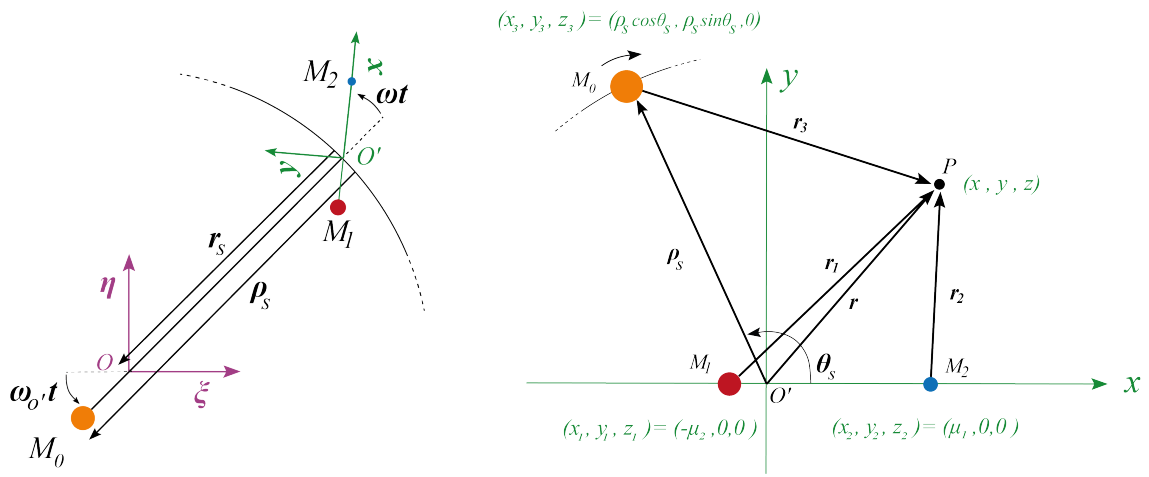

(a) Inertial view point **(b)** Rotating view point

Figure 12: Bicircular model in the Earth-Moon system

do is to assume that in the barycenter O' of M_1 and M_2 is concentrated the total mass $M_1 + M_2$, note that this approximations works well especially when $M_1 >> M_2$ like in our case.

Therefore, the acceleration of O' can be written in the following form:

$$\boldsymbol{a}_{\boldsymbol{O'}} = \frac{V_{O'}^2}{r_s}\boldsymbol{e}_r = \frac{m_s}{\rho_s^3}\boldsymbol{\rho}_s \tag{89}$$

Where $\boldsymbol{e}_r$ is the unit vector directed toward M_0, $V_{O'}$ the velocity of the barycenter while $\boldsymbol{r}_s = r_s\boldsymbol{e}_r$ and $\boldsymbol{\rho}_s = \rho_s\boldsymbol{e}_r$ represent the vector from O' to O and from O' and the Sun respectively.

In *Figure 12* is reported a schematic representation of the Bicircular model in the Earth-Moon reference frame, the angle θ_s is defined as the relative angle between the x-axis of the rotating frame and the Sun. The mass of the Sun is denoted as m_s, the position of the satellite with respect to the Sun is r_3.

Summarizing the different terms of Eq.(88) in the rotating-normalized frame are given by:

$$\boldsymbol{r}_s = (r_s\cos\theta_s, r_s\sin\theta_s, 0)^T \tag{90}$$

$$\boldsymbol{\rho}_s = (\rho_s\cos\theta_s, \rho_s\sin\theta_s, 0)^T \tag{91}$$

$$\boldsymbol{r}_3 = \boldsymbol{r} - \boldsymbol{\rho}_s = (x - \rho_s\cos\theta_s, y - \rho_s\sin\theta_s, z)^T \tag{92}$$

$$m_s = \frac{M_0}{M_1 + M_2} \approx 329006m^* \tag{93}$$

Where all distances are normalized with respect to the distance of M_1 and M_2 and the unit mass is $M_1 + M_2$ leaving the other parameters the same as the CRTBP.

Substituting Eq.(89) into Eq.(88) and using the above relations, we obtain:

$$\ddot{x} - 2\dot{y} - x = -\mu_1 \frac{x+\mu_2}{r_1^3} - \mu_2 \frac{x-\mu_1}{r_2^3} - m_s \frac{x-\rho_s \cos\theta_s}{r_3^3} - \frac{m_s}{\rho_s^3}\rho_s \cos\theta_s \tag{94a}$$

$$\ddot{y} + 2\dot{x} - y = -\frac{\mu_1}{r_1^3} y - \frac{\mu_2}{r_2^3} y - m_s \frac{y-\rho_s \sin\theta_s}{r_3^3} - \frac{m_s}{\rho_s^3}\rho_s \sin\theta_s \tag{94b}$$

$$\ddot{z} = -\left(\frac{\mu_1}{r_1^3} + \frac{\mu_2}{r_2^3} + \frac{m_s}{r_3^3}\right) z \tag{94c}$$

With:

$$\theta_s = \theta_s^0 + \dot{\theta}_s (t - t_0) \tag{95}$$

Where θ_s^0 is the initial angular position of the Sun while its angular rate $\dot{\theta}_s$ in the rotating frame, can be computed from the kinematics, expressing the relative velocity of the Sun with respect to O':

$$\boldsymbol{v}_s^{abs} = \boldsymbol{\omega}_{O'} \times (\boldsymbol{\rho_s} - \boldsymbol{r}_s) = \boldsymbol{v}_{O'} + \boldsymbol{v}_{rel} + \boldsymbol{\omega} \times \boldsymbol{\rho}_s \tag{96}$$

Therefore, since $\boldsymbol{v}_{O'} = \boldsymbol{\omega}_{O'} \times (-\boldsymbol{r}_s)$, substituting and rearranging we get:

$$\boldsymbol{v}_{rel} = (\boldsymbol{\omega}_{O'} - \boldsymbol{\omega}) \times \boldsymbol{\rho}_s = \dot{\boldsymbol{\theta}}_s \times \boldsymbol{\rho}_s \tag{97}$$

where in components, $\dot{\boldsymbol{\theta}}_s = (\boldsymbol{\omega}_{O'} - \boldsymbol{\omega}) = (0, 0, \dot{\theta}_s)^T$.
Putting some numbers, we can compute $\boldsymbol{\omega}_{O'}$ in normalized coordinates, setting in Eq.(14) the time of the period of O', we get its value in normalized time denoted as $T_{O'}$, so that:

$$\dot{\theta}_s = \omega_{O'} - \omega = \frac{2\pi}{T_{O'}} - 1 \approx -0.925287494370215 \frac{rad}{s^*} \tag{98}$$

Also in this case, Eq.(94) can be written defining a potential Ω defined as:

$$\Omega(x, y, z, \theta_s(t)) = U(x, y, z) + \frac{m_s}{r_3} - \frac{m_s}{\rho_s^2}(x \cos\theta_s + y \sin\theta_s) \tag{99}$$

So that the equations of motions become:

$$\ddot{x} - 2\dot{y} = \frac{\partial \Omega}{\partial x} \tag{100a}$$

$$\ddot{y} + 2\dot{x} = \frac{\partial \Omega}{\partial y} \tag{100b}$$

$$\ddot{z} = \frac{\partial \Omega}{\partial z} \tag{100c}$$

The Earth-Moon system is a reference in general used when modeling the motion in the Earth-Moon system when the spacecraft starts to go far away from the system, adding the presence of the sun that acts as a perturbation.

Sun-Earth rotating frame The rotating frame should has its origin coincident with the barycenter of M_0 and M_1, however, in this model, the equations of motion of the particle are not so simple, therefore we can assume that, since $M_0 \gg M_1 \gg M_2$ in our case, the two origin of the two frames are coincident, with this assumption the equations that we obtain are slightly different from Eq.(94) nevertheless give good results. If one insist to obtain exactly Eq.(94) in the Sun-Earth system, transformation of coordinate between the the two rotating frames is necessary.
Referring to *Figure 13*, most of the parameter are similar to those already defined in the CRTBP that we have already discuss, moreover, we denote with $\boldsymbol{R}_3$ the position of the mass M_2 while $\boldsymbol{r}_M$ the position of M_2 with respect to M_1 and $\boldsymbol{r}_3$ the position of P with respect to M_2.
With this choice is interesting to note that since $O \equiv O'$ and is fixed, $\boldsymbol{a}_{O'} = 0$ and therefore, as we will see, we retrieve a similar structure of equations of motion obtained in the CRTBP, the equation of motion becomes:

$$\ddot{\boldsymbol{r}} = -\frac{\mu_1}{r_1^3}\boldsymbol{r_1} - \frac{\mu_2}{r_2^3}\boldsymbol{r_2} - \frac{m_M}{r_3^3}\boldsymbol{r_3} - 2\boldsymbol{\omega} \times \boldsymbol{v} - \boldsymbol{\omega} \times (\boldsymbol{\omega} \times \boldsymbol{r}) \tag{101}$$

Where $\boldsymbol{r}_3$ is given by:

$$\boldsymbol{r}_3 = \boldsymbol{r} - \boldsymbol{R}_3 \tag{102}$$

In this case the angular velocity $\boldsymbol{\omega}$ of M_0 and M_1, is taken unitary with also its distance and the mass $M_0 + M_1$. The angular velocity of M_2, $\dot{\theta}_M$ relative to the rotating frame can be computed from kinematics, infect:

$$\boldsymbol{v}_M^{abs} = \boldsymbol{\omega} \times \boldsymbol{R}_2 + \boldsymbol{\omega}_M \times (\boldsymbol{R}_3 - \boldsymbol{R}_2) = \boldsymbol{v}_M^{rel} + \boldsymbol{\omega} \times \boldsymbol{R}_3 \tag{103}$$

Where $\boldsymbol{\omega}_M$ is the absolute angular velocity of M_2 around M_1 and:

$$\boldsymbol{R}_3 = \boldsymbol{R}_2 + \boldsymbol{r}_M = (\mu_1 + r_M \cos\theta_M, r_M \sin\theta_M, 0) \quad , \quad \theta_M = \dot{\theta}_M(t - t_0) + \theta_M^0 \tag{104}$$

Therefore Eq.(102) becomes:

$$\boldsymbol{v}_M^{rel} = (\boldsymbol{\omega}_M - \boldsymbol{\omega}) \times \boldsymbol{R}_3 = \boldsymbol{\omega}_{rel} \times \boldsymbol{R}_3 \tag{105}$$

With $\boldsymbol{\omega}_{rel} = (0, 0, \dot{\theta}_M)$.
Using again Eq.(14), substituting the period of M_2 around M_1 we get the period in nor-

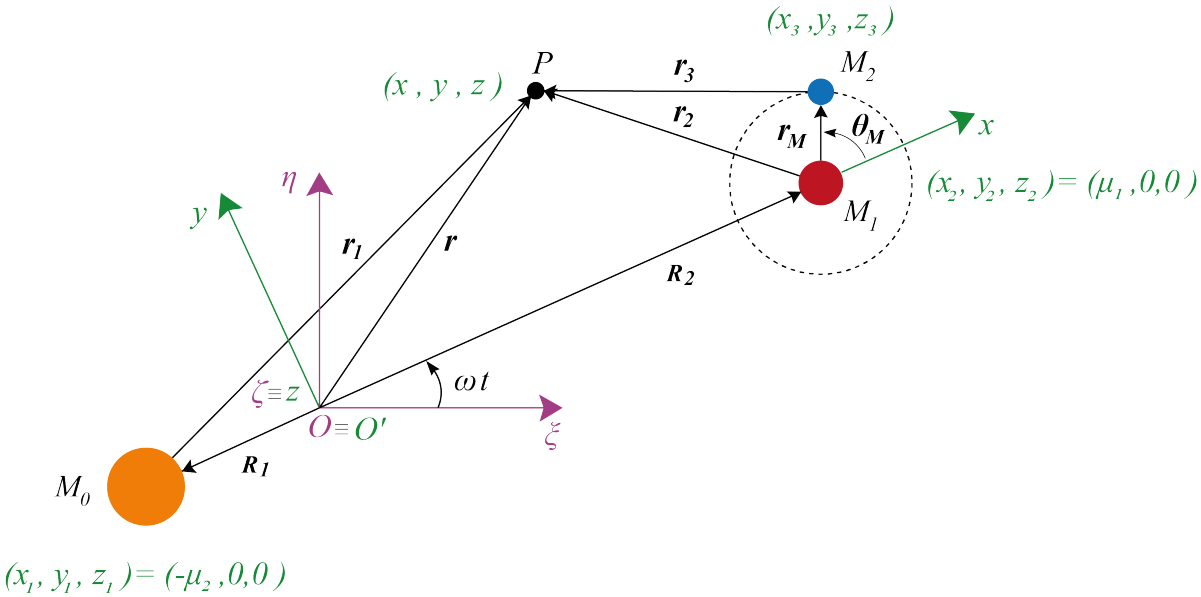

Figure 13: Sun-Earth reference system

malized time T_M, then:

$$\dot{\theta}_M = \omega_M - \omega = \frac{2\pi}{T_M} - 1 \approx 12.369326500732065 \frac{rad}{s^*} \tag{106}$$

Finally, the equations of motion can be written in scalar form as follow:

$$\ddot{x} - 2\dot{y} - x = -\mu_1 \frac{x + \mu_2}{r_1^3} - \mu_2 \frac{x - \mu_1}{r_2^3} - m_M \frac{x - \mu_1 - r_M \cos\theta_M}{r_3^3} \tag{107a}$$

$$\ddot{y} + 2\dot{x} - y = -\frac{\mu_1}{r_1^3} y - \frac{\mu_2}{r_2^3} y - m_M \frac{y - r_M \sin\theta_M}{r_3^3} \tag{107b}$$

$$\ddot{z} = -(\frac{\mu_1}{r_1^3} + \frac{\mu_2}{r_2^3} + \frac{m_M}{r_3^3}) z \tag{107c}$$

with:

$$m_M = \frac{M_2}{M_0 + M_1} \approx 3.6942 \times 10^{-8} m^* \tag{108}$$

Where also in this case, it is possible to introduce a potential Ω defined as:

$$\Omega(x, y, z, \theta_M(t)) = U(x, y, z) + \frac{m_M}{r_3} \tag{109}$$

So that we obtain the same structure of Eq.(100).
This model is in general used when modelling the motion of a particle in the Sun-Earth system taking into account the Moon as a perturbation.

As we can see, in both cases, the equation of motion that we obtain are $non-autonomous$ due to the time presence, moreover we note that the primaries M_0, M_1, M_2 move in a incoherent motion meaning that they don't satisfy Newton's equations since in reality, is not possible to have the three primaries that moves under the assumption of the Bi-circular model (the same happen in the concentric model), however the motion obtained gives very accurate results with respect to the real dynamics.

3 Low-Energy trajectory design

When considering a transfer between two bodies, an Hohmann transfer gives the lower limit of the propellant that must be used in order to transfer from one point to another one under the two-body problem assumption.
However, when considering more bodies, new transfer strategy arises so that, in particular conditions, the total amount of propellant can be significantly lower than an Hohmann transfer.
In this chapter we follow [3] to construct low energy trajectories based on the idea of manifold implemented in a CRTBP and then the idea of weak stability boundary is also presented using a formulation given in [1] and [2].

3.1 Construction of periodic orbits in the CRTBP

We have already see that third order, Richardson approximation is a very useful tool in order to construct periodic orbits when also non-linearities are considered.
However, taking the initial condition of such orbits and integrating the dynamics under the CRTBP leads to a non-closed orbits, as we can see in *Figure 14*, the integrated orbit follow the periodic orbit in the first half orbital period but then starts to diverge without return to the initial point, in order to face to this problem we need some preliminary considerations.

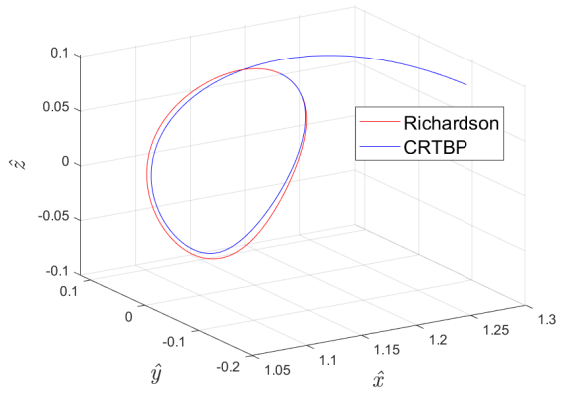

Figure 14: Comparison between Richarson and its propagated trajectory in the CRTBP

First of all we note that the CRTBP has symmetries, infect if we denote $(x, y, z, v_x, v_y, v_z, t)$ a generic solution of Eq.(27), if we making the following substitution:

$$(x, y, z, v_x, v_y, v_z, t) \rightarrow (x, -y, z, -v_x, v_y, -v_z, -t) \tag{110}$$

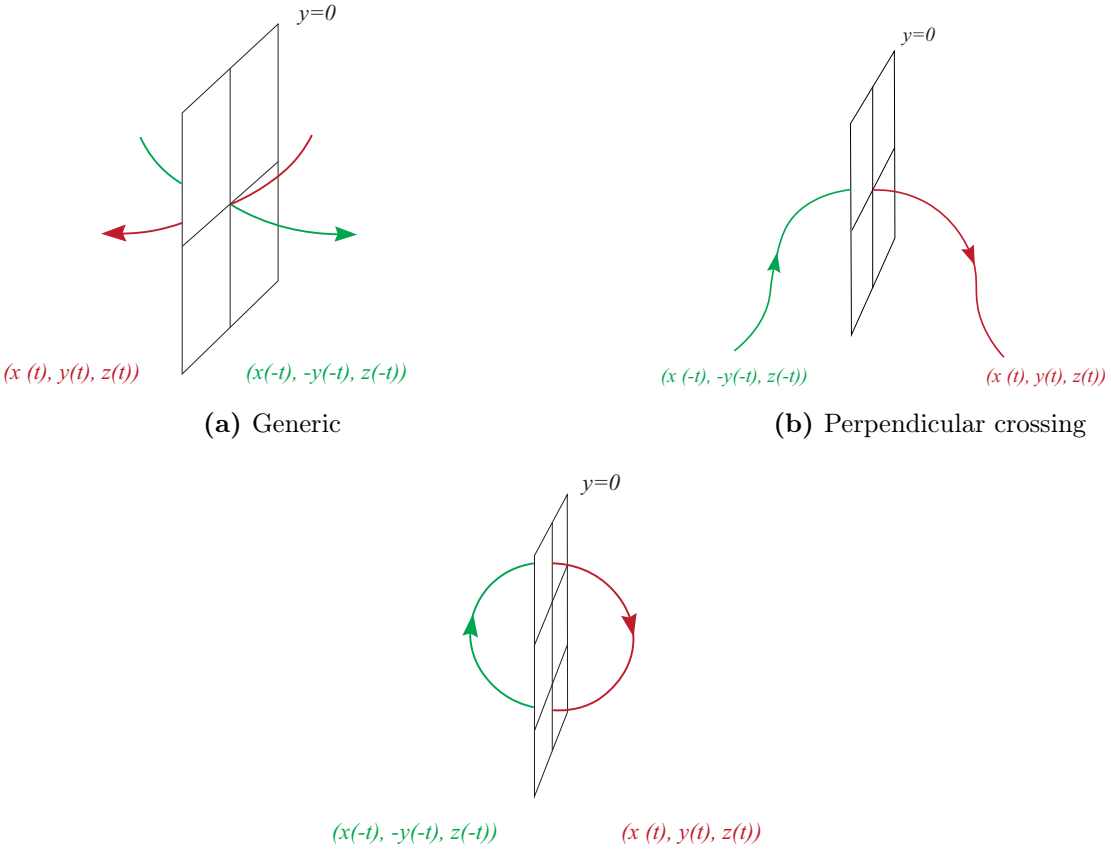

(a) Generic

(b) Perpendicular crossing

(c) Closed orbit

Figure 15: Symmetry property

we obtain that also $(x, -y, z, -v_x, v_y, -v_z, -t)$ is a solution that represents the mirrored trajectory respect to the $x-z$ plane but in this case the curve is traveled in the opposite direction as we can see in *Figure 15*a.

A closed orbit can be constructed using symmetries, if we take a trajectory, starting at p with a velocity perpendicular to the $x-z$ plane and applying Eq.110, we get that from a trajectory that flows forward from p, there exist another solution given by its mirrored image that flows toward p as in *Figure 15*b, the two trajectories are attached in p and they represent the same trajectory. However this is not sufficient to obtain a closed trajectory since also in the next crossing the velocity must be perpendicular to the plane $y = 0$ as in *Figure 15*c.

Thanks to this property, we can restrict our problem in analyze only half of the orbit, imposing to have the initial and final state in the following form:

$$\begin{aligned} \boldsymbol{x}_i &= \boldsymbol{x}(0) = (x^i, 0, z^i, 0, v_y^i, 0) \\ \boldsymbol{x}_f &= \boldsymbol{x}(T/2) = (x^f, 0, z^f, 0, v_y^f, 0) \end{aligned} \tag{111}$$

Starting from an Halo orbit and using an initial state at $y(t_0) = 0$ given by Richardson approximation, due to the higher non-linear term, the state after half orbit is of the form

$(x, \delta y, z, \delta v_x, v_y, \delta v_z)$ when integrated using the CRTBP (where with δ we denote a small value different from zero) and therefore, when integrated forward, the trajectory deviate from the nominal Halo obtaining an open trajectory. In order to drive the system to have a closed orbit, we apply a differential correction method.
The main idea behind the differential correction method is to change some free variables at the starting condition in order to obtain the desired final state.
To do so we apply Newton's method, let $\boldsymbol{X}$ the vector containing the free variables, at the initial state, that we have access in order to drive the system to the desired final target state $\boldsymbol{x}_T = (x^T, 0, z^T, 0, v_y^T, 0)$, given by:

$$\boldsymbol{X} = \begin{pmatrix} x^0 \\ z^0 \\ v_y^0 \\ t \end{pmatrix} \tag{112}$$

When integrating the trajectory the system must satisfy some constraints, in our case, related to the final state, $\boldsymbol{x}_f = (x^f, y^f, z^f, v_x^f, v_y^f, v_z^f)$, indicated as $\boldsymbol{C}(\boldsymbol{X}) = \boldsymbol{0}$, where:

$$\boldsymbol{C}(\boldsymbol{X}) = \begin{bmatrix} y^f - y^T \\ v_x^f - v_x^T \\ v_z^f - v_z^T \end{bmatrix} = \begin{bmatrix} y^f \\ v_x^f \\ v_z^f \end{bmatrix} = \boldsymbol{0} \tag{113}$$

Therefore the goal of our problem is to tune opportunely the free variables in order to satisfy Eq.(113). Due to the non-linearities, the solution is not obtained directly but through an iterative process, let $\boldsymbol{X}^j$ the j-th iteration of the free variables vector, expanding in Taylor series up to the first order $\boldsymbol{C}(\boldsymbol{X})$, we get:

$$\boldsymbol{C}(\boldsymbol{X}) \approx \boldsymbol{C}(\boldsymbol{X}^j) + \frac{\partial \boldsymbol{C}(\boldsymbol{X}^j)}{\partial \boldsymbol{X}^j}(\boldsymbol{X}^{j+1} - \boldsymbol{X}^j) = \boldsymbol{0} \tag{114}$$

Where $\frac{\partial \boldsymbol{C}(\boldsymbol{X}^j)}{\partial \boldsymbol{X}^j}$ is the Jacobian of the constrain vector, given by:

$$\frac{\partial \boldsymbol{C}(\boldsymbol{X})}{\partial \boldsymbol{X}} = \begin{bmatrix} \frac{\partial y^f}{\partial x^0} & \frac{\partial y^f}{\partial z^0} & \frac{\partial y^f}{\partial v_y^0} & \dot{y}^f \\ \frac{\partial v_x^f}{\partial x^0} & \frac{\partial v_x^f}{\partial z^0} & \frac{\partial v_x^f}{\partial v_y^0} & \dot{v}_x^f \\ \frac{\partial v_z^f}{\partial x^0} & \frac{\partial v_z^f}{\partial z^0} & \frac{\partial v_z^f}{\partial v_z^0} & \dot{v}_z^f \end{bmatrix} = \begin{pmatrix} \Phi_{21}(t_f, t_0) & \Phi_{23}(t_f, t_0) & \Phi_{25}(t_f, t_0) & \dot{y}^f \\ \Phi_{41}(t_f, t_0) & \Phi_{43}(t_f, t_0) & \Phi_{45}(t_f, t_0) & \dot{v}_x^f \\ \Phi_{61}(t_f, t_0) & \Phi_{63}(t_f, t_0) & \Phi_{65}(t_f, t_0) & \dot{v}_z^f \end{pmatrix} \tag{115}$$

First of all we note that we have four free variables but just three equations describe how are related to the constrain vector, therefore we will have an infinite possible solutions (undetermined system), this reflects the fact that the resulting jacobian is rectangular and not possible to take its inverse. What we can do is to fix one variable allowing the other to change, eliminating the corresponding column of the jacobian obtaining a diagonal matrix, otherwise the pseudo-inverse can be used, this last solution is used so

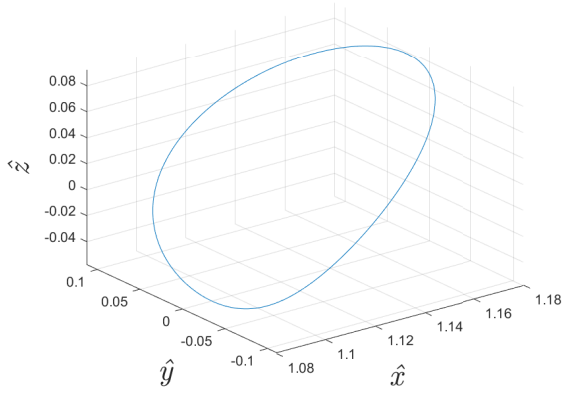

Figure 16: Halo orbit differentially corrected and propagated in the CRTBP

that inverting Eq.(114), we obtain:

$$\boldsymbol{X}^{j+1} = \boldsymbol{X}^{j} - \frac{\partial \boldsymbol{C}(\boldsymbol{X}^{j})}{\partial \boldsymbol{X}^{j}}^{T} \left[\frac{\partial \boldsymbol{C}(\boldsymbol{X}^{j})}{\partial \boldsymbol{X}^{j}} \frac{\partial \boldsymbol{C}(\boldsymbol{X}^{j})}{\partial \boldsymbol{X}^{j}}^{T} \right]^{-1} \boldsymbol{C}(\boldsymbol{X}^{j}) \tag{116}$$

Note that this can be done only if the term in parenthesis is invertible.
The iterative algorithm stops when $\boldsymbol{C}(\boldsymbol{X}^{j+1})$ is lower than a prescribe tolerance or a maximum number of iteration is reached.
In *Figure 16* is shown the resulting halo orbit corrected, propagated in the CRTBP.

Note that this can be also applied to Lyapunov orbit, imposing a planar orbit with $z(t) = 0$ we get:

$$\boldsymbol{X} = \begin{pmatrix} x^0 \\ v_y^0 \\ t \end{pmatrix} \quad , \quad \boldsymbol{C}(\boldsymbol{X}) = \begin{bmatrix} y^f \\ v_x^f \end{bmatrix} = \boldsymbol{0} \quad , \quad \frac{\partial \boldsymbol{C}(\boldsymbol{X})}{\partial \boldsymbol{X}} = \begin{bmatrix} \frac{\partial y^f}{\partial x^0} & \frac{\partial y^f}{\partial v_y^0} & \dot{y}^f \\ \frac{\partial v_x^f}{\partial x^0} & \frac{\partial v_x^f}{\partial v_y^0} & \dot{v}_x^f \end{bmatrix} \tag{117}$$

A quick consideration must be done in this case, while for Halo orbits the initial seed for the differential correction scheme is given by a Richardson approximation that considers non-linear term up to the third order, in the Lyapunov orbit, the initial guess is a linear approximation of the orbit given in Eq.(84) but for high amplitude the linear approximation is not more suitable to initiate a differential correction procedure (insisting using the linear approximation leaves to a solution which is compatible with a two-body orbit around the Moon), what we can do is to take as initial guess the Lyapunov orbit computed in the previous step and start to increase its size, this method is also known as continuation algorithm (for more detail about this method see [3]) the results is shown in *Figure 10*.

3.2 Stability of periodic orbits

When considering closed orbits around equilibrium point, it is interesting also to study its stability when a perturbation $\delta \boldsymbol{x}_0$ is applied to the orbit.
We note that for a closed orbit $\bar{\boldsymbol{x}}(t)$ of period T, the state is retrieved after one orbital period:

$$\bar{\boldsymbol{x}}(t_0) = \bar{\boldsymbol{x}}(t_0 + T) \tag{118}$$

Therefore in order to understand the behaviour of the new trajectory $\boldsymbol{x}(t)$ we can simply compare it with the nominal one at each orbital period. The new trajectory, after the perturbation, can return or diverge from the nominal orbit, in these cases the orbit is called stable or unstable respectively.
A generic orbit is completely determined by its state at one point $\boldsymbol{x}_p$, if we represent the trajectory in the state space, what we have is a closed curve in $\mathbb{R}^6$ defined by the flow ϕ as can be see in *Figure 17*.

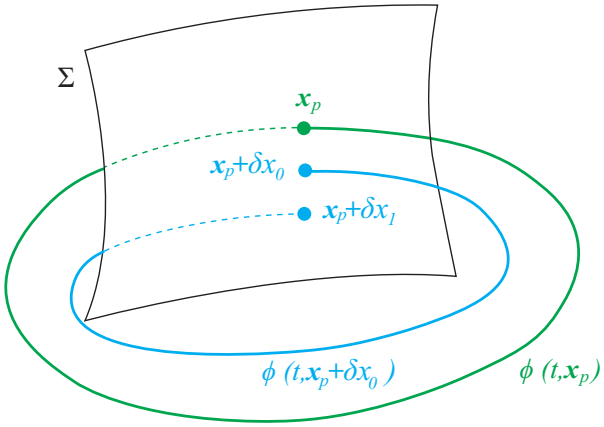

Figure 17: Example of a low-energy transfer from [3]

In order to study its stability, we need a reference so that we can compare them, to do so we can define Σ as the cross $n-1$ dimensional section (also called Poincare section) of the dynamical flow, that is a fixed section transverse to the curve at $\boldsymbol{x}_p$ that define the nominal orbit.
Applying a perturbation, the curve return to that surface with a displacement from the nominal orbit given by:

$$\delta \boldsymbol{x}(T) = \delta \boldsymbol{x}_1 = \boldsymbol{\Phi}(t_0, T + t_0)\delta \boldsymbol{x}(t_0) = \boldsymbol{M}\delta \boldsymbol{x}(t_0) = \boldsymbol{M}\delta \boldsymbol{x}_0 \tag{119}$$

Where the matrix $\boldsymbol{M} = \boldsymbol{\Phi}(t_0, T + t_0)$ is called Monodromy matrix, note that $\boldsymbol{M}$ is a discrete map whose eigenvalues determines whenever initial perturbation $\delta \boldsymbol{x}(t_0) = \delta \boldsymbol{x}_0$ will growth or decay after each revolution.

The generic solution of Eq.(119) after k revolutions is given by (note that the matrix $\boldsymbol{M}$ is evaluated in the reference trajectory and therefore doesn't change after each revolution):

$$\delta \boldsymbol{x}_k = \delta \boldsymbol{x}(kT) = \boldsymbol{M}^k \delta \boldsymbol{x}_0 \tag{120}$$

Since we have a discrete map, the condition to have stability reduce to:

$$Re(\lambda_i) < 1 \quad , \quad \forall i \tag{121}$$

In our case the eigenvalues of $\boldsymbol{M}$ can be expressed in the form:

$$\lambda_1 = \frac{1}{\lambda_2} \qquad (\lambda_1 \gg 1) \quad , \quad \lambda_3 = \bar{\lambda}_4 \quad , \quad \lambda_5 = \lambda_6 = 1 \tag{122}$$

It is possible to demonstrate that the eigenvalues λ_5 represent a neutral variation, normal to the plane and not interesting in our case. The eigenvalue λ_6 is in somehow related to the energy, it is infect possible to perturb a nominal trajectory, obtaining another closed one having the same energy (Jacobi constant), this generate different families of orbits with the same energy level.

- The eigenvalues λ_1 and λ_2 represent unstable and stable behaviour, the associated eigenvectors represent the direction, in the state space, where the spacecraft leaves as fast as possible or it is captured by the orbit, those direction are very important when define manifolds as we will see in the next section.

- (λ_3,λ_4) are complex and conjugate pairs (with $|\lambda| = 1$), in this case a perturbation along the associated eigenvector has the effect to rotate the perturbation of a certain angle after one orbital period, this kind of motion is present only for 3D orbits and generate the so called quasi-Halo and quasi-Lissajous orbit.
  These perturbations leads to new type of orbit, since in general is not useful to work in a six dimensional space for obvious reasons, its possible to study the possible orbit projecting the surface Σ in the $x - y$ plane, perturbing each nominal orbit previously studied in the direction of λ_3 and λ_4 obtaining *Figure 18*.
  Each closed circles are formed by points that represents the intersection of an orbit with the plane while the isolated points are the nominal orbits. As we can see quasi-Halo orbits are orbits that looks like torus when the integration time go to infinite while quasi-Lissajous orbits are more complicated. Note that in this case, also the intersection after half period is shown (symmetric part).

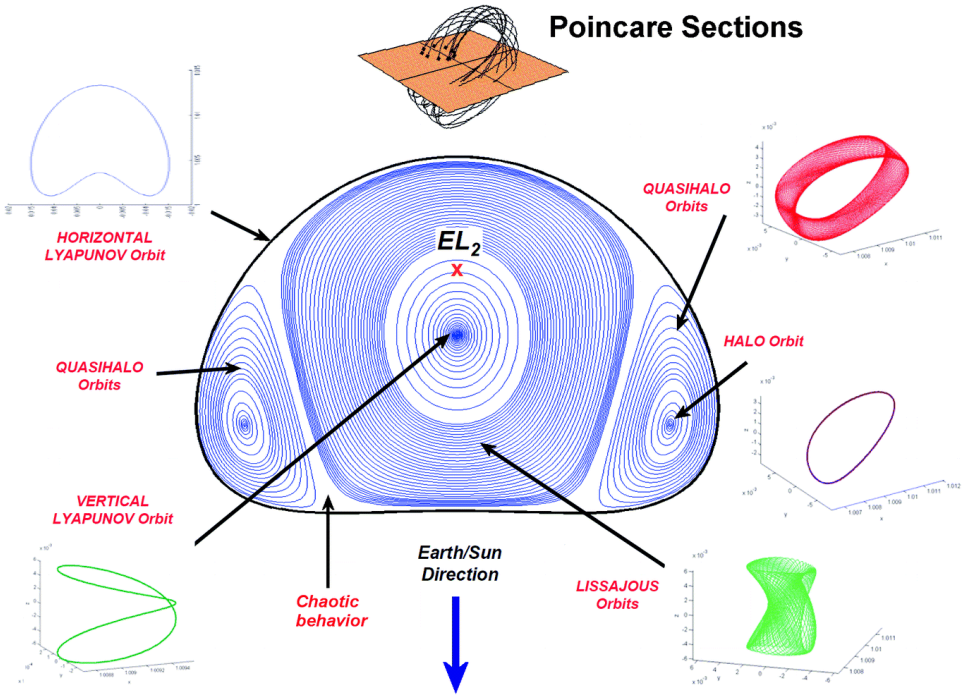

Figure 18: Example orbits representation in the Sun-Earth L_2 from [19], note that this map depend on the value of C_J

3.3 Invariant Manifolds and their computation

Periodic orbits around Lagrangian points are very important in order to design transfer trajectories however an important aspect to take into account is also how we can reach these orbits.

When designing orbit trajectories in libration point, we want, in general, reach the target saving as much as possible propellant, moreover if we look in our prospective we have no clear idea how to design such a trajectory starting from a parking orbit around the Earth, what we can do in these situations is to start from the final part, and integrate *backwards* in time.

To do so we apply a perturbation from the final orbit, among all the perturbations, the stable is the most convenient since, integrating forward, the spacecraft is attracted from that orbit.

Let $\boldsymbol{V}^s(\boldsymbol{x}_0)$ denote the normalized stable eigenvector related to the Monodromy matrix computed at $\boldsymbol{x}_0$ along the orbit, the perturbed state can be written as:

$$\boldsymbol{x}(\boldsymbol{x}_0) = \boldsymbol{x}_0 \pm \epsilon \boldsymbol{V}^s(\boldsymbol{x}_0) \tag{123}$$

The term ϵ is a quantity that must be a compromise between accuracy (if it is too high we have a big perturbation that is not representative of our problem) and time (since in this case it takes a lot of time to leave the orbit for very small perturbations), a value of

$\epsilon = 1 \times 10^{-6}$ is used.
Note also that the $\pm$ sign must be considered and derive from the definition of eigenvector (if $\boldsymbol{V}^s(\boldsymbol{x}_0)$ is an eigenvalue also $-\boldsymbol{V}^s(\boldsymbol{x}_0)$ it is).
Sometimes we are interested in leaving the orbit instead to reach it, in these cases we intergrate *forward* the trajectory along the unstable eigenvector $\boldsymbol{V}^u(\boldsymbol{x}_0)$ so that:

$$\boldsymbol{x}(\boldsymbol{x}_0) = \boldsymbol{x}_0 \pm \epsilon \boldsymbol{V}^u(\boldsymbol{x}_0) \tag{124}$$

The previous results are valid for a point $\boldsymbol{x}_0$, in order to consider all points of the orbit we propagate the successive stable/unstable perturbations $\boldsymbol{V}^{s/u}(\boldsymbol{x}(t))$ along the orbit:

$$\boldsymbol{V}^{s/u}(\boldsymbol{x}(t)) = \boldsymbol{\Phi}(t_0, t)\boldsymbol{V}^{s/u}(\boldsymbol{x}_0) \tag{125}$$

And since the state transition matrix not preserve the norm the results must be normalized.
In *Figure 19* is reported the propagated trajectory in forward (red lines) and backward (green lines) in time, if we increase the number of points that we propagate what we obtain is a stable and unstable manifold (a surface), mathematically:

$$\begin{aligned} W^s(\phi(t, \boldsymbol{x}), \boldsymbol{x}_0) &= \{\boldsymbol{x} \in X : \phi(t, \boldsymbol{x}) \longrightarrow \boldsymbol{x}_0 \in Y \;\; as \;\; t \to \infty\} \\ W^u(\phi(t, \boldsymbol{x}), \boldsymbol{x}_0) &= \{\boldsymbol{x} \in X : \phi(t, \boldsymbol{x}) \longrightarrow \boldsymbol{x}_0 \in Y \;\; as \;\; t \to -\infty\} \end{aligned} \tag{126}$$

Where Y is the set, in the state space, of all points corresponding to the closed orbit.

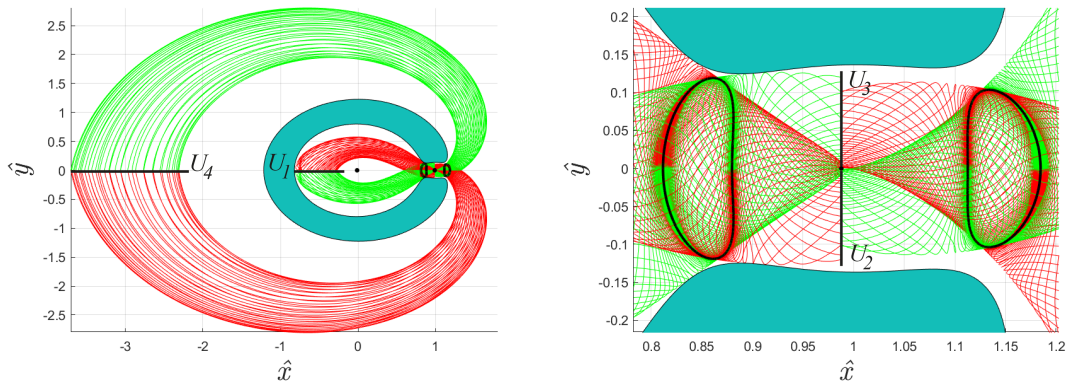

Figure 19: Stable (green) and Unstable (red) Manifold emanated from a Lyapunov orbit around L_1 and L_2

3.4 Transit and non-Transit trajectories

Manifold are useful tool when considering transfer trajectories and can be considered as a separatrix of two important transfers: non-transit and transit orbits.
Let $\bar{\boldsymbol{x}}(t)$ a planar Lyapunov periodic orbit, in these cases we only consider orbits around L_1 and L_2, since the other points have too much energy and therefore not interesting for our goal, for simplicity, we suppose that the Jacobi constant associated to $\bar{\boldsymbol{x}}(t)$ is such that the outer and internal realm can communicate through the bottleneck in order that existence of period orbit around L_1 and L_2 is granted.
In order to design trajectories that moves from one region to another we define some important Poincaré sections U_i that are useful when dealing with mission analysis:

$$\begin{aligned} U_1(x, y, v_x, v_y) &= \{(x, y, v_x, v_y) \in X : y = 0, -1 < x < 0, v_y < 0\} \\ U_2(x, y, v_x, v_y) &= \{(x, y, v_x, v_y) \in X : x = \mu_1, y < 0, v_x > 0\} \\ U_3(x, y, v_x, v_y) &= \{(x, y, v_x, v_y) \in X : x = \mu_1, y > 0, v_x < 0\} \\ U_4(x, y, v_x, v_y) &= \{(x, y, v_x, v_y) \in X : y = 0, x < -1, v_y > 0\} \end{aligned} \tag{127}$$

Where X is the set of points that belongs to the manifold and inequalities must be considered due to feasibility of the manifold trajectories.
Those sections are 3D surfaces in (x, v_x, v_y) or (y, v_x, v_y) whose projection in the $x - y$ plane are shown in *Figure 19*.
In the previous chapter we have also see that a trajectory in the CRTBP admits an integral of motion, the Jacobi constant, therefore, given a Poincaré section, only points that intersect the Jacobi surface C_J with the manifold are compatible with the motion of the spacecraft, this actually reduce the dimension of the problem from $n-1$ to $n-2$ since we can write, using Eq.(36):

$$\begin{aligned} v_x(x, y, v_y, C_J) &= \pm\sqrt{(x^2 + y^2) + 2(\frac{\mu_1}{r_1} + \frac{\mu_2}{r_2}) - v_y^2 - C_J} \\ v_y(x, y, v_x, C_J) &= \pm\sqrt{(x^2 + y^2) + 2(\frac{\mu_1}{r_1} + \frac{\mu_2}{r_2}) - v_x^2 - C_J} \end{aligned} \tag{128}$$

Where $\pm$ sign must be chosen according the sign considered in Eq.(127) for the particular section.
Now consider, for example, a Lyapunov orbit located at L_2 and propagate the internal stable manifold till reach the section U_2, if we at that point project in the $y - v_y$ plane the intersection of the manifold and Jacobi constant what we get is a closed 2D curve that divide the plane in two region one inside and another outside the curve that combined with Eq.128 and the position of the section gives a representation of the satellite's state.
It is possible to demonstrate that if a spacecraft has initial condition such that the state

is inside the curve, the satellite, when it moves toward L_2, it escape from the interior to the exterior region, accordingly, state outside the curve are not capable to escape from their region and are bounced back, these two conditions are summarized in *Figure 20* and *Figure 21*. An analogous reason can be applied for the unstable manifold with the difference that the trajectories must be propagated backward in time and for a different section.

From the plots, a transit orbit starts inside the stable manifolds and then once the spacecraft approach the closed orbit, the trajectory moves along the unstable manifold region.

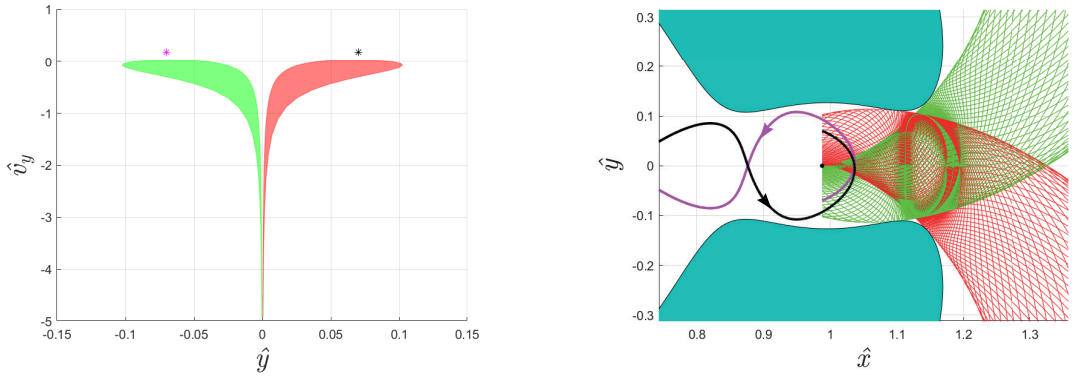

(a) Poincaré Section **(b)** Propagated Trajectory

Figure 20: Example of non-transit orbit, the point represent the initial state

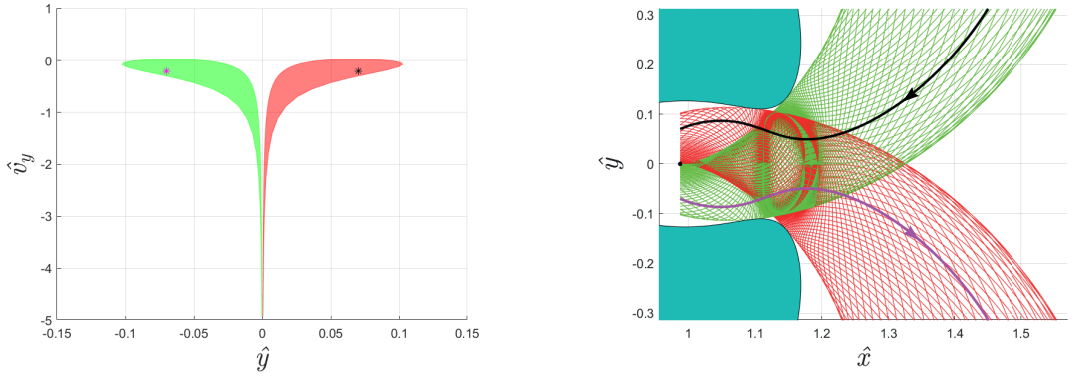

(a) Poincaré Section **(b)** Propagated Trajectory

Figure 21: Example of transit orbit, the point represent the initial state

Note that the phase plane shown is not a Poincare cut of the flow (only one velocity component is shown) but rather it represents a projection of the Poincare section, however in space mission design it is common to refer it as a Poincaré section. Moreover those section are fictitious section meaning that we can define an arbitrary section, the cuts U_i are placed there in order to compare trajectories coming from the stable/unstable in

easier way but no one prohibit to select oblique sections or to propagate the manifold also for successive time, a transit orbit can become transit after a certain number of intersection with the cut, after that it is bounced back more and more times can have the right state to escape, those are very important aspect when considering low energy transfers.
Even if the procedure to obtain a transit or a non-transit orbits are quite simple, we have discussed only planar Lyapunov orbits, the extension of 3D orbits it's more difficult since the number of state variables increase (for more detail see [20]).

3.5 Earth-Moon low-energy transfer, patched CRTBP approximation

As the patched two body problem can be used to model the dynamics with more body considering at each step a two body problem, the patched three body problem use a similar logic where the patched point is given by a Poincaré section.
While in the two body problem we have conics as trajectories in the PCRTBP we use stable and unstable manifolds because represents pathways that go from one region to another one with low fuel consumption.
When design a low energy transfer a possible idea is to transfer from a parking orbit and insert the spacecraft into an interior stable manifold emanated from L_1, using this idea, in order to intersect a parking orbit the manifold must be propagated, in some cases, for a long time, making a certain number of revolutions around the primary.
However, looking to the secondary body in *Figure 19*, the manifolds are very close to it, a situation like this would be desirable and can be obtained studying the Sun-Earth system.
Let's consider a L_2 orbit around the Moon, if we propagate backward along the exterior stable manifold we see that all the trajectories start to go very faraway so that the influence of the Sun starts to become important, in these situation where the modeled dynamic change it is possible to switch from an Earth-Moon system to an Sun-Earth dynamics by patching together the trajectories in a certain Poincaré cut.

In *Figure 22* is reported an example of patched process and the resulting trajectory is also highlighted. The trajectory is divided in two different legs, in the first leg, the planar orbit is integrated backward along the stable manifold until it reaches the Poincare cut, while in the second leg, the spacecraft is in a parking orbit around the Earth and an impulsive manoeuvre is applied, so that the spacecraft is injected in an heliocentric trajectory toward L_2, through the stable manifold of the Sun-Earth system, and then it's bounced back along the associated unstable manifold.

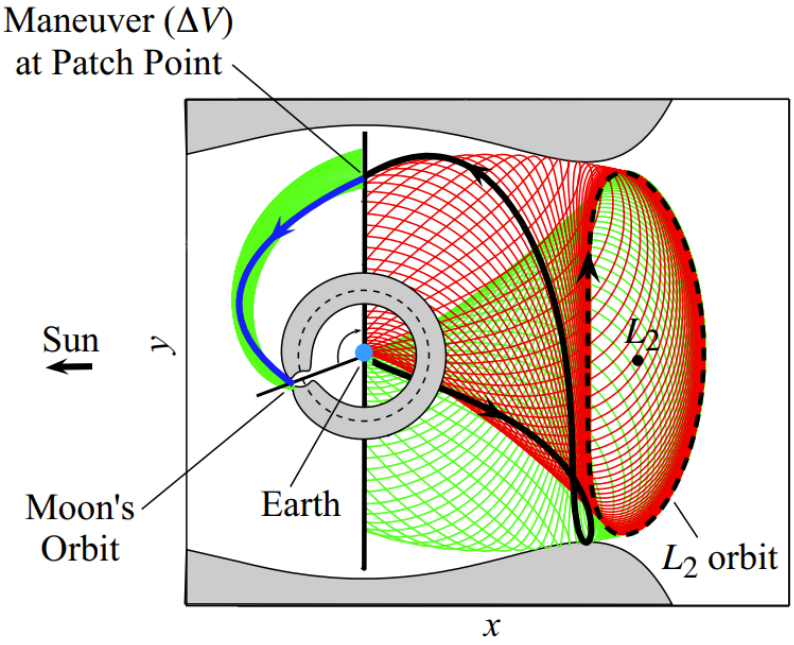

Figure 22: Example of a low-energy transfer from [3]

At this point we observe that in particular condition the 2 legs intersect in position space and a small maneuver is applied so that low energy transfer is obtained.
The main parameters that define a low energy transfer targeting libration point are the following, for more detail see [21]:

- Earth Moon orbit parameter: This value correspond to the Jacobi constant of the Halo orbit, this parameter can be useful especially when considering ballistic capture.
- Sun-Earth-Moon angle θ: We have discuss previously a low energy transfer generally happen in some particular condition related to the phase angle θ, between the Sun-Earth line and Earth-Moon line at the arrival, most of the low energy transfer have $0 < \theta < \frac{\pi}{2}$ or $\pi < \theta < \frac{3}{2}\pi$ at the capture.
- Arrival position τ, p: At the arrival the satellite can be at any point along the Halo orbit, the parameter $0 < \tau < 1$ parametrize a generic position of the Halo. Moreover since, in general, we can approach the Earth-Moon's libration point from the interior or exterior stable manifold, the parameter p can be set to 'exterior' or 'interior' accordingly.

Change any of those parameters it is possible to construct different families of low energy transfer that are captured by the Halo orbit.

3.6 Weak stability boundary and its construction

Another possible way in order to design low-energy transfer is to use the so called weak stability boundary (WSB).
The weak stability boundaries is a region, studied in [1], where the spacecraft experience gravitational force due to a central body while the other forces tends to balance, in this region, small maneuver can cause the trajectory to change dramatically obtaining a ballistic or quasi ballistic trajectory that are temporally captured by the Moon.
Let's consider the radial direction emanated from a central body, that can be the Moon in this context, using spherical coordinates, the position of the satellite is given by (θ, φ) and the distance r such that $\boldsymbol{r} = r\boldsymbol{e}_r$ as shown in *Figure 23*.
The velocity of the spacecraft is suppose to be initially contained in a plane perpendicular to the radial direction Σ while the parameter α, is the angle defined in order to span all the possible directions on the plane.
We define the Keplerian energy H as in the two body problem:

$$H = \frac{1}{2}v^2 - \frac{\mu}{r} \tag{129}$$

Where μ is the mass parameter of the central body.
With the assumption made, a temporally captured orbit is a trajectory that revolves around a central body for a certain number n of times without cycle around other bodies, this type of orbits are also called n-stable if also $H < 0$ along the trajectory (otherwise are n-unstable).
Starting from low altitude, and propagate the trajectory with a certain initial velocity $\dot{\boldsymbol{x}}$, the trajectory will cross again Σ after approximately one orbital period if the altitude is sufficient small so that the the dynamics is well approximated by a two-body problem. Increasing the distance r, keeping all the other parameters and the eccentricity $e \in [0, 1)$ (hence $H < 0$ initially) fixed and change the velocity accordingly in magnitude (needed in order to have a constant e), the trajectory starts to go faraway from the Moon till at some point, propagating further, the trajectory escape performing at least one revolution around the second primary, the Earth, before returning to the Moon as describe in *Figure 24*.
Therefore, let r^* the distance where the satellite escape, points with $r < r^*$ are called stable points while if $r > r^*$ are unstable.
Even if a stable points perform one cycle around the Moon no one grants that in the next integration the satellite remain stable again, it is possible that the point remain stable for n cycles and then become unstable.
Moreover the condition doesn't imply that other stable orbit can be found increasing r but only means that a change of stability is present as we can see in *Figure 25*.

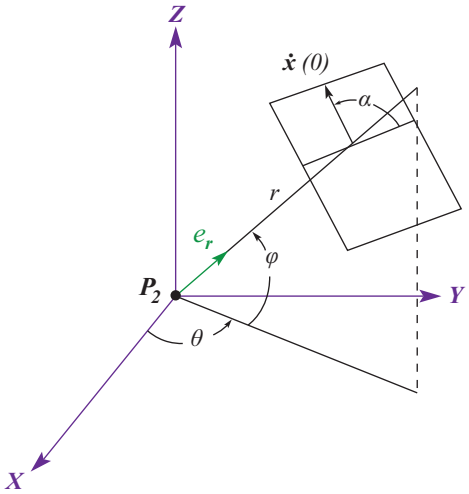

Figure 23: Polar representation, from[1]

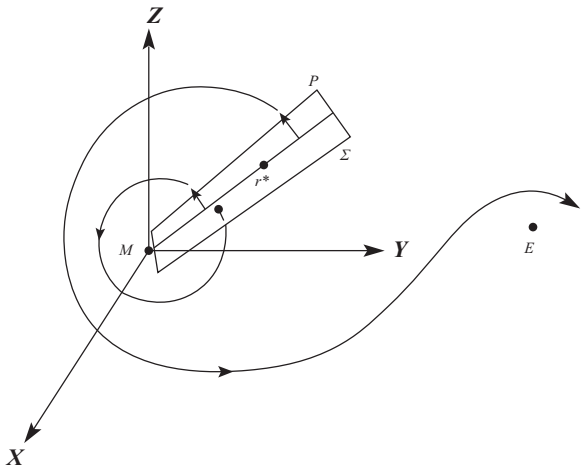

Figure 24: Definition of r^*, from [1]

Therefore, if we denote as r_k^{*n} the distance of the n-stable points, where the k-th stability transition is present, the set of n-stable point $\mathcal{W}_n$ can be written as:

$$\mathcal{W}_n(e,\theta,\varphi,\alpha,\beta) = \{\bigcup_{k\geq 1}(r_{2k-1}^{*n} - r_{2k}^{*n}) | \theta \in [0,2\pi]\,, \varphi \in \left[-\frac{\pi}{2},\frac{\pi}{2}\right], (\alpha,\beta) \in [0,2\pi], e \in [0,1)\} \tag{130}$$

This However is a specific set, the total set of stable point span every possibilities:

$$\mathcal{W}_n^* = \{\bigcup_{e,\theta,\varphi,\alpha,\beta} \mathcal{W}_n(e,\theta,\varphi,\alpha,\beta)\} \tag{131}$$

Where β is the angle between the Sun-Earth line and the Earth-Moon line.
In *Figure 26* is shown an example of 1-stable orbit, the weak stability boundaries are defined as the boundary of $\mathcal{W}_n$, that is the locus of all points r^* for which there is a change of stability of the initial trajectory:

$$WSB_n = \partial \mathcal{W}_n^* \tag{132}$$

Comparing the definition of WSB_n and the one given by Manifold we can see that given a stable manifold that revolves n times around the Moon, points in the intersection of the stable manifold and a cut that have a null initial radial velocity and $H < 0$, are points of WSB_n, even if this consideration is valid for a range of energies only (for more detail see [22]).
We can now discuss how to construct low-energy transfer.
In order to construct low energy transfer we join together a forward and backward

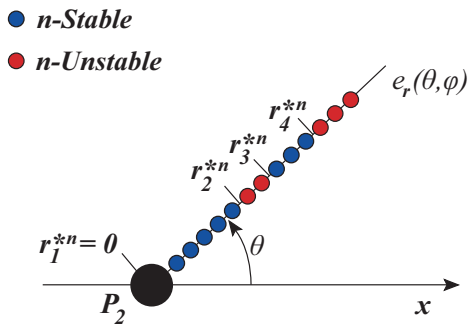

Figure 25: n-stability/instability definition, from[23]

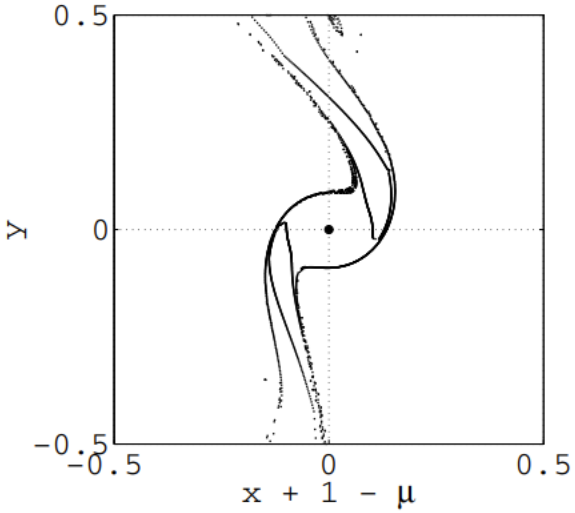

Figure 26: WSB_1 with e=0 on the plane, from[22]

trajectory like in *Figure 27*. For the backward segment, a direction of approach to the Moon is selected so that the parameters $\theta, \varphi, \alpha, \beta$ are defined, selecting a point that lies in the WSB of the Moon and propagate backward in time, the trajectory will escape and the satellite arrives approximately 1.5×10^6Km far from the Earth, this is the region of the WSB of the Earth.

In the forward segment, the satellite starts in a parking orbit and the trajectory is propagate forward, for certain combination of position and velocity, the two trajectory intersect and a small manoeuvre is applied to patch in the state space. The trajectory obtained is temporally captured by the moon, in order to stay there another small manoeuvre must be applied.

Once the trajectory is defined, it can be used as initial guess in a more refined model since, where the dynamical model is switched suddenly from a CRTBP to another one, important deviation can be present.

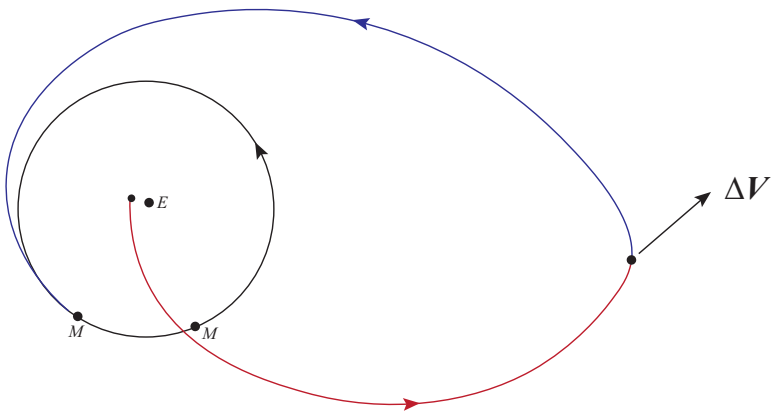

Figure 27: Example of a low-energy transfer

4 LUMIO mission

The Lunar Meteoroid Impacts Observer (LUMIO) is a 12U CubeSat that is plan to be placed in the Earth-Moon L2 point, it is equipped with a camera in order to detect flashes, in the visible radiation, coming from asteroids impacts on the farside of the Moon.
Combined with a detection of impacts in the nearside from ground, it is possible to get an estimation of the asteroids flux that hit the lunar surface.

4.1 Mission overview

In this thesis we suppose to depart as a secondary payload of ARTEMIS-2, therefore the design of LUMIO's trajectory it depends strongly by the primary mission, in *Figure 28* is shown the mission profile of ARTEMIS-2, the main goal is to carry astronauts on board and overfly the lunar surface thanks to a lunar fly-by and then return to the Earth.
LUMIO is injected in a trans-lunar orbit and, using a low-energy transfer, the satellite is placed into a Halo orbit around L_2 of the Earth-Moon system and plan to operate for at least one year.

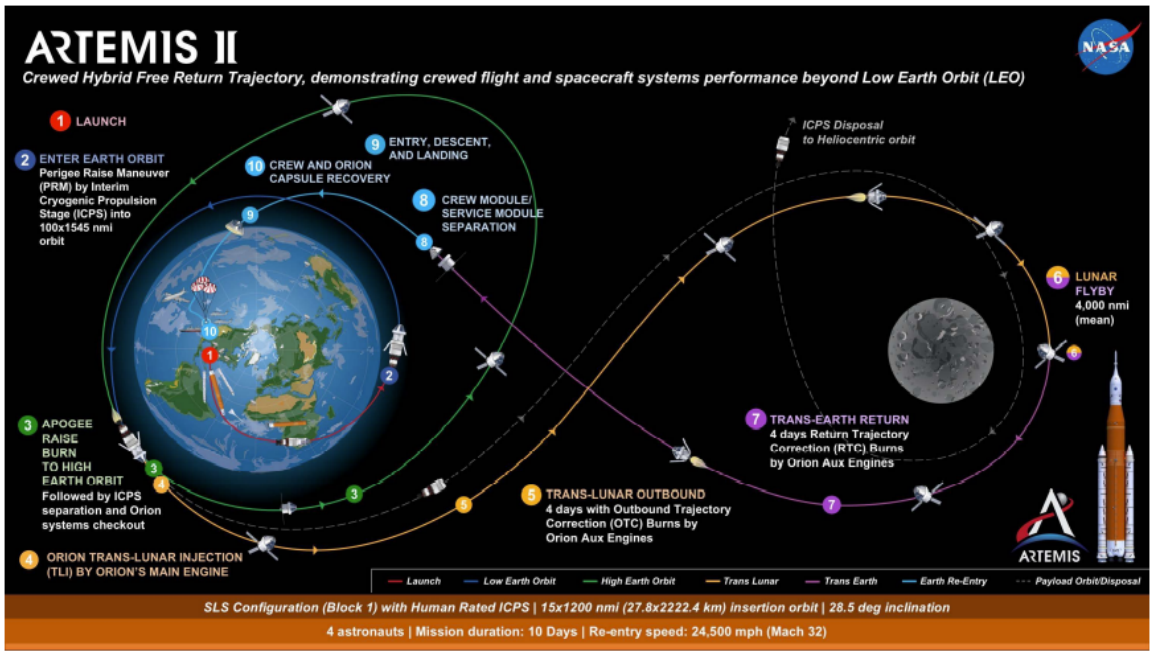

Figure 28: ARTEMIS mission profile (credits: NASA)

4.2 RPRnBP model

As we have already discuss, when considering orbits around equilibrium points or also low-energy transfer trajectories where, important deviation can be present especially in correspondence of the weak stability boundaries at the patched point, refined dynamical model is necessary in order to get more realistic results particularly when integrate for a long time.
In our case we consider a rotopulsating restricted n-body problem (RPRnBP) that is briefly describe in the following section (for more detail about the dynamics see in [24]).

4.2.1 Equation of motion RPRnBP

The equation of motion are written as perturbations of the restricted three body problem, the assumption are similar to those describe in the CRTBP, with the exception that the motion of the primaries is assume elliptical instead of circular, and perturbations due to the presence of the other bodies are added, note that ,with these approximations, the problem becomes non-autonomous.
Referring to *Figure 29*, let $(\boldsymbol{R}(t),\ \boldsymbol{V}(t))$ the position and velocity of a massless particle P, written in an inertial frame $(O; \boldsymbol{i}, \boldsymbol{j}, \boldsymbol{k})$ centered in the barycenter of the solar system, we want to make a change of coordinates in order to write the equation of motion in the synodic frame centered on the barycenter of the two primaries, M_1 and M_2, in normalized coordinates.

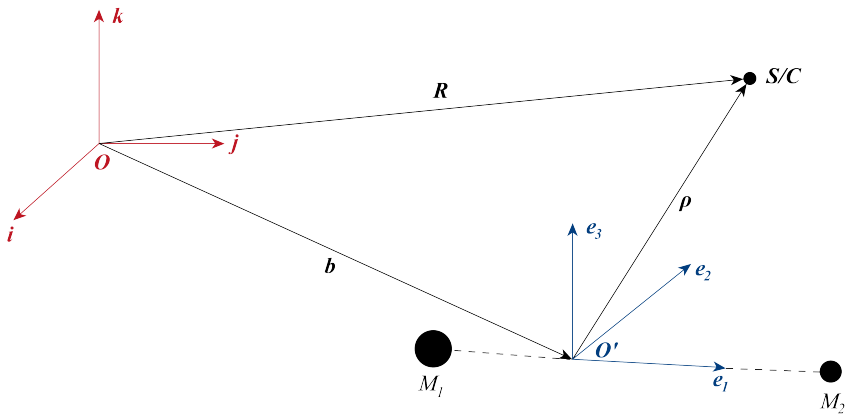

Figure 29: RPRnBP

The synodic frame $(O'; \boldsymbol{e}_1, \boldsymbol{e}_2, \boldsymbol{e}_3)$ is defined as usual like in the CRTBP, although the distance between M_1 and M_2 is not constant, the unit of length is chosen such that their distance is unitary, instant by instant, if we denote as $\boldsymbol{\rho}$ the normalized distance in the synodic frame, we can write:

$$\boldsymbol{R}_2(t) - \boldsymbol{R}_1(t) = k(t)\boldsymbol{e}_1 \quad \text{and} \quad \|\boldsymbol{\rho}_2 - \boldsymbol{\rho}_1\| = 1 \tag{133}$$

Where $\boldsymbol{R}_i$ and $\boldsymbol{\rho}_i$ are the position of the i-th primary in their reference frame and $k(t) = \|\boldsymbol{R}_2(t) - \boldsymbol{R}_1(t)\|$ depends on time.
The normal vectors $(\boldsymbol{e}_1, \boldsymbol{e}_2, \boldsymbol{e}_3)$ can be computed as:

$$\boldsymbol{e}_1 = \frac{\boldsymbol{R}_2 - \boldsymbol{R}_1}{k(t)} \tag{134a}$$

$$\boldsymbol{e}_2 = \boldsymbol{e}_3 \times \boldsymbol{e}_1 \tag{134b}$$

$$\boldsymbol{e}_3 = \frac{(\boldsymbol{V}_2 - \boldsymbol{V}_1) \times (\boldsymbol{R}_2 - \boldsymbol{R}_1)}{\|(\boldsymbol{V}_2 - \boldsymbol{V}_1) \times (\boldsymbol{R}_2 - \boldsymbol{R}_1)\|} \tag{134c}$$

The position of P in the inertial frame can be related with the normalized synodic frame through a rototrasltion:

$$\boldsymbol{R} = \boldsymbol{b} + \boldsymbol{r}_{rel} = \boldsymbol{b} + k(t)\boldsymbol{C}(t)\boldsymbol{\rho}(\tau) \tag{135}$$

Where $\boldsymbol{b}$ is just the distance between the two origin given by the center of mass in Eq.(11), that is nonzero in this case, while $\boldsymbol{C}(t)$ is a rotation matrix defined by the direction cosine, $(\boldsymbol{C}(t) = [\boldsymbol{e}_1, \boldsymbol{e}_2, \boldsymbol{e}_3])$.
The velocity will be:

$$\boldsymbol{V} = \frac{d\boldsymbol{R}}{dt} = \dot{\boldsymbol{b}} + \dot{k}\boldsymbol{C}\boldsymbol{\rho} + k\dot{\boldsymbol{C}}\boldsymbol{\rho} + \dot{\tau}k\boldsymbol{C}\boldsymbol{\rho}' \tag{136}$$

Where dots are time derivatives while primes stand for derivative in normalized time τ given by:

$$\tau = n(t - t_0) = \sqrt{\frac{G(m_1 + m_2)}{\bar{d}}}(t - t_0) \tag{137}$$

where n is the mean angular velocity obtained from Kepler third law Eq.(15) using a medium distance $\bar{d}$ from the primaries so that also n is unitary in normalized coordinates.
In order to derive the equation of motion we consider Newton's law:

$$m\ddot{\boldsymbol{R}} = \boldsymbol{\nabla}U + \boldsymbol{F}_{nc} \tag{138}$$

Where $\boldsymbol{F}_{nc}$ are the forces that are not conservative.
The potential is written considering each body as an extended object, the major diffi-

culty in doing this is that the shape of the planet is not perfectly spherical and therefore the derivation of its potential is not straightforward, remanding to orbital mechanics textbook, it is possible to demonstrate that in this case the potential of a body with mass M_B and mean radius R_B at a distance r, can be written as:

$$U = \frac{GM}{r}\left[1 - \sum_{k=2}^{\infty} J_k \left(\frac{R_B}{r}\right)^k P_k(\sin\delta)\right] \tag{139}$$

Where $P_k(\sin\delta)$ is the Legendre polynomial of degree k given by:

$$P_k(x) = \frac{1}{2^n n!}\frac{d^n}{dx^n}[(x^2-1)^n] \tag{140}$$

While the generic J_k is called zonal harmonics and δ is the declination of P. As a matter of fact the term that most influence the dynamics is J_2 while higher terms are relatively small compared to it, therefore the potential can be simplified, computing $P_2(\sin\delta)$ and substituting in Eq.(139), obtaining:

$$U = \frac{GM}{r}\left[1 - \frac{J_2}{2}\left(\frac{R_B}{r}\right)^2\left(3\frac{r_z^2}{r^2} - 1\right)\right] \tag{141}$$

Since $\sin\delta = \frac{r_z}{r}$.
Transforming each term in normalized coordinate and considering n bodies, the potential of P will be, by superposition:

$$U = m\sum_{j=1}^{n}\frac{\mu_j}{k\left\|\boldsymbol{\rho}-\boldsymbol{\rho}_j\right\|}\left[1 + \frac{J_{2j}R_{B_j}^2}{2k^2\left\|\boldsymbol{\rho}-\boldsymbol{\rho}_j\right\|^2}\left(1 - \frac{3(\boldsymbol{\rho}-\boldsymbol{\rho}_j)^T\boldsymbol{C}^T\boldsymbol{I_z}\boldsymbol{C}(\boldsymbol{\rho}-\boldsymbol{\rho}_j)}{(\left\|\boldsymbol{\rho}-\boldsymbol{\rho}_j\right\|)^2}\right)\right] \tag{142}$$

Where I_z is a 3×3 zero matrix with the third diagonal term unitary needed in order to consider a vectorial form of the third component, $\boldsymbol{r}_z = [0,0,r_z]$:

$$\boldsymbol{r}_z = k\boldsymbol{I_z}\boldsymbol{C}(\boldsymbol{\rho}-\boldsymbol{\rho}_j) \tag{143}$$

And hence:

$$r_z^2 = \boldsymbol{r}_z^T\boldsymbol{r}_z = k^2(\boldsymbol{\rho}-\boldsymbol{\rho}_j)^T\boldsymbol{C}^T\boldsymbol{I_z}^T\boldsymbol{I_z}\boldsymbol{C}(\boldsymbol{\rho}-\boldsymbol{\rho}_j) \tag{144}$$

Substituting the previous equation into the equation of motion and computing all the derivatives we obtain:

$$\boldsymbol{\rho}'' = -\frac{1}{\dot\tau}\left(\frac{2\dot k}{k}\boldsymbol{I} + 2\boldsymbol{C}^T\dot{\boldsymbol{C}}\right)\boldsymbol{\rho}' - \frac{1}{\dot\tau^2}\left[\left(\frac{\ddot k}{k}\boldsymbol{I} + 2\frac{\dot k}{k}\boldsymbol{C}^T\dot{\boldsymbol{C}} + \boldsymbol{C}^T\ddot{\boldsymbol{C}}\right)\boldsymbol{\rho} + \boldsymbol{C}^T\ddot{\boldsymbol{b}}\right] + \boldsymbol{\nabla}U + \boldsymbol{a}_{nc} \tag{145}$$

Where $\mu_j = \frac{m_j}{m_1+m_2}$ and:

$$\boldsymbol{\nabla} U = -m\left(\sum_{j=1}^{n}\frac{\mu_j}{k\left\|\boldsymbol{\rho}+\boldsymbol{\rho}_j\right\|^3}(\boldsymbol{\rho}+\boldsymbol{\rho}_j)+\sum_{j=1}^{n}\frac{3\mu_j J_{2j}R_{B_j}^2}{2k^3\left\|\boldsymbol{\rho}-\boldsymbol{\rho}_j\right\|^5}(\boldsymbol{\rho}-\boldsymbol{\rho}_j)\right.$$
$$\left.+\sum_{j=1}^{n}\frac{3\mu_j J_{2j}R_{B_j}^2}{2k^3\left\|\boldsymbol{\rho}-\boldsymbol{\rho}_j\right\|^5}\left(2\boldsymbol{C}^T\boldsymbol{I_z}\boldsymbol{C}(\boldsymbol{\rho}+\boldsymbol{\rho}_j)-\frac{5(\boldsymbol{\rho}+\boldsymbol{\rho}_j)^T\boldsymbol{C^T}\boldsymbol{I_z}\boldsymbol{C}(\boldsymbol{\rho}+\boldsymbol{\rho}_j)}{\left\|\boldsymbol{\rho}-\boldsymbol{\rho}_j\right\|^2}(\boldsymbol{\rho}+\boldsymbol{\rho}_j)\right)\right) \tag{146}$$

Eq.(145) is the equation of motion of the RPRnBP written in the synodic frame of M_1 and M_2, in this case we have added an acceleration to take into account possible other forces that acts on P.
An example of a non conservative force is the solar radiation pressure that imparts an acceleration $\boldsymbol{a}_{SRP}$ to P given by:

$$\boldsymbol{a}_{SRP} = \frac{\boldsymbol{F}}{m} = (1+c_r)\frac{A_{SC}}{m}\frac{\Psi d}{c}\boldsymbol{e}_r \tag{147}$$

With Ψ the energy flux at a distance d from the Sun, $\boldsymbol{e}_r$ the radial direction directed toward P from the Sun and c_r the reflectivity coefficient.
Note that also in this case, the equation of motion can be written as a system of ordinary differential equations:

$$\dot{\boldsymbol{x}} = \boldsymbol{f}(\boldsymbol{x},\tau) \tag{148}$$

The equation of motion can be used also to obtain the state transition matrix following the same procedure discuss in 2.2.4, the equation are quite long and complicated, for more details see [24].

4.3 Multiple shooting method

4.3.1 Motivation

Before starting to optimize trajectories is necessary to understand how they are constructed, infect simply integrate the trajectory starting from a certain initial condition leave to inconsistent result.
The major difficulty that we encounter with this approach is due to the chaotic behaviour of Eq.(145). For example, integrating directly a halo orbit trajectory using a RPRnBP with initial condition given by a CRTBP, what we get is that the trajectory is too much

sensitive to a small variations and even if initially a halo like shape is obtained then starts to diverge dramatically. Compared with the RPRnBP model, the solution of the CTBP is not capable to give satisfactory initial conditions to get something which is similar to a Halo orbit therefore, what condition take in this situation?.
The answer is unknown, using this approach the results is inconclusive, even if we know that there exist path similar to a Halo since the predominant dynamics is always given by a CRTBP approximation, a similar consideration is valid when considering a generic trajectory.
In order to solve this problem we need something different, which is more robust and capable to desensitize the dynamics, especially when no maneuver are present, the multiple shooting method.

4.3.2 Overview

The multiple shooting method is describe in *Figure 30*, the trajectory is subdivided in multiple segments, obtained propagating some selected points, also called nodes.

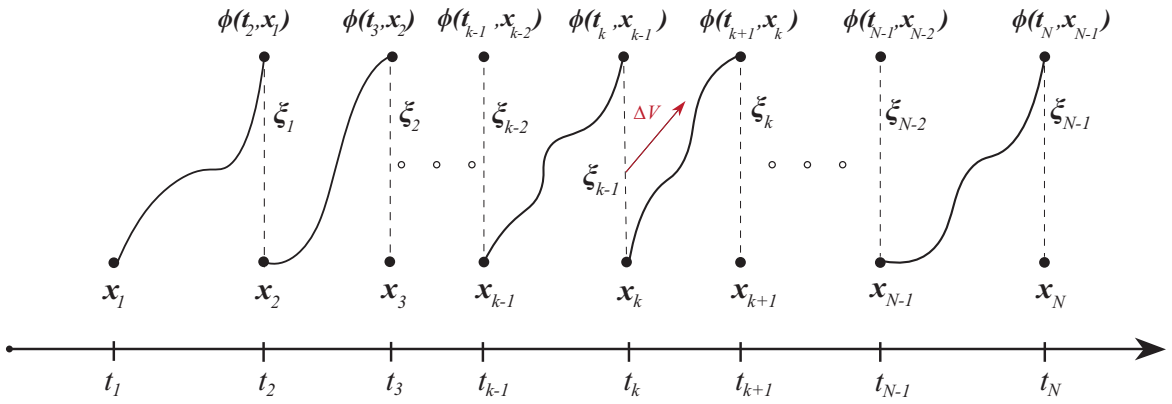

Figure 30: Multiple shooting method

When these points are propagated forward in a more fidelity model, different segments are generated, a shooting method is applied for each arc, adjusting the initial conditions in order to satisfy some constrain like the continuity of the trajectory and, eventually, constraints at the boundaries.
In this case the vector of free variable $\boldsymbol{Y}$ that can be tune to reach the desired results is of the form:

$$\boldsymbol{Y} = \begin{pmatrix} \boldsymbol{X} \\ \boldsymbol{\tau} \end{pmatrix} = \begin{bmatrix} \boldsymbol{x}_1 \\ \vdots \\ \boldsymbol{x}_i \\ \vdots \\ \boldsymbol{x}_N \\ t_1 \\ \vdots \\ t_i \\ \vdots \\ t_N \end{bmatrix} \tag{149}$$

Where $\boldsymbol{x}_i$ is the state vector evaluated at the i-th node, at the normalized time t_i and N is the number of nodes.

4.4 Problem definition

In all orbital mechanical problem involving parameters that must be changed in order to full fill some constrain, paying attention also to the "performance" of the trajectory, an optimization process is needed. The optimization problem can be formulated as follows:

$$\begin{aligned} \min J(\boldsymbol{Y}) \quad & \text{Subject to:} \\ \boldsymbol{A}_{eq}(\boldsymbol{Y}) = \boldsymbol{b}_{eq} \quad & \text{Equality linear constrains} \\ \boldsymbol{A}(\boldsymbol{Y}) \leq \boldsymbol{b} \quad & \text{Inequality linear constrains} \\ \boldsymbol{H}(\boldsymbol{Y}) = \boldsymbol{0} \quad & \text{Non linear equality constrains} \\ \boldsymbol{G}(\boldsymbol{Y}) \leq \boldsymbol{0} \quad & \text{Non linear inequality constrains} \end{aligned}$$

Where J is the objective functions that rules the quality of the solution that satisfy the constrains.
In order to find a minimum of this problem, the solution must satisfy KKT that gives a necessary condition of a solution to be optimal, note however that this condition is not sufficient in general and therefore, no one tell us if the solution is a global or a local minimum, for more details see [25].
In the following are summarized most used constrains when design a transfer trajectory.

4.4.1 Equality linear constrain

Equality linear constraints are those associated to known quantities, in some cases, position or velocity or both may be not allowed to vary in particular nodes.
However in most cases, constraints at the boundaries are probably the most important since are related to insertion point or because mission need to reach a particular point at the end of the transfer, the constrain can be written as:

$$\boldsymbol{\mathcal{C}}(\boldsymbol{x}_1, \boldsymbol{x}_N) = \bar{\boldsymbol{b}} \tag{150}$$

Where $\bar{\boldsymbol{b}}$, is a vector of known quantities.
Note that Eq.(150) involve position or velocity constrain, however also time constraint must be set in order to have a consistent problem, in most of the cases, time at the initial node is set:

$$t_1 = \bar{t}_0 \tag{151}$$

Note however that this constrain must be apply when the initial time is well defined, in some cases, in a preliminary analysis, time window could be more appropriate.

4.4.2 Inequality linear constrain

Inequality constrain are related to the arc duration between two successive nodes, this is due to the fact that maneuvers are supposed to be impulsive but in reality they need time and cannot operate as continuous thrusters, therefore:

$$t_k - t_{k-1} \geq \Delta\bar{t}_0 \qquad i = 2, \ldots, N \tag{152}$$

Even if we optimize a trajectory, the overall duration can be very high especially when low-cost trajectory are considered, therefore condition related to a maximum time of flight TOF_{max} must be considered:

$$t_N - t_1 \leq TOF_{max} \tag{153}$$

As already noted, in some cases, initial time is not clear and a time window of the initial node is necessary, this is mostly due to delays of the nominal operations:

$$t_{min} \leq t_1 \leq t_{max} \tag{154}$$

4.4.3 Equality non linear constrain

In order to introduce this type of constrain, let $\boldsymbol{\rho}$ and $\boldsymbol{\eta}$ the position and velocity in normalized coordinates, so that, the state at each nodes and their components, can be written in the following form:

$$\boldsymbol{x}_k = \begin{bmatrix} \boldsymbol{\rho}_k \\ \boldsymbol{\eta}_k \end{bmatrix} = \begin{bmatrix} \rho_k^x \\ \rho_k^y \\ \rho_k^z \\ \eta_k^x \\ \eta_k^y \\ \eta_k^z \end{bmatrix} \quad , \quad k = 1, .., N \tag{155}$$

The dynamical flow in the RPRnBP, starting at $\boldsymbol{x}_k$ and propagated till $t = t_{k+1}$ is denoted as usual, $\phi(t_{k+1}, \boldsymbol{x}_k)$ as already discuss. The defects $\boldsymbol{\xi}_i$, in state space, from the propagated node and its successive can be computed as:

$$\boldsymbol{\xi}_k = \phi(t_{k+1}, \boldsymbol{x}_k) - \boldsymbol{x}_{k+1} = \mathbf{0} \quad , \quad k = 1, \ldots, N-1 \tag{156}$$

Condition in Eq.(156) enforce the system to be continuous at each patched point in state space, however a maneuver could be present, in those situations Eq.(156), valid for no maneuver, must be modify, to do so, let's consider the following partitions:

$$\phi(t_{k+1}, \boldsymbol{x}_k) = \begin{bmatrix} \phi_{\boldsymbol{\rho}}(t_{k+1}, \boldsymbol{x}_k) \\ \phi_{\boldsymbol{\eta}}(t_{k+1}, \boldsymbol{x}_k) \end{bmatrix} \quad \boldsymbol{\Phi}^k(t_k, t_{k+1}) = \begin{bmatrix} \boldsymbol{\Phi}^k_{\boldsymbol{\rho}}(t_k, t_{k+1}) \\ \boldsymbol{\Phi}^k_{\boldsymbol{\eta}}(t_k, t_{k+1}) \end{bmatrix} \quad k = 1, \ldots, N-1 \tag{157}$$

Let n_m the set of nodes where ΔV is present, continuity condition becomes:

$$\boldsymbol{\xi}_j = \phi_{\boldsymbol{\rho}}(t_{j+1}, \boldsymbol{x}_j) - \boldsymbol{\rho}_{j+1} = \mathbf{0} \quad , \quad j+1 \in n_m \tag{158}$$

Where only continuity in position is enforced, while:

$$\Delta V_{j+1} = \left\| \phi_{\boldsymbol{\eta}}(t_{j+1}, \boldsymbol{x}_j) - \boldsymbol{\eta}_{j+1} \right\| \quad \text{if} \quad j+1 \in n_m \tag{159a}$$

$$\Delta V_1 = \| \boldsymbol{\eta}_0 - \boldsymbol{\eta}_1 \| \quad \text{if} \quad n_m = 1. \tag{159b}$$

Where ΔV_1 is the impulsive maneuver at the first node (if present) while $\boldsymbol{\eta}_0$ is the initial velocity before the manoeuvre which is known.
When dealing with optimization process in a computer, also gradients must be taken into account. In general gradients need not to be set, they are computed by the machine step by step and thus can require a lot of time, however if we are able to give also the

gradients the optimization process benefits and time require is much less.
Lets consider the vector of constraints:

$$\boldsymbol{c}(\boldsymbol{X},\boldsymbol{\tau}) = (\boldsymbol{\xi}_1,\ldots,\boldsymbol{\xi}_i,\ldots,\boldsymbol{\xi}_j,\ldots,\boldsymbol{\xi}_{N-1}) \tag{160}$$

Consisting in a column vector with $6(N-1)-3N_{man}$ or $6(N-1)-3(N_{man}-1)$ components depending if a maneuver at the initial node is present or not, the gradient of $\boldsymbol{c}(\boldsymbol{X},\boldsymbol{\tau})$ reads:

$$\boldsymbol{\nabla c}(\boldsymbol{X},\boldsymbol{\tau}) = \left[\begin{array}{ccc|ccc} \frac{\partial c_1}{\partial \rho_1^x} & \frac{\partial c_1}{\partial \rho_1^y} & \cdots & \frac{\partial c_1}{\partial t_1} & \cdots & \frac{\partial c_1}{\partial t_N} \\ \frac{\partial c_2}{\partial \rho_1^x} & \frac{\partial c_2}{\partial \rho_1^y} & \cdots & \frac{\partial c_2}{\partial t_1} & \cdots & \frac{\partial c_2}{\partial t_N} \\ \vdots & \ddots & \vdots & \vdots & \ddots & \vdots \end{array}\right] = \left[\frac{\partial \boldsymbol{c}}{\partial \boldsymbol{X}} \;\middle|\; \frac{\partial \boldsymbol{c}}{\partial \boldsymbol{\tau}}\right] \tag{161}$$

Remembering the definition of $\Phi(t,t_0)$ in Eq.(46), the term $\frac{\partial \boldsymbol{c}}{\partial \boldsymbol{X}}$ can be express in the following form:

$$\frac{\partial \boldsymbol{c}}{\partial \boldsymbol{X}} = \begin{bmatrix} \boldsymbol{\Phi}^1 & -\boldsymbol{I} & \boldsymbol{0} & \ldots & \ldots & \ldots & \boldsymbol{0} \\ \boldsymbol{0} & \boldsymbol{\Phi}^2 & -\boldsymbol{I} & \ddots & \ldots & \ldots & \vdots \\ \vdots & \ddots & \ddots & \ddots & \ddots & \ldots & \vdots \\ \boldsymbol{0} & \ldots & \ddots & \boldsymbol{\Phi}_{\boldsymbol{\rho}}^j & -\tilde{\boldsymbol{I}} & \ddots & \boldsymbol{0} \\ \vdots & \ldots & \ldots & \ddots & \ddots & \ddots & \vdots \\ \boldsymbol{0} & \ldots & \ldots & \ldots & \boldsymbol{0} & \boldsymbol{\Phi}_{\boldsymbol{\rho}}^{N-1} & -\tilde{\boldsymbol{I}} \end{bmatrix} \tag{162}$$

Note that in how is written Eq.(162) a maneuver is present at the final node.
Where $\boldsymbol{I}$ is a 6×6 identity matrix while:

$$\tilde{\boldsymbol{I}} = \begin{bmatrix} 1 & 0 & 0 & 0 & 0 & 0 \\ 0 & 1 & 0 & 0 & 0 & 0 \\ 0 & 0 & 1 & 0 & 0 & 0 \end{bmatrix} \tag{163}$$

Regarding the time derivatives:

$$\frac{\partial \boldsymbol{x}_k(t_k)}{\partial t_k} = \dot{\boldsymbol{x}}_k(t_k) = \boldsymbol{f}^k(\boldsymbol{x}_k(t_k),t_k) = \begin{bmatrix} \boldsymbol{f}_{\boldsymbol{\rho}}^k(\boldsymbol{x}_k(t_k),t_k) \\ \boldsymbol{f}_{\boldsymbol{\eta}}^k(\boldsymbol{x}_k(t_k),t_k) \end{bmatrix} \quad k=1,\ldots,N \tag{164a}$$

$$\frac{\partial \phi(t_{k+1},\boldsymbol{x}_k)}{\partial t_{k+1}} = \boldsymbol{f}^k(\phi(t_{k+1},\boldsymbol{x}_k)) = \begin{bmatrix} \boldsymbol{f}_{\boldsymbol{\rho}}^k(\phi(t_{k+1},\boldsymbol{x}_k)) \\ \boldsymbol{f}_{\boldsymbol{\eta}}^k(\phi(t_{k+1},\boldsymbol{x}_k)) \end{bmatrix} \quad k=1,\ldots,N-1 \tag{164b}$$

Where we have used Eq.(43).
A more difficult derivative is the following:

$$\frac{\partial \phi_{\boldsymbol{\rho}}(t_{k+1}, \boldsymbol{x}_k)}{\partial t_k} = -\boldsymbol{\Phi}^k_{\boldsymbol{\rho}}(t_k, t_{k+1}) \boldsymbol{f}^k(\boldsymbol{x}_k, t_k) \tag{165a}$$

$$\frac{\partial \phi(t_{k+1}, \boldsymbol{x}_k)}{\partial t_k} = -\boldsymbol{\Phi}^k(t_k, t_{k+1}) \boldsymbol{f}^k(\boldsymbol{x}_k, t_k) \tag{165b}$$

The derivation of this relations can be seen in [26].
Summarizing, the derivative of the constrain are the following:

$$\frac{\partial \boldsymbol{\xi}_k}{\partial t_k} = -\boldsymbol{\Phi}^k(t_k, t_{k+1}) \boldsymbol{f}^k(\boldsymbol{x}_k, t_k) \tag{166a}$$

$$\frac{\partial \boldsymbol{\xi}_k}{\partial t_{k+1}} = \boldsymbol{f}^k(\phi(t_{k+1}, \boldsymbol{x}_k)) - \boldsymbol{f}^{k+1}(\boldsymbol{x}_{k+1}, t_{k+1}) \tag{166b}$$

$$k = 1, \ldots, N-1 \tag{166c}$$

If no maneuver is present, or:

$$\frac{\partial \boldsymbol{\xi}_k}{\partial t_k} = -\boldsymbol{\Phi}^k_{\boldsymbol{\rho}}(t_k, t_{k+1}) \boldsymbol{f}^k_{\boldsymbol{\rho}}(\boldsymbol{x}_k, t_k) \tag{167a}$$

$$\frac{\partial \boldsymbol{\xi}_k}{\partial t_{k+1}} = \boldsymbol{f}^k_{\boldsymbol{\rho}}(\phi_{\boldsymbol{\rho}}(t_{k+1}, \boldsymbol{x}_k)) - \boldsymbol{f}^{k+1}_{\boldsymbol{\rho}}(\boldsymbol{x}_{k+1}, t_{k+1}) \tag{167b}$$

$$k = 1, \ldots, N-1 \tag{167c}$$

If maneuver is present at node $k+1$ (note that a maneuver at the first node is not 'seen' by the constrain).
Now that we have all the derivatives the gradient can be computed, *Figure 31* shows an example of sparsity patter.

4.4.4 Inequality nonlinear constrain

During optimization process the spacecraft can take beneficial effect from fly-by's in this case the satellite is in proximity of a body and impact constraints must be considered. Constrain are the following:

$$\psi_k = -(\rho^x_k - \mu_1)^2 - (\rho^y_k)^2 - (\rho^z_k)^2 + R^2_M \tag{168a}$$

$$\zeta_k = -(\rho^x_k + \mu_2)^2 - (\rho^y_k)^2 - (\rho^z_k)^2 + R^2_E \tag{168b}$$

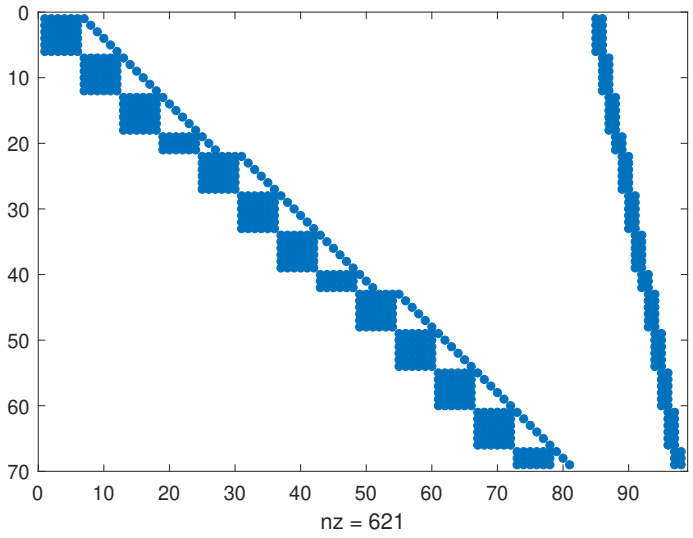

Figure 31: Sparsity pattern example of constraints gradient with $N_{man} = 4$ (one at the initial node, not shown), the colored dots are nonzero values

Where R_M and R_E are the normalized mean radius of the Moon and Earth respectively.

$$\psi_k = -(\rho_k^x - \mu_1)^2 - (\rho_k^y)^2 - (\rho_k^z)^2 + R_M^2 \tag{169a}$$

$$\zeta_k = -(\rho_k^x + \mu_2)^2 - (\rho_k^y)^2 - (\rho_k^z)^2 + R_E^2 \tag{169b}$$

Considering the vector $\boldsymbol{\sigma}$ containing all the constrain:

$$\boldsymbol{\sigma}(\boldsymbol{X}, \boldsymbol{\tau}) = (\psi_1, \dots, \psi_N, \zeta_1, \dots, \zeta_N) \tag{170}$$

The gradient will be:

$$\boldsymbol{\nabla\sigma}(\boldsymbol{X}, \boldsymbol{\tau}) = \begin{bmatrix} \frac{\partial\psi_1}{\partial\rho_1^x} & \frac{\partial\psi_1}{\partial\rho_1^y} & \dots & \frac{\partial\psi_1}{\partial\eta_N^z} & \frac{\partial\psi_1}{\partial t_1} & \dots & \frac{\partial\psi_1}{\partial t_N} \\ \vdots & \vdots & \vdots & \vdots & \vdots & \vdots & \vdots \\ \frac{\partial\zeta_1}{\partial\rho_1^x} & \frac{\partial\zeta_1}{\partial\rho_1^y} & \dots & \frac{\partial\zeta_1}{\partial\eta_N^z} & \frac{\partial\zeta_1}{\partial t_1} & \dots & \frac{\partial\zeta_1}{\partial t_N} \\ \vdots & \vdots & \vdots & \vdots & \vdots & \vdots & \vdots \\ \frac{\partial\zeta_N}{\partial\rho_1^x} & \frac{\partial\zeta_N}{\partial\rho_1^y} & \dots & \frac{\partial\zeta_N}{\partial\eta_N^z} & \frac{\partial\zeta_N}{\partial t_1} & \dots & \frac{\partial\zeta_N}{\partial t_N} \end{bmatrix} \tag{171}$$

With derivatives given by:

$$\frac{\partial \psi_k}{\partial \boldsymbol{x}_k} = \begin{bmatrix} -2(\rho_k^x - \mu_1) \\ -2\rho_k^y \\ -2\rho_k^z \\ 0 \\ 0 \\ 0 \end{bmatrix} \quad , \quad \frac{\partial \psi_k}{\partial t_k} = 0 \tag{172}$$

and:

$$\frac{\partial \zeta_k}{\partial \boldsymbol{x}_k} = \begin{bmatrix} -2(\rho_k^x + \mu_2) \\ -2\rho_k^y \\ -2\rho_k^z \\ 0 \\ 0 \\ 0 \end{bmatrix} \quad , \quad \frac{\partial \zeta_k}{\partial t_k} = 0 \tag{173}$$

And all the other derivatives are null.

4.5 Construction of Halo orbit in the RPRnBP

As we have already discuss, when considering orbits around equilibrium points unmodeled dynamics starts to become important and must be taken into account when propagate the trajectory for a long time, this section is dedicated to the refinement of periodic orbit in the RPRnBP.

4.5.1 Implementation

In this case we consider a free trajectory, no maneuver is present, moreover we consider a fixed time grid equally spaced:

$$t_k = t_1 + \frac{j-1}{N-1}(t_N - t_1) \quad , \quad j = 1, \dots, N \tag{174}$$

So that the free variables are only those related to the state $\boldsymbol{x}_k$.
Therefore Eq.(162) simplify becoming:

$$\boldsymbol{\nabla c} = \frac{\partial \boldsymbol{c}}{\partial \boldsymbol{X}}(\boldsymbol{X}) = \begin{bmatrix} \boldsymbol{\Phi}^1 & -\boldsymbol{I} & 0 & \dots & 0 \\ 0 & \boldsymbol{\Phi}^2 & -\boldsymbol{I} & \ddots & \vdots \\ \vdots & \ddots & \ddots & \ddots & 0 \\ 0 & \dots & 0 & \boldsymbol{\Phi}^{N-1} & -\boldsymbol{I} \end{bmatrix} \tag{175}$$

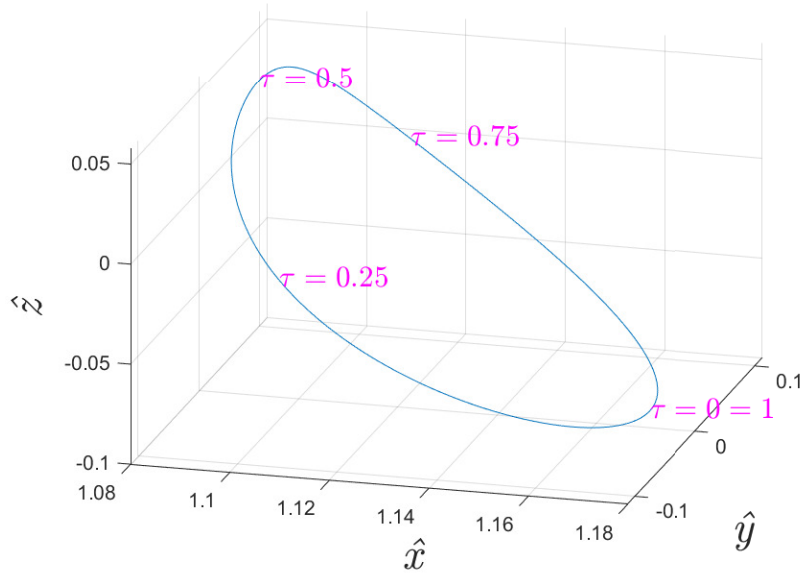

Figure 32: Parametrization of τ

The initial conditions are specified at the initial time only and is taken from the solution of the CRTBP.
Each point along the Halo orbit can be parametrized through the value τ, introduced in the previous chapter, therefore the initial condition can be set accordingly:

$$\boldsymbol{x}_1(t_1) = \bar{\boldsymbol{x}}(\tau) \tag{176}$$

The parametrization selected is shown in *Figure 32*.
Then an objective function must be set, in this case we force the solution to be continuous so that we express the objective as a quadratic form of the constraints:

$$J(\boldsymbol{X}) = \frac{1}{2}\boldsymbol{c}\mathcal{M}\boldsymbol{c}^T \tag{177}$$

Where the matrix $\mathcal{M}$ must be positive definite in order to enforce the optimization to have $J_{opt}(\boldsymbol{X}) \approx 0$, in this case the matrix $\mathcal{M}$ can be taken as the identity matrix $\boldsymbol{I}$.
Also the gradient of the objective can be computes as:

$$\boldsymbol{\nabla} J(\boldsymbol{X}) = \frac{1}{2}\boldsymbol{\nabla}\boldsymbol{c}(\boldsymbol{I}\boldsymbol{c}^T) + \frac{1}{2}\boldsymbol{c}\boldsymbol{\nabla}\big(\boldsymbol{I}\boldsymbol{c}^T\big) = (\boldsymbol{\nabla}\boldsymbol{c})\boldsymbol{c}^T \tag{178}$$

The implementation of the optimization algorithm is done with MATLAB®, through

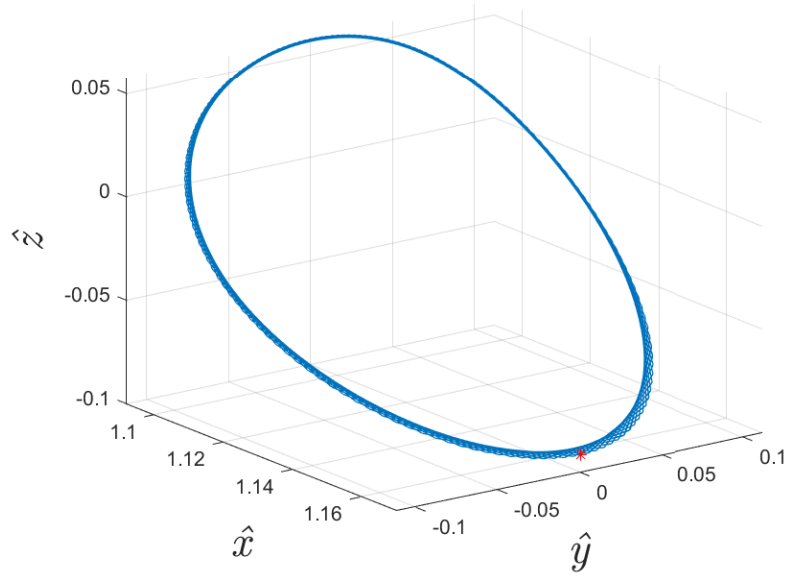

Figure 33: First guess discrete and repeated Halo, in red is shown the starting point with $\tau = 0$

`fmincon`, using `interior-point` algorithm.
In this case the dynamics is integrated, the PrinceDormand78 integrator is chosen (`ode78`) that uses a Runge-Kutta scheme up to the 7^{th} order and then verified with an 8^{th} order scheme, with a tolerance set to 2.5×10^{-12}.
However before to start the optimization process an initial seed must be applied, the selected initial guess, samples N times, is taken from the CRTBP orbit, differentially corrected and repeated with a certain number of times in order to span the desired time interval.
The selection of this repeated closed orbit is due to the fact that its construction is done through an iterative process, therefore, errors at the second crossing of the $y = 0$ plane are present so that when propagated for a long time, due to the chaotic behaviour and computer errors, the trajectory will diverge after few revolutions.
LUMIO orbit is selected to be a L_2 Southern Halo orbit with $A_z = 28418.41$Km, obtained after a trade-off analysis that can be found in [13].

4.5.2 Results

The trajectory is integrated for one year, starting on 21 March 2024, time difference between successive nodes of 2 days is chosen ($N = 183$), the repeated Halo guess is shown in *Figure 33*.
Solar radiation pressure is also consider, using a cannon-ball model, the main geometric parameter are shown in *Table 2*

Table 2: Main parameters of LUMIO spacecraft

Area $[m^2]$	Mass $[Kg]$	Reflectivity Coeff. C_r	Radiation flux Ψ $[\frac{W}{m^2}]$
0.4	24	1.08	1371

While the mean parameter of `fmincon` are the following:

```
options =optimoptions('fmincon','Display','Iter','Algorithm',...
'interior-point','SpecifyObjectiveGradient',true,...
'SpecifyConstraintGradient',true,'CheckGradients',false,'StepTolerance'...
,1e-10,'MaxIterations',300,'FiniteDifferenceType','central'...
,'ConstraintTolerance',5e-04,'EnableFeasibilityMode',true,...
'SubproblemAlgorithm','cg');
```

It is interesting to highlight the possibility to check the gradients, setting the corresponding option to `'true'` once gradient of objective or constrains or both are specified.

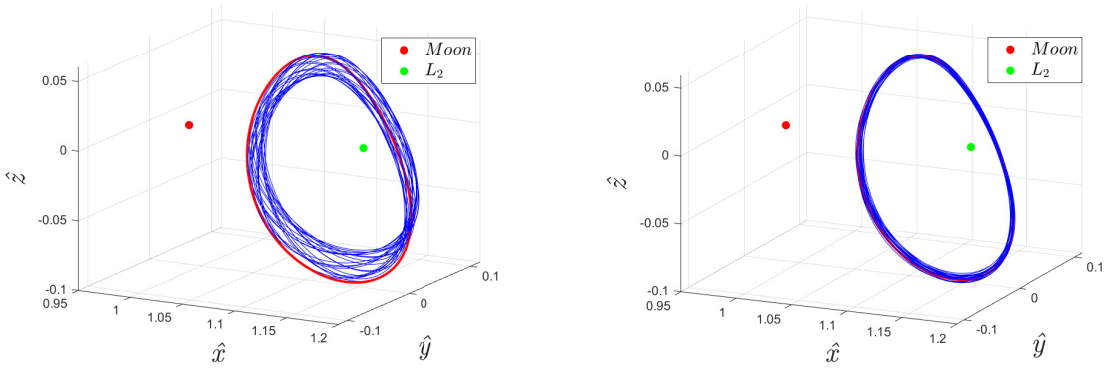

(a) Constrained Case **(b)** Unconstrained Case

Figure 34: Optimize trajectory (blue) compared with the initial guess (red)

The trajectory results is shown in *Figure 34* and *Table 3*, where is compared with the Halo obtained in the CRTBP, with initial condition in $\tau = 0$, note also that with this procedure, it is also possible to formulate an optimization process without any constrain at the boundaries, this situation can be used when studying closed orbits alone, without be interested to the insertion point.

As suspected, the unconstrained case is more prone to be optimize and gives better results, even if no clear initial condition is defined.
According to [24], the trajectories obtained have the free boundaries removed (10% of

Table 3: Comparison solutions

Case	$J(\boldsymbol{X})$	Max constrain violation	N_{iter}
Constrained	1.486414e-07	4.143e-04	23
Unconstrained	2.974350e-09	2.346e-05	5

the total time), this because in an optimization process, no one grants that a quasi Halo trajectory is obtained also propagating further the trajectory, since the optimal solution is optimal within the time interval selected and divergence behaviour can be found in proximity of the free boundaries. Note that this is not a problem, in reality since station keeping maneuvers are present, in order to maintain LUMIO inside its operative ranges and to design a more robust trajectory against inevitable errors.

5 Conclusion

When dealing with trajectory in high fidelity models, no closed solution exist and the solution must be integrated numerically, moreover, optimization process is necessary in order to search for an optimal solution among all the feasible one.
When considering closed orbits, multiple shooting algorithm is capable of desensitize the dynamics, especially when no maneuver are present, providing a more robust construction of closed orbits, starting from a solution differentially corrected in the CRTBP.
For LUMIO, low-energy transfer strategy is used in order to reach Earth-Moon L_2 libration point, those trajectories can be designed using weak stability boundaries, or exploiting manifolds, obtained perturbing the closed trajectory, that allow to the spacecraft to reach the target, saving a lot of propellant but with a considerable time of flight.

5.1 Recommendations

This section some recommendations are presented:

- About the model, the RPRnBP takes into account the Eath-Moon system, the other planets and the Sun, however when propagating for a long time the trajectory, other perturbations start to become significant. Firstly, asteroids, opportunely modeled, can be taken into account, especially those on the triangular points of the Sun-Jupiter system, moreover, also relativistic effect starts to enter in the game.

- As already note, errors are always present, the theory is different from the real dynamics, therefore, in order to have a Halo-like trajectory, small corrective maneuvers are always present.

Appendices

A Quintic equation

Here is briefly reported the computation of the quintic equation for each collinear point:

- L_1: Taking the different sign we have:

$$x - \mu_1 \frac{x+\mu_2}{(x+\mu_2)^3} + \mu_2 \frac{x-\mu_1}{(x-\mu_1)^3} = 0 \tag{179}$$

  Simplifying and manipulating we get:

$$\begin{aligned} x^5 + (2\mu_2 - 2\mu_1)x^4 + (\mu_1^2 + \mu_2^2 - 4\mu_1\mu_2)x^3 + (-2\mu_1\mu_2^2 + 2\mu_2\mu_1^2 - \mu_1 + \mu_2)x^2 \\ +(\mu_1^2\mu_2^2 + 2\mu_1^2 + 2\mu_2^2)x + (\mu_2^3 - \mu_1^3) = 0 \end{aligned} \tag{180}$$

  In this case a polynomial of fifth degree has five solutions four are complex and conjugate pairs the last instead is real and is what we are looking for.

- L_2: Taking the different sign we have in this case:

$$x - \mu_1 \frac{x+\mu_2}{(x+\mu_2)^3} - \mu_2 \frac{x-\mu_1}{(x-\mu_1)^3} = 0 \tag{181}$$

  Obtaining the following polynomial:

$$\begin{aligned} x^5 + (2\mu_2 - 2\mu_1)x^4 + (\mu_1^2 + \mu_2^2 - 4\mu_1\mu_2)x^3 + (-2\mu_1\mu_2^2 + 2\mu_2\mu_1^2 - \mu_1 - \mu_2)x^2 \\ +(\mu_1^2\mu_2^2 + 2\mu_1^2 - 2\mu_2^2)x + (-\mu_2^3 - \mu_1^3) = 0 \end{aligned} \tag{182}$$

- L_3: In this case we get:

$$x - (-\mu_1 \frac{x+\mu_2}{(x+\mu_2)^3} - \mu_2 \frac{x-\mu_1}{(x-\mu_1)^3}) = 0 \tag{183}$$

  Therefore:

$$x^5 + (2\mu_2 - 2\mu_1)x^4 + (\mu_1^2 + \mu_2^2 - 4\mu_1\mu_2)x^3 + (-2\mu_1\mu_2^2 + 2\mu_2\mu_1^2 + \mu_1 + \mu_2)x^2 + (\mu_1^2\mu_2^2 - 2\mu_1^2 + 2\mu_2^2)x + (\mu_2^3 + \mu_1^3) = 0 \tag{184}$$

B Richardson third order approximation

In this section is describe the procedure in order to obtain a Halo orbit, knowing its amplitude, around a collinear point $L_i = (\gamma_i, 0, 0)$, for more detail about the method, see [27]:

- **Step 1:** Once that the position of the interested libration point has been computed, the distance from each primary to the generic Lagrangian point is:

$$r_1 = |\gamma_i + \mu_2| \qquad \text{for } M_1 \tag{185a}$$

$$r_2 = |\gamma_i - \mu_1| \qquad \text{for } M_2 \tag{185b}$$

  Then it is possible to compute c_n as follows:

$$c_n = \frac{\mu_2}{r_1^3} + (-1)^n \frac{\mu_1 r_1^{n-2}}{r_2^{n+1}} \qquad \text{for } L_1 \tag{186a}$$

$$c_n = (-1)^n \frac{\mu_2}{r_1^3} + (-1)^n \frac{\mu_1 r_1^{n-2}}{r_2^{n+1}} \qquad \text{for } L_2 \tag{186b}$$

$$c_n = (-1)^n \frac{\mu_1}{r_1^3} + (-1)^n \frac{\mu_2 r_1^{n-2}}{r_2^{n+1}} \qquad \text{for } L_3 \tag{186c}$$

  Compute the values of k and the linearized frequency λ:

$$\lambda = \sqrt{\frac{2 - c_2 + \sqrt{9c_2^2 - 8c_2}}{2}} \tag{187a}$$

$$k = \frac{\lambda^2 + 1 + 2c_2}{2\lambda} \tag{187b}$$

- **Step 2:** Some important constants are computed:

$$
\begin{aligned}
d_1 &= \frac{3\lambda^2}{k}(k(6\lambda^2-1)-2\lambda)\\
d_2 &= \frac{8\lambda^2}{k}(k(11\lambda^2-1)-2\lambda)\\
a_{21} &= \frac{3c_3(k^2-2)}{4(1+2c_2)}\\
a_{22} &= \frac{3c_3}{4(1+2c_2)}\\
a_{23} &= -\frac{3c_3\lambda}{4kd_1}(3k^3\lambda-6k(k-\lambda)+4)\\
a_{24} &= -\frac{3c_3\lambda}{4kd_1}(2+3k\lambda)\\
b_{21} &= -\frac{3c_3\lambda}{2d_1}(3k\lambda-4)\\
b_{22} &= \frac{3c_3\lambda}{d_1}\\
d_{21} &= -\frac{c_3}{2\lambda^2}\\
a_{31} &= -\frac{9\lambda}{4d_2}(4c_3(ka_{23}-b_{21})+kc_4(4+k^2))+\\
&+\frac{9\lambda^2+1-c_2}{2d_2}(3c_3(2a_{23}-kb_{21})+c_4(2+3k^2))\\
a_{32} &= -\frac{9\lambda}{4d_2}(4c_3(ka_{24}-b_{22})+kc_4)-\frac{3}{2d_2}(9\lambda^2+1-c_2)(c_3(kb_{22}+d_{21}-2a_{24})-c_4)\\
b_{31} &= \frac{3}{8d_2}8\lambda(3c_3(kb_{21}-2a_{23})-c_4(2+3\lambda^2))+\\
&+\frac{3}{8d_2}((9\lambda^2+1+2c_2)(4c_3(ka_{23}-b_{21})+kc_4(4+k^2)))\\
b_{32} &= \frac{9\lambda}{d_2}(c_3(kb_{22}+d_{21}-2a_{24})-c_4)+\frac{3(9\lambda^2+1+2c_2)}{8d_2}(4c_3(ka_{24}-b_{22})+kc_4)\\
d_{31} &= \frac{3}{64\lambda^2}(4c_3a_{24}+c_4)\\
d_{32} &= \frac{3}{64\lambda^2}(4c_3(a_{23}-d_{21})+c_4(4+k^2))\\
s_1 &= \frac{1}{2\lambda(\lambda(1+k^2)-2k)}(\frac{3}{2}c_3(2a_{21}(k^2-2)-a_{23}(k^2+2)-2kb_{21})\\
&-\frac{3}{8}c_4(3k^4-8k^2+8))\\
s_2 &= \frac{1}{2\lambda(\lambda(1+k^2)-2k)}(\frac{3}{2}c_3(2a_{22}(k^2-2)+a_{24}(k^2+2)+2kb_{22}+5d_{21})+\\
&+\frac{3}{8}c_4(12-k^2))\\
l_1 &= -\frac{3}{2}c_3(2a_{21}+a_{23}+5d_{21})-\frac{3}{8}c_4(12-k^2)+2\lambda^2s_1\\
l_2 &= \frac{3}{2}c_3(a_{24}-2a_{22})+\frac{9}{8}c_4+2\lambda^2s_2
\end{aligned}
\tag{188}
$$

- **Step 3:** Compute Δ, defined as:

$$\Delta = \lambda^2 - c_2 \tag{189}$$

Then it is possible to use the following equations in order to compute the unknown amplitude and the frequency of the orbit:

$$l_1 A_x^2 + l_2 A_z^2 + \Delta = 0 \tag{190a}$$
$$\tag{190b}$$

While the frequency ω and the period T are:

$$\omega = \lambda(1 + s_1 A_x^2 + s_2 A_z^2) \tag{191}$$
$$T = \frac{2\pi}{\omega} \tag{192}$$

- **Step 4:** Now that all the terms are computed, the solution of the Halo orbit is the following:

$$x = a_{21}A_x^2 + a_{22}A_z^2 - A_x \cos\tau + (a_{23}A_x^2 - a_{24}A_z^2)\cos 2\tau + (a_{31}A_x^3 - a_{32}A_x A_z^2)\cos 3\tau \tag{193a}$$
$$y = kA_x \sin\tau + (b_{21}A_x^2 - b_{22}A_z^2)\sin 2\tau + (b_{31}A_x^3 - b_{32}A_x A_z^2)\sin 3\tau \tag{193b}$$
$$z = \delta_m A_z \cos\tau + \delta_m d_{21} A_x A_z(\cos 2\tau - 3) + \delta_m(d_{32}A_z A_x^2 - d_{31}A_z^3)\cos 3\tau \tag{193c}$$

Where $\tau = \omega t + \phi$ being ϕ the initial phase and $\delta_m = 1, 3$ that correspond to a northern ($\delta_m = 3$) or southern ($\delta_m = 1$) Halo orbit.
With the velocity given by:

$$v_x = \omega A_x \sin\tau - 2\omega(a_{23}A_x^2 - a_{24}A_z^2)\sin 2\tau - 3\omega(a_{31}A_x^3 - a_{32}A_x A_z^2)\sin 3\tau \tag{194a}$$
$$v_y = \omega k A_x \cos\tau + 2\omega(b_{21}A_x^2 - b_{22}A_z^2)\cos 2\tau + 3\omega(b_{31}A_x^3 - b_{32}A_x A_z^2)\cos 3\tau \tag{194b}$$
$$v_z = -\omega\delta_m A_z \sin\tau - \delta_m \omega d_{21} A_x A_z \sin 2\tau - 3\omega\delta_m(d_{32}A_z A_x^2 - d_{31}A_z^3)\sin 3\tau \tag{194c}$$

Note that, the equations just shown are valid in a reference frame centered in the corresponding Lagrangian point, in order to transform into CRTBP normalized

coordinates the following transformation must be applied:

$$x^{CRTBP} = xr_j + \gamma_i \quad , \quad y^{CRTBP} = yr_j \quad , \quad z^{CRTBP} = zr_j \tag{195a}$$

$$v_x^{CRTBP} = v_x r_j \quad , \quad v_y^{CRTBP} = v_y r_j \quad , \quad v_z^{CRTBP} = v_z r_j \tag{195b}$$

Where r_j is the distance defined in Eq.(185) and must be replaced with $j = 2$ in the L_1 and L_2 point, while $j = 1$ in L_3.
In *Table 4* are summarized the different coefficent:

Table 4: Coefficients for Halo orbit Computation

Coefficient	Value
A_z	0.4404
A_x	0.2439
a_{21}	-1.7519
a_{22}	-0.2702
a_{23}	0.8179
a_{24}	0.1208
a_{31}	0.6936
a_{32}	0.0909
b_{21}	0.4727
b_{22}	-0.0770
b_{31}	0.6836
b_{32}	0.0033
d_1	192.9385
d_2	995.9668
d_{21}	0.3833
d_{31}	0.0175
d_{32}	0.3732
s_1	-0.3476
s_2	0.1469
Δ	0.2790
δ_m	1
λ	1.8626
k	2.9126
T	3.3471
ω	1.8772

References

[1] Edward A. Belbruno and James K. Miller. "Sun Perturbed Earth to Moon transfers with Ballistic Capture". In: *Guidance, Control, and Dynamics* (1993).

[2] Edward A. Belbruno and John P. Carrico. "Calculation of weak stability boundary ballistic lunar transfer trajectories". In: *AIAA/AAS Astrodynamics Specialist Conference* (2000).

[3] W. Koon et al. *Dynamical System, the Three-body Problem and Space Mission Design*. 2006.

[4] Jeffrey S. Parker and Rodney L. Anderson. *Targeting low-energy transfers to low lunar orbit*. 2013.

[5] Jeffrey S. Parker. *Targeting low-energy ballistic lunar transfers*.

[6] Jeffrey S. Parker. "Surveying Ballistic Transfers to Low Lunar Orbit". In: *Guidance, Control, and Dynamics* (2013).

[7] Y.Qia, S. Xua, and R. Qib. "Transfer from Earth to libration point orbit using lunar gravity assist". In: *Acta Astronautica* (2017).

[8] Martin W. Yu Lo, Bobby G. Williams, and W. Boliman. "Genesis mission design". In: *Journal of the Astronautical Sciences* (1998).

[9] Ralph B. Roncoli and Kenneth K. Fujii. "Mission Design Overview for the Gravity Recovery and Interior Laboratory (GRAIL) Mission". In: *AIAA/AAS Astrodynamics Specialist Conference* (2010).

[10] K. Oguri et al. "EQUULEUS trajectory design". In: *Journal of the Astronautical Sciences* (2020).

[11] S. Campagnola et al. "Mission Analysis for the EM-1 CubeSats EQUULEUS and OMOTENASHI". In: *IEEE Aerospace and Electronic Systems Magazine* (2019).

[12] C. Giordano et al. *LUMIO Phase A*. 2021.

[13] Ana M. Cipriano, Diogene A. Dei Tos, and F. Topputo. "Orbit design for LUMIO: the lunar meteoroid impacts observer". In: *frontiers in Astronomy and Space Science* (2018).

[14] Diogene A. Dei Tos and F. Topputo. "On the advantages of exploiting the hierarchical structure of astrodynamical models". In: *Acta Astronautica* (2017).

[15] C. D. Murray and S.F. Dermott. *Solar System Dynamics*. Cambridge University Press, 2008.

[16] F. Topputo. *Astrodynamics Lectures*.

[17] Wikipedia. *Solar and Heliospheric Observatory*. URL: https://en.wikipedia.org/wiki/Solar_and_Heliospheric_Observatory.

[18] Wikipedia. *James Webb Space Telescope*. URL: https://en.wikipedia.org/wiki/James_Webb_Space_Telescope.

[19] U. Walter. *Astronautics, the physics of space flight*. Springer, 2019.

[20] G. Gomez et al. *Invariant Manifolds, the Spatial Three-Body Problem and Space Mission Design*. 2001.

[21] Jeffrey S. Parker. "Families of low-energy lunar Halo transfers". In: *Advances in the Astronautical Science* (2006).

[22] E.Belbruno, M. Gidea, and F. Topputo. *Weak Stability Boundary and Invariant Manifolds*. 2010.

[23] E. Belbruno. *Weak stability boundary*. URL: https://www.youtube.com/watch?v=rp0SAAsY0CY.

[24] D. A. Dei Tos. *Trajectory optimization of limited control authority spacecraft in high-fidelity models*. 2016.

[25] Frederick S. Hillier and Gerald J. Lieberman. *Introduction to operations research, 9th.ed*. Mc Graw Hill, 2010.

[26] E. Veruari. *Space trajectory optimization in high fidelity models*. 2017.

[27] David L. Richardson. *Periodic and Quasi Periodic Halo Orbits in the Earth-Sun/Earth-Moon Systems*. 2011.